Universitá degli Studi di Pisa

Facoltá di Scienze Matematiche Fisiche e Naturali

Dipartimento di Fisica

Scuola di Dottorato Galileo Galilei - Ciclo XVIII

PARTICLE ACCELERATION AT ASTROPHYSICAL SHOCKS: A DETAILED STUDY OF THE ENERGY SPECTRUM IN TEST-PARTICLE RELATIVISTIC THEORY AND NON-LINEAR NEWTONIAN THEORY

A Thesis in

Astronomy & Astrophysics

by

Morlino Giovanni

SUPERVISOR

Mario Vietri & Pasquale Blasi

Submitted in Partial Fulfillment
of the Requirements
for the Degree of

Dottorato in Fisica

December 2008

We approve the thesis of Morlino Giovanni.

Date of Signature

Prof. Kenichi Konishi Direttore del consiglio di Dottorato	
Prof. Mario Vietri Supervisor	
Giovanni Morlino Candidato	

Abstract

Diffusive Shock Acceleration (DSA), applied in different astrophysical environment, has provided by far the most popular model for the origin of Cosmic Rays (CRs), both for what concern the Galactic CRs (from GeV to PeV energies), through the application of DSA at the outer front of expanding supernova remnants, as well as for extragalactic CRs (beyond PeV energies), applying the DSA to extragalactic sources like Gamma Ray Bursts, Active Galactic Nuclei and Radio Galaxies. Beyond the considerable successes that this theory has achieved in the past years, lots of obscure points still remains to be enlightened. In particular the explanation of ultra high energy CRs seems to require the extension of DSA for shock at relativistic speed. Moreover recent studies of nonthermal emission at young SNRs shock has revealed the importance of developing a fully non liner theory capable to include the dynamical effects of accelerated particles, but a full understanding of all the phenomenology related to the nonlinearity is far to be reached.

In this work we study several aspects relating to DSA both for newtonian and for relativistic shocks. A mathematical approach to investigate particle acceleration at shock waves moving at arbitrary speed in a medium with arbitrary scattering properties was first discussed in Vietri (2003) and Blasi & Vietri (2005). In the fist part of this thesis we use this method and somewhat extend it in order to include the effect of a large scale magnetic field in the upstream plasma, with arbitrary orientation with respect to the direction of motion of the shock. We also use this approach to investigate the effects of anisotropic scattering on spectra and anisotropies of the distribution function of the accelerated particles. A furter step in the analysis of the DSA process is put forward introducing a general equation of state to describe the shocked downstream plasma. More specifically we consider the effect of energy exchange between the electron and proton thermal components downstream, and the effect of generation of a turbulent magnetic field in the downstream plasma. The slope of the spectrum turns out to be appreciably affected by all these phenomena, especially in the Newtonian and trans-relativistic regime, while in the ultra-relativistic limit the universal spectrum $s \approx 4.3$ seems to be a very solid prediction.

In the second part of the thesis we present the general solution for the non linear (time independent) theory of particle accelerated at Newtonian shocks in the presence of a pre-existing non-thermal particle population and for arbitrary diffusion coefficient. Using this solution we show that, in general, the contribution of a pre-existing energetic particle's flux, like the galactic CRs, cannot be neglected in determine the shock dynamics. The first consequence of this statement is that shocks like SNRs' ones, that propagates into the Galactic environment can evolve in a nonlinear way even if the injection of fresh particles were an inefficient process.

Table of Contents

List of Figures

Acknowledgments

First of all I would like to thank my thesis adviser, Mario Vietri. I have learnt a lot of physics talking and working with him. He was able to show me the beauty hidden behind a formula written on a blackboard.

I also want to thank Pasquale Blasi, for his support and advises. This work wouldn't be done without his help and suggestions.

A special thank goes to Steve Shore, for fruitful discussions ranging from physics to politics, from food to philosophy, I enjoyed it very much. I also want to thank all the Astrophysics group at the University of Pisa and especially to Scilla Degl'Innocenti, Carlo Ungarelli, Giada Valle, Pier Giorgio Prada Moroni and Rosa Poggiani.

Few words in my vocabulary can express the importance of a person among all the others: my dear *fellow traveller* Nicoletta. I cannot even think a single day without her presence and her influence in all my act. Thank you.

Tre sò li putent': lu papa, lu rrè e chi nun' tene nient.

–detto popolare lucano

La storia non si ripete totalmente, ma fa rima.

–Mark Twain

Introduction

Matter in astrophysical context foundamentally occurs in rarefied ionized plasma state. When a rarefied plasma collides with a "stiff" obstacles or with another plasma with a relative speed greater than the magnetosonic speed of the plasma itself, a collisionless shock is produced[1]. Because such kind of collisions are extremely frequent in the Universe, both in the galactic and in the extragalactic context, the study of collisionless shock has an important role in the understanding of several astrophysical phenomena. In particular collisionless shock in magnetized plasma are believed to be one of the principal responsable for the production of non thermal particle population into astrophysical environments by the so called *Diffusive Shock Acceleration*, a mechanism able to transfer energy from bulk macroscopic motion of plasma to single charged particles[2].

Historically, the first theory of magnetized shock, due to De Hoffman & Teller (1950), was stimulated by the study of atmospheric nuclear explosion. This work ignited an avalanche of theoretical investigations of magnetohydrodynamic shocks. But during the same years, a second strong motivations for a deeper investigation of shock physics come about through the study of Cosmic Rays' (CRs) origin. The seminal idea was put forward by Fermi (1949, 1954) who proposed that CRs could be accelerated by repeated stochastic scattering with moving magnetized clouds. Actually in its original form this idea does not work neither to explain the shape of the observed CRs energy spectrum, nor to account for their total energy density. This is because the average energy that a particle gains per each encounter with a cloud is only proportional to v_c^2/c^2, where v_c is the clouds mean speed and c the speed of light, and it turn out to be a small quantity for any reasonable v_c. The proportionality of the energy gain to the second power of the speed justify the name of *II order* Fermi mechanism.

Only in the seventies, several authors independently realized that the Fermi's idea could be applied to particles in the vicinity of a shock wave (Axford et al. 1977; Krymskii 1977; Bell 1978a,b; Blandford & Ostriker 1978). The scattering action of magnetic turbulence can confine such particles around the shock wave, and each time a particle perform a cycle, crossing the shock from one side to the other and coming back, it gains a bit of energy, subtracting it from the bulk motion of the plasma. With respect to the Fermi's original idea, in this case the energy gain of particles is always positive and, when averaged over spatial direction, it is proportional to v_s/c, where v_s is the shock speed. As one can easily understand, this is referred to as *I order* Fermi mechanism. In this process the competition between the energy gain per cycle and the escape probability from the acceleration region, determines the spectrum of accelerated particles. If both

[1]The term *collisionless* refers to the fact that any dissipative process that occurs across the shock transition cannot be attributed to mechanisms based on collisions between particles, simply because, for the context we are interested in, the shock thickness is several order of magnitude smaller than the mean free path of particles. The shock transition is instead due to collective wave-particle interactions.

[2]It is worth mentioning that the existence of collisionless shocks and their connection with non-thermal particles has been proved directly by spacecraft observations when satellites passed the *bow shock* standing upstream of the Earth's magnetosphere in the solar wind.

are independent of energy, or have the same dependence, the resulting energy spectrum is a power-law, $f(E) \propto E^{-s}$, with a slope s that depends only by the compression factor r at the shock, namely $s = (r+2)/(r-1)$. If the plasma is assumed to behave like an ideal gas, the compression factor for strong shocks is 4, and one easily get $s = 2$. The fact that the observed CRs up to the energy of the knee (3×10^{15} eV) requires an injected spectrum $Q_{inj}(E) \propto E^{-s}$ with $s \sim 2.1$, has been considered a strong evidence in favor of the hypothesis that I order Fermi acceleration can account for the Galactic component of CRs.

Cosmic Rays. Cosmic Rays are ionized nuclei coming from the outer space and detected at the Earth, or in the space just around the Earth, with balloon, satellite experiments or air-shower detectors. One of the impressive feature of the CRs is that they are detected over a huge range of energy: measurements with modern air-shower detectors infer particles with an energy up to 3×10^{20} eV, the most energetic particles ever measured. In spite of this large energy interval, extracting information from the CRs spectrum is hard because it is nearly featureless. For energies greater than $\sim$ 1 GeV, where the Solar wind screening effect become negligible, the spectrum resembles to a broken power-law with a spectral index changing from 2.7 to 3.1 at an energy of 3×10^{15} eV (a feature called *knee*). A second change in the spectrum occurs around 3×10^{18} eV where the slope flattens again towards a value close to 2.7 (usually referred to as the *ankle*). In the highest energy region the flux falls to very low values, hence measurement becomes extremely difficult (at 3×10^{20} eV the flux is 1 particle per km^2 each 350 years) and the energy determination is also affected by strong uncertainties. Despite such difficulties the most recent data from the Auger experiment seems to confirm the theoretical prediction of a sharp drop of the flux beyond 4×10^{19} eV (Pierre AUGER Collaboration 2008), due to CRs interaction with the Microwave Background photons (the so called *GZK* effect).

CRs up to an energy around 10^{17} eV are believed to originate in our own Galaxy. The flux is nearly isotropic and does not mirror the distribution of matter in the Galaxy. This means that they are produced somewhere in the Galaxy and diffuse toward us, loosing any information about the incoming direction. The diffusion process that confines CRs in the Galaxy is believed to be due to the scattering by the irregularities in the Galactic magnetic field. The residence time depends on the particle energy and charge Z, following an apparently simple law, i.e. $\tau_{esc}(E) \simeq 5 \times 10^6 \, (\frac{E}{Z \cdot 10\mathrm{GeV}})^{-\delta}$ yr, with $\delta = 0.6$. Estimate of this escaping time is inferred from the chemical composition of the secondary CRs produced by spallation between CRs themselves and the interstellar gas, and in particular from the relative abundance of some radioactive and stable isotopes. Because the observed flux is due to the competition between the particles injected end those escaping, i.e. $N(E) \propto Q_{inj}(E)\, \tau_{esc}(E)$, it turn out, as mentioned above, that taking the injection spectrum as a simple power-law with an index of ~ 2.1 could account for the observations.

Particles with energy beyond the ankle, usually referred to as *Ultra-High Energy Cosmic Rays* (UHECRs), cannot be confined in the Galaxy, because their Larmor radius in the typical Galactic magnetic field is of the same order of the Galaxy size, or even greater. Hence the particle deflection should be small enough that the arrival direction

should trace the sources position in the sky. On the contrary the incoming spatial distribution of UHECRs is nearly isotropic, hence the general opinion is that these particles come from extragalactic sources. This idea is also supported by the measured composition that at this energy seems to change from heavy nuclei (iron) to predominantly protons or possibly light nuclei, even if the lower statistic and the uncertainties related to the shower physics, make this data difficult to interpret.

SNRs paradigm for Galactic CRs. A connection between CRs and supernovae was firstly proposed more than seventy years ago by Baade & Zwicky (1934). Their hypothesis is suggested by a simple energetic argument. The power needed to maintain the Galactic CRs at the observed level against losses due to escape from the Galaxy can be estimated as follows

$$P_{CR} \sim U_{CR} V_{CR} / \tau_{res} \approx 10^{40} \mathrm{erg/s}\,,$$

where $U_{CR} \approx 0.5$ eV/cm^3 is the CRs energy density measured at the Earth and $V_{CR} \sim 400$ kpc^3 is the volume of CRs halo around the Galactic disk. The tipical residence time of a cosmic ray in the Galaxy we assume $\tau_{esc} \sim 5 \times 10^6$ yr. Now we know that the energy realased by a single supernova explosion is around 10^{53} erg. About 99% is radiated away by escaping neutrinos, while the remaining 1% is transfer as mechanical energy to the stellar envelope, that expands and produces a shock wave propagating into the interstellar medium (ISM), with a typical speed of $10^4 - 10^5$ Km/s. The total energy injected into the Galactic environment is

$$P_{SNR} = R_{SNR} E_{SNR} \approx 3 \times 10^{41} \mathrm{erg/s}\,.$$

where $R_{SNR} \sim 0.03$ yr^{-1} is the rate of supernova explosion in the Galaxy. The energy density of the Galactic CRs component can be accounted for if one assume that only a fraction around 3%[3] of the total supernovae mechanical energy is transferred to nonthermal particles.

The previous energetic argument and the hypothesis that the I order Fermi acceleration can occurs at the shocks formed by espanding shells of SNRs, strongly support the idea that SNRs are the factories of CRs production. Indeed things are never simple as they appears. From this simple picture several problem arises. First of all the maximum energy of CRs cannot be explained if one assume a magnetic turbulence of the same order of the Galactic magnetic field: only energy up to $Z \times 10^{14} - 10^{15}$ eV can be explained (Lagage & Cesarsky 1983), more than an order of magnitude below the knee position. Secondly a back of the envelope calculation of the amount of energy transfered form shock motion towards accelerated particles reveals an energetic problem: assuming a reasonable quantity of particles injected into the acceleration process, in such a waythat the that the observed flux can be explained, the energy they gain can be of

[3]This number has to be considered carefully, because it refers to particles that escape the accelerator and propagate freely into the Galaxy. Nowadays it is still not clear how the accelerated particles can escape from the remnant without loosing a considerable fraction of their energy because of the adiabatic expansion.

the same order of the total shock bulk energy, even assuming a maximum achievable energy less that what inferred from CRs spectrum. This means that the shock evolution is strongly affected by the presence of nonthermal population, and the back reaction of CRs cannot be neglected in theoretical calculation. This was realized only at the end of the century, and the investigation of non linear effect produced by the CRs action onto the shock dynamics has revealed a variety of intriguing phenomena, most of them are still far to be completely understood.

Relativistic shocks and the connection with UHECRs. Many mechanisms have been proposed to explain UHECRs, but nowadays none of them seems to provide a definite answer. As we have discussed above, particle acceleration by shock waves remains the principal mechanism to explain the existence of Galactic CRs. Hence the idea that some modified version of such mechanism can account also for UHECRs is a natural speculation.

Acceleration at relativistic shocks, i.e. shocks with speed close to c, is one of the favorite candidate. It was already discussed in late seventies (Blandford & McKee 1976; Blandford & Ostriker 1978; Peacock 1981). Such shocks are present in several astrophysical contexts: in collimated jets associated with AGNs and quasars, in the microquasar associated with compact object in our Galaxy, and in the relativistic fireballs believed to be associated with Gamma Ray Bursts.

The theory of particle acceleration at relativistic shock is complicated by several aspects. First of all, the distribution of particles near the shock front is strongly anisotropic, because particles and shock speeds are of the same order. This imply that the diffusion approximation cannot be used. Also, the energy gain per cycle in no more a small quantities, we instead have $\Delta E \sim E$, and it cannot be related to the shock speed in a straightforward way, as for the non relativistic shock case. Moreover in the framework of relativistic, or even mildly-relativistic shocks, the importance of back reaction of particles is still not understood as well as some aspects concerning the magnetic turbulence.

Fortunately, at least in the limit of *test particle* approximation, which neglects the dynamical reaction of accelerated particles we mentioned above, the theory of particle acceleration at shock fronts can be formulated in a simple and exact form (Vietri 2003), irrespective of shock speed. In this framework all the basic physical ingredients can be taken into account in an exact way, with special reference to the type of scattering that is responsible for the particles to return to the shock front from the upstream and downstream plasmas.

The importance of study of relativistic shocks goes beyond the understanding of UHECRs' origin. Nonthermal particle population exist anyway in powerfull objects like AGNs, microquasars or GRBs, where relativistic or mildly-relativistic shock are supposed to be generated. This is inferred by the observation of radiation that is clearly nonthermal in origin, like synchrotron emission from relativistic electrons. The same is true for young SNRs, where nonthermal X-ray and TeV γ-ray radiation, coming from the outer region of the remnants, has been detected in the past few years. The idea that behind all these phenomena could stand the same fundamental mechanism is rather

fascinating.

Aims. This short introduction wants to underline that shock physics cover a primary role in the field of cosmic accelerators, and its connection with the 'violent' Universe is tight.

The aim of the present work is an in-depth study of several aspects of particle acceleration mechanism for *i)* relativistic shock in the test-particle limit and for *ii)* Newtonian shocks when nonlinear effects are included. The thesis is structured as follows. In Chapter 1 we briefly summarize the basic features of shock acceleration for Newtonian shock in the case of test-particle approach. Always in the case of test-particle approximation, in Chapter 2 we introduce the general framework to solve the acceleration problem regardless of the shock speed. Newtonian, mildly-relativistic and fully relativistic shocks can be handle solving the same relativistic equation for the particle distribution function. This general method is applied in Chapters 3 and 4 where we specialize the study of particle acceleration in several situation of physical interests. Chapter 3 is dedicated to the study of the diffusive properties of the medium where a shock can propagate. Two situation are analyzed: shock propagating in presence of a static magnetic field and shock propagating in a medium with anisotropic scattering properties. In Chapter 4 we study the effects produced to the acceleration mechanism when the plasma equation of state deviates from the usual ideal-gas approximation. As a matter of fact, the equation of state of a plasma can be notably altered when the collective wave-particle interactions are take into account. Such interactions, that are usually produced when the plasma deviates from the equilibrium state, can account for energy exchange between protons, electrons and electromagnetic field. In all the situations mentioned, we show how the slope of the accelerated particle' spectrum can deviate from the values usually adopted in the literature. Consequences of this study can be especially important for the GRBs physics.

In the last Chapter, we come back to Newtonian shocks and we illustrate the basic features of the *non-linear* acceleration theory: we show how to include the back-reaction of accelerated particles into the shock dynamics, under the hypothesis that the shock is stationary in time. We present the general solution for the modified stationary shocks also in presence of a pre-existing non-thermal particle population. Using this solution we show that, in general, the contribution of a pre-existing energetic particle's flux, like the CRs observed at the Earth, cannot be neglected in determine the shock dynamics. The first consequence of this statement is that shocks like SNRs' ones, that propagates into the Galactic environment, can evolve in a nonlinear way even if the injection of fresh particles were inefficient.

In the Conclusions we briefly summarize our results, while a short Appendix is dedicated to summarize the dynamical rule of a coherent magnetic field both for Newtonian and for relativistic shocks.

Chapter 1

Diffusive shock acceleration: Newtonian theory in the test-particle limit

Collisionless shocks are believed to be the principal mechanism able to convert plasma bulk kinetic energy into energy of non-thermal particle population. Here we introduce the basic idea of diffusive shock acceleration, summarizing only the relevant results that can be usefull for the rest of this work. In this Chapter we only deal with non-relativistic linear shocks. The full relativistic theory for linear shock will be present in Chapter 2, while the general method to handle non-linear shocks for Newtonian velocity will be described and developed in the Chapter 5.

1.1 Second order Fermi mechanism

Before discussing the particle acceleration by shock waves, we briefly describe the original idea of Fermi about the stochastic acceleration. In his seminal papers Fermi (1949, 1954) proposed such a mechanism to explain the observed cosmic rays spectrum. The basic idea concerns the interaction between particles and Galactic turbulent magnetic field. Fermi idealized the turbulent magnetic field as magnetized clouds moving around into the Galaxy with random velocity. In the frame of the clouds the magnetic field is assumed to be static. A particle entering a cloud interacts in a collisionless way: its direction is randomized by the turbulent magnetic field but the particle energy remains unchanged in the reference frame of the cloud. Nevertheless the overall process lead to a net gain of energy, as we can seen simply applying the Lorentz transformation between the Galaxy and the cloud reference frame.

Energy gain. Let us consider a single particle with energy E_1, in the Galaxy's frame, and a cloud with Lorentz factor γ and speed $u = \beta c$. For simplicity we assume only relativistic particle, i.e. $E \sim pc$. In the reference frame of the cloud the energy is

$$E_1' = \gamma E_1 (1 - \beta \cos\theta_1)\,, \tag{1.1}$$

where θ_1 is the angle between particle's and clouds velocities. After the interaction the energy remains unchanged , $E_2' = E_1'$, and the exit angle is θ_2' (in the clouds' frame). The final energy in the Galaxy frame is

$$E_2 = \gamma E_2' (1 + \beta \cos\theta_2')\,. \tag{1.2}$$

After a single interaction the energy gain is

$$\frac{E_2 - E_1}{E_1} \equiv \frac{\Delta E}{E_1} = \frac{1 - \beta\cos\theta_1 + \beta\cos\theta_2' - \beta^2\cos\theta_1\cos\theta_2'}{1-\beta^2} - 1\,. \tag{1.3}$$

To get the mean energy gain we need to average over the incoming and the outcoming directions. Because the scattering in the cloud frame is isotropic, we have $\langle\cos\theta_2'\rangle = 0$. On the other hand, the mean incoming direction can be computed averaging over the particle flux, which is proportional to the relative velocity, $\beta_r = 1 - \beta\cos\theta_1$. Hence, if the particle distribution is isotropic, we simply have:

$$\langle\cos\theta_1\rangle = \frac{\int d\Omega\,\beta_r\cos\theta_1}{\int d\Omega\,\beta_r} = \frac{\int_{-1}^{1} d\cos\theta_1\,(1-\beta\cos\theta_1)\cos\theta_1}{\int_{-1}^{1} d\cos\theta_1\,(1-\beta\cos\theta_1)} = -\frac{\beta}{3} \tag{1.4}$$

The average energy gain become:

$$\frac{\Delta E}{E_1} = \frac{1+\frac{1}{3}\beta^2}{1-\beta^2} - 1 \sim \frac{4}{3}\beta^2\,. \tag{1.5}$$

The last passage is obtained under the assumption that $\beta \ll 1$. In spite of the fact that in each interaction a particle can both gain or lose energy, the average energy gain is positive simply because the cloud is moving, hence the flux of particle crossing the cloud in front is greather then the one from behind. In other words this result is a consequence of the beaming effect.

This mechanism is called second order Fermi mechanism because the energy gain is proportional to the velocity squared. In such a mechanism a particle needs too mutch time to reach very hight energy, and this mechanism turn out to be inefficient to explain the Galactic cosmic rays spectrum.

Particle spectrum. Let us consider a generic stochastic acceleration process where in each interaction the particle's energy gain is proportional to its initial energy, $\Delta E = \xi E$. If the particle start with an energy E_0, after n interaction its energy become $E_n = E_0(1+\xi)^n$. This means that the particle needs a number of interaction equal to

$$n = \frac{\ln(E/E_0)}{\ln(1+\xi)} \tag{1.6}$$

to have an energy equal to E. We now assume that after each interaction a particle has only a probability $P_{ret} = 1 - P_{esc}$ to undergo another acceleration cycle; we can also say that P_{esc} is the probability of escaping from the acceleration mechanism. After n interaction the number of particles which have an energy greater then E is proportional to

$$N_{>E} \propto \sum_{k=n}^{\infty}(1-P_{esc})^k = \frac{(1-P_{esc})^n}{P_{esc}} \tag{1.7}$$

Using the expression (1.6) we get a power law

$$N_{>E} \propto \frac{1}{P_{esc}} \left(\frac{E}{E_0} \right)^{-\delta} , \tag{1.8}$$

where

$$\delta = -\frac{\ln(1 - P_{esc})}{(1 + \xi)} . \tag{1.9}$$

Note that here we assumed P_{esc} to be independent of particle energy. Usually both P_{esc} and ξ are small quantities, hence the previous expression reduce to $\delta \sim P_{esc}/\xi$. The differential energy spectrum $n(E) = dN/dE$ is a power law with an index

$$\alpha = 1 + \delta \sim 1 + P_{esc}/\xi . \tag{1.10}$$

The key ingredients to get a power law distribution is that the energy gained by each particle in a single acceleration cycle should be proportional to the particle energy itself and to the escaping probability should be energy independent.

1.2 Acceleration at shock front: first order Fermi mechanism

More than twenty years later, the Fermi's idea was applied in the context of collisionless shock to get a more efficient acceleration mechanism. In the following we discuss two different approach: the microscopic one proposed by Bell (1978a) (and partially developed in the previous paragraph), where the energy history of each particle is followed; the second equivalent approach introduced by Blandford & Ostriker (1978) makes use of the formalism of the particle distribution function and the corresponding transport equation.

As often happen in the science, the use of different approaches in describing the same phenomena allows one to go deeper inside the physical mechanism. Moreover different formalisms can be more or less suitable to extend the theory to different contexts or to include complications into the problem.

1.2.1 The Bell approach

Bell discussed what happen to energetic particles in the vicinity of a shock wave. A shock wave can be generally defined as a transition layer which propagates through a plasma and changes its state. The incoming plasma is compressed and a fraction of its bulk kinetic energy is converted into internal energy of the downstream plasma, resulting in an increase of the plasma entropy. Because the astrophysical plasmas are usually very tenuous, the microscopic interactions responsable of the state transition are not the collisions between particles, but the interaction of particles with the plasma waves generated by collective processes. The tickness of the shock layer is determined by these processes, hence it should be of the order of the gyroradius of the downstream thermal particles.

Bell considered a plane shock propagating parallel to the background magnetic field direction and takes into account only particles with an energy sufficiently higher

that they cannot resonate with the waves in the shock layer. Such particles see the shock only as a discontinuity in the plasma.

Another assumption is that the energetic particles are efficiently scattered by the plasma turbulence, in such a way that they can be considered isotropically distributed both in the upstream and the downstream reference frame.

Consider a shock moving with velocity $u_s = \beta_s c$. In the frame where the shock is at rest the upstream plasma moves towards the shock with velocity $\beta_1 = \beta_s$, while the downstream plasma moves away form the shock with velocity $\beta_2 c$. The situation is similar to what happen in the case of moving cloud described in the previous section, but this time the relative velocity between downstream and upstream plasma is $\beta_r = \beta_1 - \beta_2$. The flux of particle crossing the shock from downstream region towards the upstream one is

$$J_- = \int \frac{d\Omega}{4\pi} nc \cos\theta = \frac{nc}{4}\,, \tag{1.11}$$

where n is the number density and the integration is performed in the interval $-1 \leqslant \cos\theta \leqslant 0$. Hence the average value of the incoming angle is

$$\langle \cos\theta_1 \rangle = \frac{1}{J_-} \int \frac{d\Omega}{4\pi} nc \cos^2\theta_1 = -\frac{2}{3} \tag{1.12}$$

while for the outcoming direction we have $\langle \cos\theta_2' \rangle = 2/3$ because the integration is performed for $0 \leqslant \cos\theta \leqslant 1$. According to Equation (1.3) the average energy gain in a single cycle downstream-upstream-downstream is:

$$\frac{\Delta E}{E} = \frac{1 + \frac{4}{3}\beta_r + \frac{4}{9}\beta_r^2}{1 - \beta_r^2} - 1 \sim \frac{4}{3}\,\beta_r\,. \tag{1.13}$$

Compared to the collision with clouds, the shock acceleration is more efficient, resulting in an energy gain proportional to the relative velocity between upstream and downstream plasmas. This is because in each shock encounter the particle gains a positive amount of energy, while in the case of cloud collision it can both gain or lose energy. For this reason the shock acceleration is also called *first order* Fermi mechanism.

After each cycle a particle has a finite probability to escape from the shock region because of the advection of the downstream plasma. In a steady state situation the particle flux advected towards downstream infinity is simply $J_\infty = nu_2$, while no particle can escape towards upstream infinity. Hence, for the flux conservation we have $J_+ = J_- + J_\infty$, where J_+ is the flux of particles crossing the shock from upstream towards downstream. The escaping probability can be expressed as follows:

$$P_{esc} = \frac{J_+}{J_-} = \frac{J_- + J_\infty}{J_-} = \frac{4u_2}{c}\,, \tag{1.14}$$

where we used Equation (1.12). The escaping probability is independent from particle energy, hence, as showed in the precedent paragraph, the resulting energy spectrum is a

power law whit an index

$$\alpha = \delta + 1 = \frac{P_{esc}}{\Delta E/E} + 1 = \frac{3u_2}{u_1 - u_2} + 1 = \frac{r+2}{r-1}\,. \tag{1.15}$$

The last equality makes use of the compression factor $r = u_1/u_2$, that can be obtained using the flux conservation of mass, momentum and energy across the shock layer. For a standard Newtonian hydrodynamic shock propagating with a Mach number M into a gas with adiabatic index γ, the very well know result is:

$$r = \frac{(\gamma+1)M^2}{(\gamma-1)M^2+2}\,. \tag{1.16}$$

For very strong shock ($M \gg 1$) and an ideal gas ($\gamma = 5/3$) this value reduces to $r = 4$, hence the predicted cosmic rays spectrum becomes $n(E) \propto E^{-2}$.

1.2.2 Approach using the transport equation

Blandford & Ostriker (1978) obtained the same result of Bell solving the transport equation for the particle distribution function. Let $f(x,p)$ be the particle distribution, whit p the particle momentum, such that $n(x) = 4\pi \int p^2 dp\, f(x,p)$ is the local number density. The interaction between particles and magnetic turbulence can be described as a diffusion process in the x space. Let $D(x)$ be the diffusion coefficient. The particle diffusion equation in the frame where the plasma is at rest is

$$\frac{\partial f}{\partial t} = \frac{\partial}{\partial x}\left(D\frac{\partial f}{\partial x}\right)\,. \tag{1.17}$$

In a frame where the plasma moves with velocity u the time derivative must be replaced by the convective derivative, $\partial_t \to \partial_t + u\,\partial_x$. Moreover, if the plasma velocity is not constant, i.e. $u = u(x)$, we must add a term to take into account the plasma compression effect onto the particle momentum, i.e. $\dot{p} = \frac{1}{3}p\frac{du}{dx}$. Equation (1.17) can be rewritten in the more general form as:

$$\frac{\partial f}{\partial t} + u(x)\frac{\partial f}{\partial x} = \frac{\partial}{\partial x}\left(D(x)\frac{\partial f}{\partial x}\right) - \frac{1}{3}p\frac{du}{dx}\frac{\partial f}{\partial x} + Q_0(p)\delta(x)\,. \tag{1.18}$$

The last term, $Q_0(p)\delta(x)$, takes into account the injection of fresh particles that is supposed to occur only at the shock position ($x = 0$).

In the first instance we are interested in the stationary solution, hence $\partial_t f \equiv 0$. Moreover we note that for a stationary problem the solution in the downstream section must be homogeneous, i.e. $[\partial_x f = 0]_2$. To get the solution of Equation (1.18) we first integrate it around the shock discontinuity, where the plasma velocity change from u_1 to u_2; we get:

$$D_1\left[\frac{\partial f}{\partial x}\right]_1 = -\frac{u_2 - u_1}{3}\,p\,\frac{\partial f_0}{\partial x} + Q_0\,. \tag{1.19}$$

$f_0(p) \equiv f(0,p)$ is the distribution function at the shock position. Now we can use the second boundary condition, i.e. the homogeneity of the distribution function at upstream infinity, $[\partial_x f = 0]_\infty$. Integrating Equation (1.18) between 0^- and $-\infty$ we get:

$$D_1 \left[\frac{\partial f}{\partial x}\right]_1 = u_1 \left(f_0 - f_\infty\right) . \tag{1.20}$$

Using both Eqs. (1.19) and (1.20) we finally get the solution for f_0:

$$f_0(p) = s\, p^{-s} \int_0^p dp' p'^{s-1} \left(\frac{Q_0(p')}{u_1} + f_\infty(p')\right) , \tag{1.21}$$

where

$$s = \frac{3u_1}{u_1 - u_2} = \frac{3r}{r-1} . \tag{1.22}$$

At least two physical situation can be of interest. The first one correspond to the monochromatic injection, $Q_0(p) \propto \delta(p - p_{\rm inj})$. This is exactly the same case discussed in the previous paragraph using the Bell approach and the result turn out to be the same. In fact Equation (1.21) reduces to a simple power law in the momentum, $f(p) \propto p^{-s}$. For hight energy particle the distribution in energy is $n(E) \sim p^2 f(p) \propto p^{2-s}$, and from Eqs. (1.15) and (1.22) we see that $\alpha = s - 2$.

The second interesting case concerns the presence of a pre-existing non thermal particle distribution that can be re-accelerated by a shock (Bell 1978b). For the sake of simplicity we suppose that the pre-existing population is a power law, $f_\infty(p) \propto p^{-s_1}$, for p above a minimum momentum p_0; this could be the case if the particles come from a previous shock acceleration with compression ratio r_1. Neglecting a possible injection term, the integration of Equation (1.21) gives us:

$$f(p) \propto \left(\frac{p}{p_0}\right)^{-s_2} \left| \left(\frac{p}{p_0}\right)^{s_2 - s_1} - 1 \right| . \tag{1.23}$$

The spectrum (1.23) is a power law in the hight momentum limit, with an index equal to the smallest one between s_1 and s_2, i.e. the one corresponding to the strongest shock. For momentum near p_0 the spectrum become flatter and vanishes at $p = p_0$.

In the case of multiple shocks acceleration the particle distribution become flatter and flatter. Suppose to have an initial population given by $f_0 = Ap^{-s}$, with a minimum momentum equal to p_0, passing through n subsequent shocks. For simplicity we assume all the shocks having the same Mach number. The repeated integration of the Equation (1.21) gives us the following simple result:

$$f_n(p) = Ap^{-s} \frac{s^n}{n!} p_0^{n-1} \left[\ln \frac{p}{p_0}\right]^n . \tag{1.24}$$

1.2.3 Limitation and problems of linear Newtonian approach

It is worth noting that both the macroscopic and the microscopic approaches summarized in this chapter, suffer of some important limitations. The convection-diffusion equation (1.18) implicitly assumes an isotropic particle distribution in all the relevant reference frames. The same assumption is implemented in the microscopic approach in the computation of both the energy gain and the escaping probability (Eqs (1.12) and (1.14), respectively). We note that even if the isotropic assumption were correct in the plasma reference frame (as a consequence of a very efficient diffusion process), the same assumption loses its validity when the distribution is busted in the shock frame, because an anisotropy of the order of u_s/c is introduced. This correction is negligible for Newtonian shocks, but becomes of primary importance when one deals with relativistic shocks. In a consistent treatment the angular distribution can not be decided *a priori*, but it has to be an output of the calculation. We will show how to address this point in the Chapter 2.

A second consideration concerns the contribution of the accelerated particle in the shock dynamics. The theory presented in this chapter considers the shock as a pre-existing phenomena whose dynamics is fixed by the hydrodynamic (or magnetohydrodynamics) conditions. We have seen that the predicted energy spectrum is $n(E) \sim E^{-2}$; this mean that the energy content in non-thermal particles diverges. It is clear that a real physical process can only reach a maximum energy $E_{\max}$, determined by the shock size, the magnetic field strength and the timelife of the shock. On the other hand in several astrophysical situations $E_{\max}$ can easily becomes sufficiently large such that the fraction of energy transferred to the accelerated particles is no more negligible ($\gtrsim 10\%$), and accelerated particles become able to modify the plasma state and the shock structure itself. In such a regime the shock is called *non-linear* because this back reaction effect. Several non linear processes can be expected when the back reaction of non thermal particles is included in the computation: some of them tend to enhance the efficiency of the shock acceleration, while others tend to reduce it:

1. If the accelerated particle pressure is sufficiently strong, the incoming upstream plasma is smoothly compressed before the encounter with the shock discontinuity. In such a modified velocity profile particles experience a different velocity jump in passing from upstream to downstream, according to their energy. The net effect is an acceleration more efficient for hight energy particles and less efficient for the less energetic ones.

2. We know that usually the diffusion coefficient increases with energy. If the shock produces sufficient hight energy particles such that their diffusion length becomes larger than the shock acceleration region, these particles can escape towards upstream infinity, carring away a considerable fraction of energy and pressure. In this picture the shock becomes "radiative" and the compression ratio increases, allowing a more efficient acceleration.

3. Energetic particles streaming into the upstream plasma can produce plasma instabilities able to amplify the magnetic turbulence. This mechanism can strongly reduce the diffusion coefficient, enhancing the number of shock encounter that a

particle experiences per unit time. Also this process translates in an enhancement of the acceleration efficiency.

4. A more efficient acceleration as predicted by points (1)-(3), tends to reduce the downstream plasma temperature simply because an increasing fraction of the total energy is channelled into the non-thermal particles. On the other hand the particles injected at the shock front are belived to come from the tale of the maxwellian distribution of downstream particles. As a consequence a more efficient acceleration should implies a less efficient injection.

5. If the production of magnetic turbulence by the accelerated particles (point[3]) becomes energetically important, CRs lose a fraction of their energy that is converted into magnetic energy and pressure. While energetic particles cannot directly affect the sub-shock discontinuity transition, the produced magnetic turbulence enhances the total pressure and reduces the compression factor r.

As is clear the overall picture is extraordinary complicated and hightly non linear. We have a competition between positive feedback mechanisms (1)-(3), which tend to enhance the acceleration efficiency, and negative ones (4)-(5). In the recent years a lot of work were done to address one or more of the points listed above, but a fully consistent treatment of all these effects does not still exist.

Moreover there are serious doubts about the existence of a static solution of the non linear problem. A more realistic solution should be time dependent.

Chapter 2

Diffusive shock acceleration: the relativistic theory in the test-particle limit

2.1 Introduction

In this chapter we summarise the main characteristics of the theory of particle acceleration developed by Vietri (2003) and Blasi & Vietri (2005). The reader is referred to this previous work for further details. The power of this novel approach is in its generality: it provides an exact solution for the spectrum of the accelerated particles and at the same time the distribution in pitch angle that the particles acquire due to scattering in the upstream and downstream fluids. This mathematical approach is applicable without restrictions on the velocity of the fluid speeds (from Newtonian to ultra-relativistic) and irrespective of the scattering properties of the background plasmas (small as well as large angle scattering, isotropic or anisotropic scattering). The only condition which is necessary for the theory to work is common to most if not all other semi-analytical approaches existing in the literature, namely that the acceleration must take place in the test particles regime: no dynamical reaction is currently introduced in the calculations. As a consequence, the shock is assumed to conserve its strength during the acceleration time, and the acceleration is assumed to have reached a stationary regime.

A basic ingredient of the shock acceleration mechanism is the diffusion of particles in the media both upstream and downstream with respect to the shock. This diffusion allows a particle to cross and re-cross the shock, acquiring a certain amount of energy at each cycle upstream $\rightarrow$ downstream $\rightarrow$ upstream. The information about scattering is introduced in the problem through a function $w(\mu, \mu')$ which expresses the probability per unit length that a particle moving in the direction μ' is scattered to a new direction μ. It is worth stressing that w can have a different functional form in the upstream and downstream plasmas, in particular in the case of relativistic shocks.

The repeated scatterings of the particles lead eventually to return to the shock front, as described in terms of the conditional probability $P_u(\mu_\circ, \mu)$ ($P_d(\mu_\circ, \mu)$) that a particle entering the upstream (downstream) plasma in the direction $\mu_\circ$, returns to the shock and crosses it in the direction of the downstream (upstream) plasma in the direction μ. The mathematical method adopted to calculate the two very important functions P_u and P_d based upon the knowledge of the elementary scattering function w was described in detail in Blasi & Vietri (2005), and is based on solving two non-linear integral-differential equations in the two independent coordinates $\mu_\circ$ and μ.

Vietri (2003) showed on very general grounds that the spectrum of accelerated particles is a power law for all momenta exceeding the injection momentum. The slope of such power law and the anisotropy pattern of the accelerated particles near the shock

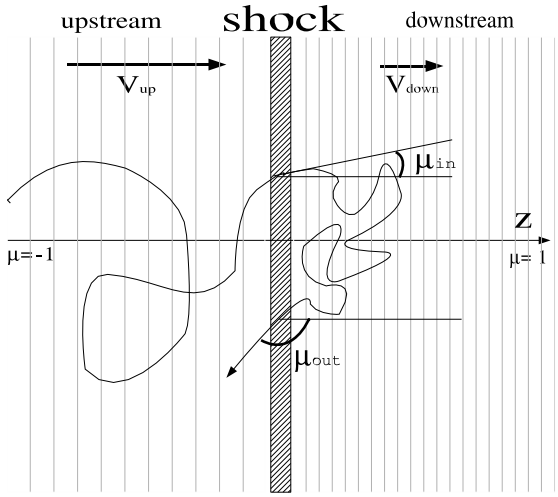

Fig. 2.1 Pictorial view of particle scattering process around a plane shock wave as seen by shock stationary frame.

front are fully determined by the conditional probabilities P_d and P_u and by the equation of state of the downstream plasma. Particle acceleration at shock fronts has been previously investigated through different methods, both semi-analytical (see e.g. Kirk & Schneider (1987); Gallant & Achterberg (1999); Kirk et al. (2000); Achterberg et al. (2001)) and numerical, by using Monte Carlo simulations (*e.g.* Bednarz & Ostrowski (1998); Lemoine & Pelletier (2003); Niemiec & Ostrowski (2004); Lemoine & Revenu (2006)). The theory of particle acceleration developed by Vietri (2003) and Blasi & Vietri (2005) has been checked versus several of these calculations existing in the literature, both in the case of non relativistic shocks and for relativistic shocks, and assuming small as well as large pitch angle isotropic scattering (see Blasi & Vietri (2005) for an extensive discussion of these results).

2.2 An exact solution for the accelerated particles in arbitrary conditions

The directions of motion of the particles in the downstream and upstream frames are identified through the cosine of their pitch angles, all evaluated in the comoving frames of the fluids that they refer to. The direction of motion of the shock, identified as the z axis, is assumed to be oriented from upstream to downstream, following the direction of motion of the fluid in the shock frame ($\mu = 1$ corresponds to particles moving toward the downstream section. Refer to Fig. 2.1 to a pictorial view). The transport equation for the particle distribution function g, as obtained in Vietri (2003) in a relativistically covariant derivation reads

$$\gamma\,(u+\mu)\,\frac{\partial g}{\partial z} = \iint \left[-W(\mu',\mu,\phi',\phi)g(\mu,\phi) + W(\mu,\mu',\phi,\phi')g(\mu',\phi')\right] d\mu' d\phi' + \omega\,\frac{\partial g}{\partial \tilde{\phi}}\,, \tag{2.1}$$

in which both scattering and regular deflection in a large scale magnetic field are taken into account.

Here all quantities are written in the fluid frame, with the exception of the spatial coordinate z, the distance from the shock along the shock normal, which is measured in the shock frame. u and γ are, respectively, the velocity and the Lorentz factor of the fluid with respect to the shock. θ and ϕ are the polar coordinates of particles in momentum space, measured with respect to the shock normal, while $\tilde{\phi}$ is the longitudinal angle around the magnetic field direction. As usual $\mu = \cos\theta$ and $\omega = eB/E$ is the particle Larmor frequency. $W(\mu,\mu',\phi,\phi')$ is the scattering probability per unit length, namely the probability that a particle moving in the direction (μ',ϕ') is scattered to a direction (μ,ϕ) after travelling a unit length.

An important simplification of Eq. (2.1) occurs when an axial symmetry is assumed. In this case the scattering probability depends only on $\Delta \equiv \phi - \phi'$ and the large scale magnetic field can be either zero or different from zero but parallel to the shock normal. In both cases it is straightforward to integrate eq. (2.1) over ϕ: the two-dimensional integral on the right-hand side simplifies to an integral in one dimension, while the term $\omega(\partial g/\partial\tilde{\phi})$ disappears.

These simplifications lead to

$$\gamma\,(u+\mu)\,\frac{\partial g}{\partial z} = \int \left[-w(\mu',\mu)g(\mu) + w(\mu,\mu')g(\mu')\right] d\mu', \tag{2.2}$$

where

$$w(\mu,\mu') \equiv \int W(\mu,\mu',\Delta)\,d\Delta \qquad \text{and}$$
$$g(\mu) \equiv \frac{1}{2\pi}\int g(\mu,\phi)\,d\phi\,.$$

The physical ingredients are all contained in the two conditional probabilities $P_u(\mu_\circ,\mu)$ and $P_d(\mu_\circ,\mu)$: these two functions provide respectively the probability that a particle entering the upstream (downstream) plasma along a direction μ_0 exits it along a direction μ. In the absence of large scale coherent magnetic fields, the two functions $P_u(\mu_\circ,\mu)$ and $P_d(\mu_\circ,\mu)$ were defined through a set of two integral-differential non linear equations by Blasi & Vietri (2005). We report these equations here for completeness:

$$P_u(\mu_\circ,\mu)\left(\frac{d(\mu_\circ)}{u+\mu_\circ}-\frac{d(\mu)}{u+\mu}\right)=\frac{w(\mu,\mu_\circ)}{u+\mu_\circ}-\int_{-u}^{1}d\mu'\frac{w(\mu,\mu')P_u(\mu_\circ,\mu')}{u+\mu'}+$$
$$\int_{-1}^{-u}d\mu'\frac{w(\mu',\mu_\circ)P_u(\mu',\mu)}{u+\mu_\circ}-\int_{-1}^{-u}d\mu'P_u(\mu',\mu)\int_{-u}^{1}d\mu''\frac{w(\mu',\mu'')P_u(\mu_\circ,\mu'')}{u+\mu''},\qquad(2.3)$$

$$P_d(\mu_\circ,\mu)\left(\frac{d(\mu_\circ)}{u+\mu_\circ}-\frac{d(\mu)}{u+\mu}\right)=\frac{w(\mu,\mu_\circ)}{u+\mu_\circ}+\int_{-u}^{1}d\mu'\frac{P_d(\mu',\mu)w(\mu',\mu_\circ)}{u+\mu_\circ}-$$
$$\int_{-1}^{-u}d\mu'\frac{P_d(\mu_\circ,\mu')w(\mu,\mu')}{u+\mu'}-\int_{-u}^{1}d\mu'P_d(\mu',\mu)\int_{-1}^{-u}d\mu''\frac{w(\mu',\mu'')P_d(\mu_\circ,\mu'')}{u+\mu''}.\qquad(2.4)$$

In the equations above we used:

$$d(\mu)\equiv\int_{-1}^{+1}w(\mu',\mu)d\mu'\,,\qquad(2.5)$$

which is unity by definition.

It is worth stressing that Eq. (2.3) provides automatically the correct normalization for the return probability from upstream: $\int_{-u}^{1}d\mu' P_u(\mu_\circ,\mu')=1$, independent of the entrance angle $\mu_\circ$. In §3.2.1 we will generalize the method to include the possibility of deflection by large scale magnetic fields, which is one of the achievements of this work. In that case we will show that the return probability from upstream is no longer bound to be unity, due to the escape of particles from the upstream region.

The procedure for the calculation of the slope of the spectrum of accelerated particles, as found by Vietri (2003) and Blasi & Vietri (2005), is as follows: for a given Lorentz factor of the shock (γ_s), the velocity of the upstream fluid $u=\beta_s$ is calculated. The velocity u_d of the downstream fluid is found from the usual jump conditions at the shock and through the adoption of an equation of state for the downstream fluid.

Once the two functions P_u and P_d have been calculated, the slope of the spectrum, as discussed in Vietri (2003), is given by the solution of the integral equation:

$$(u_d+\mu)g(\mu)=\int_{-u_d}^{1}d\xi Q^T(\xi,\mu)(u_d+\xi)g(\xi),\qquad(2.6)$$

where

$$Q^T(\xi,\mu)=\int_{-1}^{-u_d}d\nu P_u(\nu,\mu)P_d(\xi,\nu)\left(\frac{1-u_{rel}\mu}{1-u_{rel}\nu}\right)^{3-s}.\qquad(2.7)$$

Here $u_{rel}=\frac{u-u_d}{1-uu_d}$ is the relative velocity between the upstream and downstream fluids and $g(\mu)$ is the angular part of the distribution function of the accelerated particles, which contains all the information about the anisotropy. Note that in Eq. (2.7) all variables and functions are evaluated in the downstream frame, while the P_u calculated through Eq. (2.3) is in the frame comoving with the (upstream) fluid. The P_u that need

to be used in Eq. (2.7) is therefore

$$P_u(\nu,\mu) = P_u(\tilde{\nu},\tilde{\mu})\frac{d\tilde{\mu}}{d\mu} = P_u(\tilde{\nu},\tilde{\mu})\left[\frac{1-u_{rel}^2}{(1-u_{rel}\mu)^2}\right].$$

The solution for the slope s of the spectrum is found by solving Eq. (2.6). In general, this equation has no solution but for one value of s. Finding this value provides not only the slope of the spectrum but also the angular distribution function $g(\mu)$.

2.3 The special case of isotropic scattering

No assumption has been introduced so far about the scattering processes that determine the motion of the particles in the upstream and downstream plasmas, with the exception of the axial symmetry of the function $W(\mu,\mu',\phi,\phi')$.

A special case of this symmetric situation is that of isotropic scattering, that takes place when the scattering probability W only depends upon the deflection angle Θ, related to the initial and final directions through

$$\cos\Theta \equiv \mu\mu' + \sqrt{1-\mu^2}\sqrt{1-\mu'^2}\cos(\phi-\phi'). \tag{2.8}$$

Among the many functional forms that correspond physically to isotropic scattering, the simplest one is

$$W(\mu,\mu',\phi,\phi') = W(\cos\Theta) = \frac{1}{\sigma}e^{-\frac{1-\cos\Theta}{\sigma}}, \tag{2.9}$$

where σ is the mean scattering angle. Integration of eq. (2.9) over $\phi-\phi'$ leads to

$$w(\mu,\mu') = \frac{1}{\sigma}\,e^{-\frac{1-\mu\mu'}{\sigma}}\,I_0\left(\frac{\sqrt{1-\mu^2}\sqrt{1-\mu'^2}}{\sigma}\right), \tag{2.10}$$

with $I_0(x)$ the Bessel function of order 0. Eq. (2.9), first introduced in Blasi & Vietri (2005), naturally satisfies the requirement of being symmetric under rotations around the normal to the shock surface. In the limit $\sigma \ll 1$ this function becomes a Dirac Delta function, strongly peaked around the forward direction, corresponding to isotropic Small Pitch Angle Scattering (SPAS). For the opposite limit, that is $\sigma \gg 1$, w becomes flat and corresponds to the case of isotropic Large Angle Scattering (LAS). In §3.3.2 we will modify this functional form to introduce the possibility of anisotropic scattering.

Chapter 3

The plasma diffusion properties

3.1 Introduction

In this Chapter we extend the application of the new theoretical framework summarized in the previous Chapter to two new interesting situations: 1) presence of a coherent large scale magnetic field in the upstream fluid; 2) anisotropic scattering. In both cases we calculate the spectrum of accelerated particles and the distribution in pitch angle (upstream and downstream) for shock fronts moving with arbitrary velocity. The results of point 1) are compared with those obtained in Achterberg et al. (2001), carried out for a parallel ultra-relativistic shock.

The work presented in this Chapter has been inspired by the need to address several points of phenomenological relevance. As far as relativistic shocks are concerned, it was understood that the return of the particles to the shock surface from the upstream region can be warranted even in the absence of scattering, provided the background magnetic field is at an angle with the shock normal (e.g. Achterberg et al. (2001)). This is due to the fact that the shock and the accelerated particles remain spatially close and regular deflection takes place before particles can experience the complex, possibly turbulent structure of the upstream magnetic field. This implies that the calculation of the spectrum of the accelerated particles cannot be calculated using a formalism based on the assumption of pitch angle diffusion, as in the vast majority of the existing literature.

In the downstream region, the motion of the shock is always quasi-newtonian, even when the shock moves at ultra-relativistic speeds. This implies that the propagation of the particles is generally well described by (small or large) pitch angle scattering. However, the turbulent structure of the magnetic field, responsible for the scattering, is likely to have an anisotropic structure and be therefore responsible for anisotropic scattering. In fact, even in the case of isotropic turbulence, the scattering can determine an anisotropic pattern of particle scattering. It follows that a determination of the spectrum able to take into account these potentially important situations is very important.

The outline of the Chapter is the following: in §3.2 we consider in detail the case of a large scale magnetic field in the upstream frame and no scattering of the particles. The scattering is assumed to be isotropic in the downstream plasma. In §3.3 we introduce the possibility of anisotropic scattering in both upstream and downstream plasmas. We summarize in §3.4.

3.2 Acceleration in the presence of static magnetic field

3.2.1 Particles' deflection in the upstream region

It is well known that particle acceleration at a shock front with parallel magnetic field without scattering centers does not work. This magnetic scattering may be self-generated by the same particles, but the process of generation depends on the conditions in specific astrophysical environments. The case in which a regular magnetic field not parallel to the shock normal is present in the upstream fluid is quite interesting in that it allows for the return of the particles to the shock front even in the absence of scattering (see Fig. 3.1). In this section we investigate in detail the process of acceleration at shocks with arbitrary velocity when only a regular large scale magnetic field is present upstream (no scattering). We assume that enough turbulence is instead present in the downstream plasma to guarantee magnetic scattering of the particles.

There are two main differences introduced by this situation when compared with the standard case considered in the previous section:

- *(a)* Particle motion in the upstream region is deterministic: the stochasticity introduced by the interaction with scattering centers is assumed to be absent. This requires a new determination of the return probability P_u introduced in the Chapter 2.
- *(b)* The presence of regular magnetic field with arbitrary orientation breaks the axial symmetry around the shock normal. This, in principle, would force us to treat the problem in the four angular variables $\mu_\circ, \phi_\circ, \mu$ and ϕ.

In the following we will show how addressing point *(a)* in fact solves point *(b)* as well.

3.2.2 Upstream return probability

Let us Consider a particle entering upstream in the direction identified by the two angles $\mu_\circ$ and $\phi_\circ$, and returning to the shock along the direction identified by μ and ϕ. Since the motion of the particle is deterministic, the return direction is completely defined by the incoming coordinates, and we can write in full generality:

$$P_u(\mu_\circ, \phi_\circ; \mu, \phi) = (2\pi)^{-1} \delta\left(\mu - \mu_1(\mu_\circ, \phi_\circ)\right)\, \delta\left(\phi - \phi_1(\mu_\circ, \phi_\circ)\right)\,, \tag{3.1}$$

where μ_1 and ϕ_1 are obtained from the solution of the equation of motion, as discussed below. One can see that P_u is effectively a function of only two variables.

In order to apply the same mathematical procedure introduced in §2.2, we need to write P_u as a function of azimuthal angles only. Therefore we use the properties of the delta function in $\delta(\mu - \mu_1(\mu_\circ, \phi_\circ))$, to write:

$$\begin{aligned} P_u(\mu_\circ, \phi_\circ; \mu, \phi) &= \frac{1}{2\pi} \left| \frac{\partial \phi_\circ(\mu_\circ, \mu)}{\partial \mu} \right| \delta\left(\phi_\circ - \bar{\phi_\circ}\right)\, \delta\left(\phi - \phi_1\right) \\ &\equiv P_u(\mu_\circ, \mu)\, \delta\left(\phi_\circ - \bar{\phi_\circ}\right)\, \delta\left(\phi - \phi_1\right)\,. \end{aligned} \tag{3.2}$$

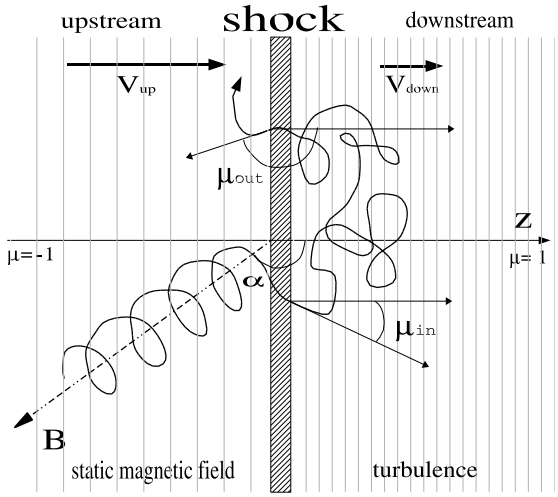

Fig. 3.1 Pictorial view of particle scattering process around a plane shock wave as seen by shock stationary frame. Upstream only a static large-coherence magnetic field is present, while downstream the diffusion is due to magnetic turbulence.

We now show that $P_{u}(\mu_{\circ},\mu)$, as defined by Eq. (3.2), is exactly the function to be used in eq. (2.7). This is easily shown by writing the fluxes of particles ingoing and outgoing the upstream plasma:

$$J_{+}(\mu,\phi)=\int_{-1}^{-u}d\mu^{'}\int_{0}^{2\pi}d\phi^{'}\,P_{u}(\mu^{'},\phi^{'},\mu,\phi)J_{-}(\mu^{'},\phi^{'})\,, \tag{3.3}$$

which, when integrated over ϕ, yields

$$J_{+}(\mu)\equiv\int d\phi J_{+}(\mu,\phi)=\int_{-1}^{-u}d\mu^{'}\,P_{u}(\mu^{'},\mu)J_{-}(\mu^{'})\,, \tag{3.4}$$

where we assumed that J_{-} is independent of ϕ. This is exactly the same relationship as was used in Vietri (2003), and proves our point that the system may, in the average, still be treated as if it were symmetric about the shock normal.

The key assumption here is that the flux crossing back into the upstream region from the downstream one, J_{-}, be independent of the azimuthal angle ϕ. This is of course true in the Newtonian regime, because there the residence time for all particles diverges, and there is time for deflections to effectively erase anisotropies in the ϕ direction. But this must be true *a fortiori* in the relativistic regime, when one considers that the properties of scattering are of course still the same as in the Newtonian regime, while the surface to be recrossed, *i.e.*, the shock, is running away from the particles at a speed that becomes, asymptotically, a fair fraction of the particles' speed. So, while not exactly true, the independence of J_{-} from ϕ is at least a good approximation.

In order to write $P_u(\mu_\circ, \mu)$ in a more explicit way, we need to solve the equation of motion of the particles, namely find the direction at which the particles re-cross the shock front as a function of the incoming direction. Particles move following a helicoidal trajectory around the magnetic field direction, indicated here as $\tilde{z}$. The problem is simplest if expressed in the frame $\tilde{O}$ comoving with the upstream fluid but with the polar axis coincident with $\tilde{z}$. We mark with a tilde all quantities expressed in this frame. The equations of motion in the frame $\tilde{O}$ are:

$$\tilde{\mu}(t) = \tilde{\mu}_\circ \,, \tag{3.5}$$

$$\tilde{\phi}(t) = \tilde{\phi}_\circ + \omega t \,, \tag{3.6}$$

where t is time and ω is the Larmor frequency. The particles re-cross the shock when $z_{\rm particle}(t) = z_{\rm shock}(t)$. This condition expressed in the frame $\tilde{O}$ reads

$$\sin(\omega\, t + \tilde{\phi}_\circ) - \sin\tilde{\phi}_\circ = \frac{\tilde{\mu}_\circ \cos\alpha + \beta_s}{\sin\alpha\, \sin\tilde{\theta}_\circ}\, \omega t \,, \tag{3.7}$$

where α is the angle between the shock normal z and the magnetic field direction $\tilde{z}$. The solution of Eq. (3.7) gives the upstream residence time t^* of the particles, to be evaluated numerically.

The angles that identify the re-crossing direction, as functions of the residence time, are

$$\tilde{\mu}_1 = \tilde{\mu}_\circ \,, \qquad \text{and} \tag{3.8}$$

$$\tilde{\phi}_1 = \tilde{\phi}_\circ + \omega t^*(\tilde{\mu}_\circ, \tilde{\phi}_\circ) \,. \tag{3.9}$$

A rotation by the angle α provides us with the re-crossing coordinates μ_1 and ϕ_1 in the fluid frame. At this point the Jacobian in Eq. (3.2) can be calculated, although some care is needed because this Jacobian is not a single valued function: for each pair $(\mu_\circ, \mu)$ the Jacobian has two values. This degeneracy arises because of the substitution of $\phi_\circ$ with μ, since each μ corresponds in general to two possible values of $\phi_\circ$. This is clear from Fig. 3.2, where we show some examples of solutions: the directions of entrance and escape from the upstream fluid are plotted for different values of the shock speed and for different orientations of the large scale magnetic field.

Eq. (3.7) admits a solution $t^* > 0$ only if the two following conditions are fulfilled:

i) the initial velocity of a particle along the shock normal must be larger than the shock speed (otherwise the particle is prevented from crossing the shock to start with). This implies:

$$\mu_\circ < -\beta_s \,. \tag{3.10}$$

ii) The particle velocity along the shock normal has to be less than the shock speed, namely

$$\tilde{\mu}_\circ \cos\alpha > -\beta_s \,. \tag{3.11}$$

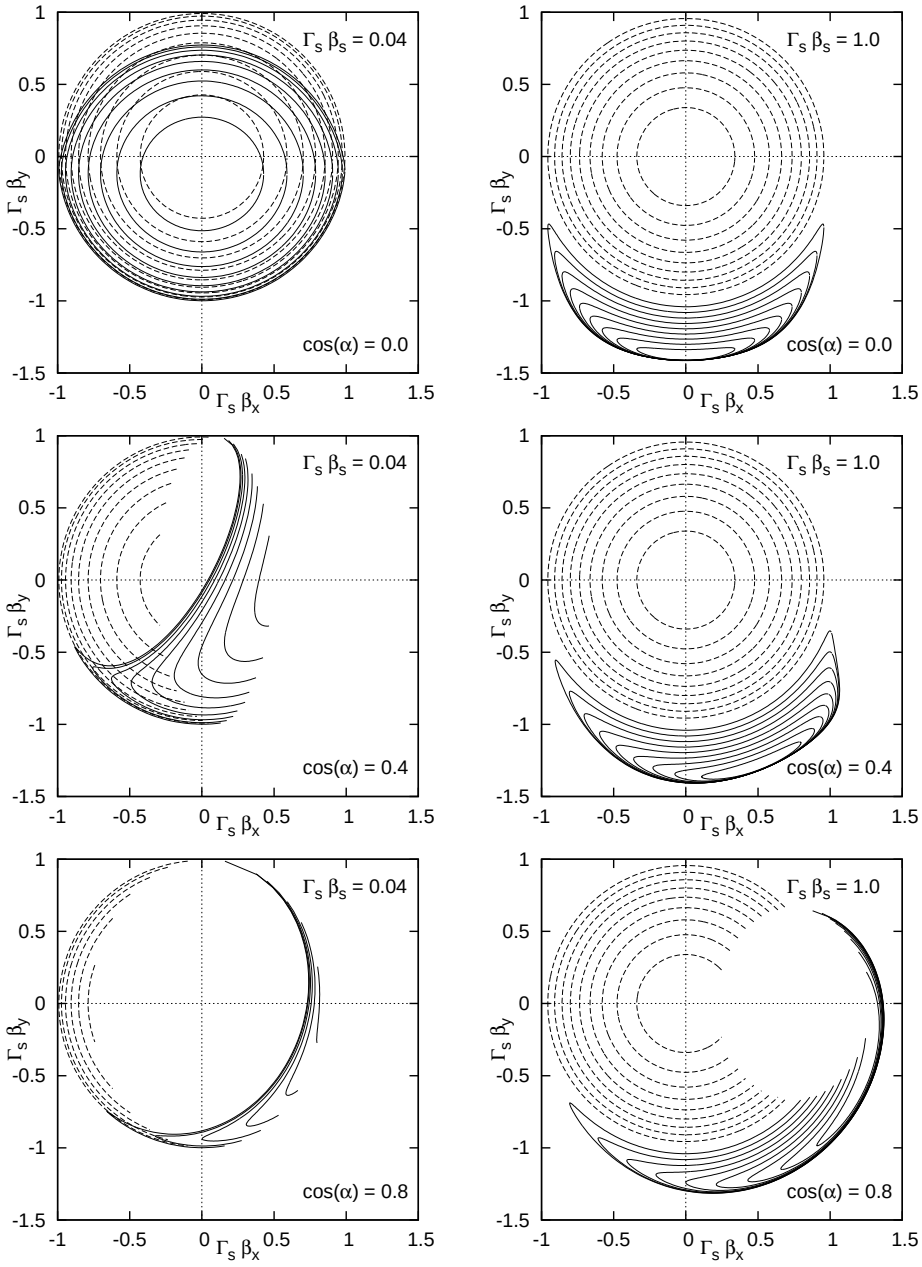

Fig. 3.2 Location of the particles entering the upstream region (dashed lines) and returning to the downstream region (solid lines) after being deflected by the magnetic field upstream. The directions are plotted in the plane $\Gamma_s\beta_{p,x}$ - $\Gamma_s\beta_{p,y}$. $\beta_{p,x}$ and $\beta_{p,y}$ are the components of the particle velocity along the x and the y axis respectively. The origin corresponds to particles entering along the shock normal. Circles correspond to particles having constant $\mu_\circ$. The left panels refer to $\Gamma_s\beta_s = 0.04$. The right panels refer to $\Gamma_s\beta_s = 1.0$. In both cases we show the effects of three different orientations of the magnetic field (from the top to the bottom $\cos\alpha = 0.0, 0.4, 0.8$). The presence of an empty region when $\cos\alpha > \beta_s$ is due to particle leakage from upstream [Compare with Fig.1 in Achterberg et al. (2001)].

Particles not satisfying this last condition escape the shock region towards upstream infinity, a situation which is not realized in the case of scattering considered in §2.2. This escape process occurs only for $\cos\alpha > -\beta_s$, and results in the loss of particles having the entrance pitch angles cosine exceeding $\mu_{\rm min}(\mu_\circ, \phi_\circ)$. In fact for $\cos\alpha < -\beta_s$, $\mu_{\rm min} = {\rm const} = -1$ and all particles eventually re-cross the shock.

When the particles are allowed to escape upstream, the acceleration is clearly expected to become less efficient and give rise to softer spectra of the accelerated particles (see §3.2.3).

Putting together all of the above, we can finally write the upstream conditional probability as

$$P_u(\mu_\circ, \mu) = \frac{1}{2\pi} \sum_{i=1,2} \left| \frac{\partial \phi_\circ}{\partial \mu} \right|_i \theta\left(-\mu_\circ - \beta_s\right) \, \theta\left(\mu_\circ - \mu_{\rm min}(\mu_\circ, \mu)\right) \,, \tag{3.12}$$

where the sum is extended over the two branches of the Jacobian.

For $\cos\alpha < -\beta_s$ the particles always return to the shock front and this forces the return probability to be unity when integrated over all outgoing directions:

$$\int_{-u}^{1} d\mu \, P_u(\mu_\circ, \mu) = 1 \,. \tag{3.13}$$

This integral condition is trivially satisfied by Eq. (3.12) and is used as a check for P_u after its numerical computation.

Figs. 3.3, 3.4 and 3.5 show some examples of our calculations of $P_u(\mu_\circ, \mu)$ as a function of μ for different values of $\mu_\circ$, for a Newtonian, a trans-relativistic and a relativistic shock respectively. For each case we show the results for different inclinations of the magnetic field with respect to the shock normal. It is worth noticing that P_u does not change significantly when the inclination of the magnetic field varies in the range $0 < \cos\alpha < \beta_s$, at a given shock speed. Therefore we do not expect a significant variation of the spectral slope in this range. In §3.2.3 we show that this is in fact the case.

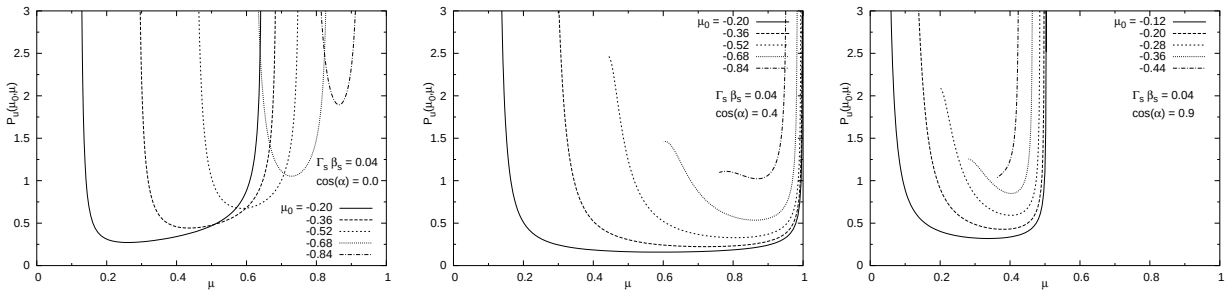

Fig. 3.3 Conditional probability $P_u(\mu_\circ, \mu)$ as a function of the outgoing direction μ, for a fixed value of the shock speed ($\Gamma_s\beta_s = 0.04$) with three different inclinations of the magnetic field ($\cos\alpha = 0.0, 0.4, 0.9$). For each plot the different lines correspond to different values of the ingoing direction $\mu_\circ$.

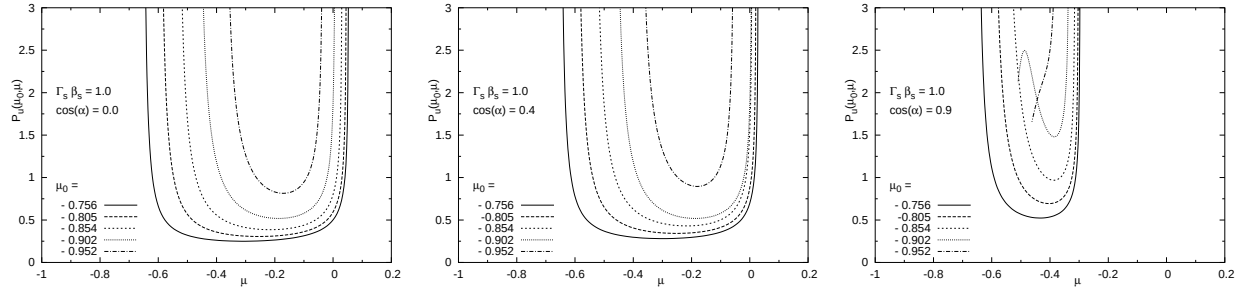

Fig. 3.4 Like Fig.3.3 but for a trans-relativistic shock ($\Gamma_s\beta_s = 1.0; \beta_s = 0.707$).

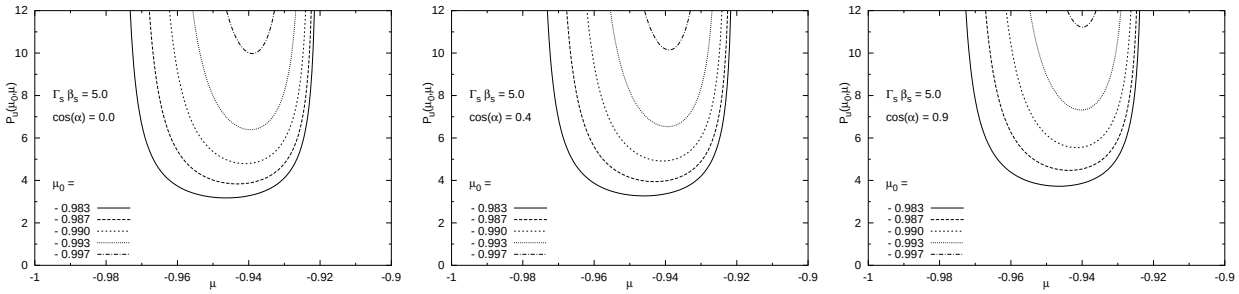

Fig. 3.5 Like Fig.3.3 but for a relativistic shock ($\Gamma_s\beta_s = 5.0; \beta_s = 0.98$). The three plots are very similar to each other because the condition $\cos\alpha > \beta_s$ is never reached.

3.2.3 Results for spectrum and angular distribution of the accelerated particles

In this section we use Eq. (2.6) and Eq. (2.7) to calculate the spectrum and angular distribution of the accelerated particles at the shock front. The return probabilities are calculated assuming that in the downstream fluid there is isotropic scattering, so that P_d can be calculated from Eq. (2.4) using Eq. (2.10) as a scattering function. We assume $\sigma = 0.01$ for the SPAS regime and $\sigma = 10$ for the LAS regime. In the upstream fluid we assume that particles can only be deflected by a large scale coherent magnetic field with arbitrary orientation with respect to the normal to the shock front. The return probability P_u is therefore calculated as discussed in detail in §3.2.2.

The only information still lacking to proceed further is an equation of state for the medium, that would allow us to compute the velocity of the downstream fluid from the jump conditions at the shock front (see for instance Gallant (2002)). We assume that the gas upstream has zero pressure. Moreover, in the following we assume everywhere that the magnetic field has no dynamical role, so that the standard jump conditions for an unmagnetized shock can be adopted (the role of the magnetic field becomes important

when the magnetic energy density becomes comparable with the thermal energy density Kirk & Duffy (1999)).

Following much of the previous literature, we adopt the Synge equation of state for the downstream gas Synge (1957), assuming that only protons contribute. Although used widely, this assumption may not be well justified in a general case. We will illustrate our conclusions on the role of the equation of state for the spectrum and anisotropy of the accelerated particles in a separate paper.

Within this set of assumptions it is worth reminding that the velocity ratio $r = u_{\rm up}/u_{\rm down}$ tends asymptotically to 4 for a non relativistic shock (even for shock speeds that are known to give lower compression factors) and to 3 for ultra-relativistic shocks.

The simplest case to consider is that of a shock in which the large scale coherent magnetic field in the upstream region is parallel to the shock front ($\cos\alpha = 0$). This is known as a perpendicular shock. The angular distribution and the slope of the spectrum of the accelerated particles are plotted in Fig. 3.6 (the LAS (SPAS) case is shown in the left (right) panel) and Fig. 3.7 respectively, for various shock velocities ranging from newtonian to relativistic.

Looking at Fig. 3.6 some comments are in order. First of all the angular distribution extends in the range $-1 < \mu < \mu_{\rm max}$. As seen in the upstream frame, $\mu_{\rm max}$ corresponds to particles that enter downstream after a deflection with initial coordinates $\tilde{\mu}_\circ = -\beta_s$ and $\tilde{\theta}_\circ = \pi/2$. We can easily estimate $\mu_{\rm max}$ in the limit of relativistic shock using Eq. (3.7). In the present case $\alpha = \theta_\circ = \pi/2$ and $\sin\phi_\circ = -1/\Gamma_s$, so Eq. (3.7) gives

$$\Gamma_s\beta_s = \frac{1-\cos\xi}{\xi-\sin\xi} \equiv f(\xi)\,, \tag{3.14}$$

where $\xi = \omega t$. Hight values of $\Gamma_s\beta_s$ correspond to small values of ξ, therefore we can use the first order Taylor expansion of f around zero: $f(\xi) = 3/\xi + O(\xi)$. Hence we get $\xi \simeq 3/\Gamma_s\beta_s$ and

$$\mu_{\rm max} = \cos(\xi + \tilde{\phi}_\circ) = \left(1 - 4/\Gamma_s^2\right)^{1/2}. \tag{3.15}$$

Finally this value can be expressed in the downstream reference frame

$$\mu'_{\rm max} = \frac{\mu_{\rm max} - v_{\rm rel}}{1 + \mu_{\rm max} v_{\rm rel}} \tag{3.16}$$

and with a little algebra one can see that $\mu'_{\rm max} \to 1/3$ for $\beta_s \to 1$, as can be seen from Fig. 3.6.

A second comment concerns the discontinuity that the angular distribution shows in passing from upstream to downstream sector. The jump can be easily understood looking at the panel in Fig. 3.2 with $\Gamma_s\beta_s = 1$ and $\cos(\alpha) = 0$: the biggest dashed circle represents the particle that enter upstream with the maximum allowed value $\mu_{\circ,max} = -\beta_s$; only a fraction of these particles, about one half, recross the shock with an angle infinitely close to $\mu_{\circ,max}$. This explain why the jump is roughly one half, and is located

at $\mu_{\circ,max}$ as appear in the downstream frame, *i. e.*

$$\mu'_{\circ,max} = \frac{-\beta_s + v_{rel}}{1 - \beta_s v_{rel}} = -\frac{\beta_s}{r}\,. \tag{3.17}$$

For relativistic shock $r \to 3$, and $\mu'_{\circ,max} \to -1/3$, as results from Fig. 3.6.

The last note concerns the anisotropy. The angular distribution of the particles in the downstream frame is seen to be rather anisotropic for the SPAS case, even in the newtonian regime. Large angle scattering (LAS) is evidently more efficient in isotropizing the accelerated particles. On the other hand, because the regular magnetic field deflection, the particles in the upstream section accumulate towards the maximum value μ_{max}.

The anisotropies do not seem to affect the spectrum of the accelerated particles in the case of non relativistic shocks: the slope of the spectrum for both SPAS and LAS is 4.000 ± 0.001. The effect becomes more prominent for faster shocks and in particular for relativistic shocks. In the SPAS case, for $\Gamma_s\beta_s = 10$, we found $s = 4.272 \pm 0.001$, compatible with $s = 4.28 \pm 0.01$, obtained by Achterberg et al. (2001) for $\Gamma_s = 10$, with a Monte-Carlo simulation.

In Fig. 3.7, the dotted and dashed lines refer to the SPAS and LAS cases respectively. At first sight it may appear rather surprising that in the limit of relativistic shocks the spectrum of accelerated particles is softer in the LAS regime than it is in the SPAS regime, since LAS is envisioned as more efficient in redirecting the particles to the shock front. This intuitive vision turns out to be incorrect, as also shown in Table 1, where we list the slope, the average energy gain and the return probability from downstream (as defined in Eqs. (3.20) and (3.23)) for a relativistic shock with $\Gamma_s\beta_s = 5.0$.

Table 3.1 Exact spectral slope, mean amplification and downstream return probability (as defined in eq. (3.20) and (3.23) respectively) for $\Gamma_s\beta_s = 5.0$.

	slope	$\langle G \rangle$	$\langle P_{\rm ret}^{\rm (down)} \rangle$
SPAS	4.218 ± 0.001	2.0387	0.4165
LAS	4.445 ± 0.001	2.0753	0.3430

One can see that while the average energy gain is similar in the two cases, the return probability in the case of LAS is 20% lower than for the SPAS case. Qualitatively this can be understood as follows: when the shock velocity increases, particles are caught up by the shock front when they have travelled only a small fraction (of order $1/\Gamma_s$) of their gyration. Once downstream, LAS is likely to swing them far from the shock front in a few interactions, while SPAS deflects their trajectories rather slowly yet remaining in the vicinity of the shock surface. This is responsible for the 20% difference in the average return probabilities in the two cases. This is also shown in Fig. 3.8, where we plot the particles flux, $J(\mu) \equiv |\mu + u_d| g(\mu)$ in terms of downstream coordinates: the total

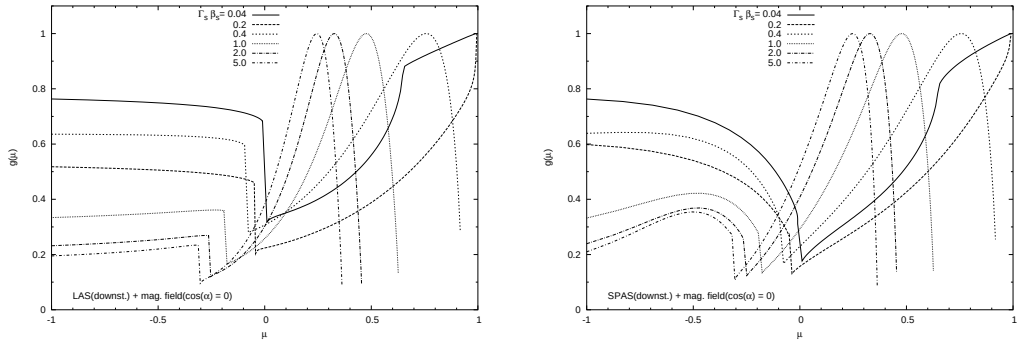

Fig. 3.6 Particle distribution function at the shock front when a large scale coherent magnetic field is present in the upstream region, with a direction parallel to the shock plane. In the downstream region particles are scattered in the LAS (left plot) or in the SPAS regime (right plot) (here the maximum of the distribution is arbitrarily set equal to 1). Several values of shock speeds are shown. The particle distribution functions always show a jump at $\mu = -\beta_s$. Large angle scattering makes distribution functions flatter compared with the small angle scattering case for $-1 < \mu < -u_d$.

flux of particles entering the downstream section ($-u_d < \mu < 1$) is normalized to unity. It is clear from Fig. 3.8 that the flux of particles returning to the shock is slightly larger for the case of SPAS (dashed line in the range $-1 < \mu < -u_d$).

A more interesting question concerns the effect of the orientation of the large scale magnetic field with respect to the normal to the shock. We have already emphasized that for any orientation different from that of a perpendicular shock, and in the absence of scattering processes upstream, particles are lost from the upstream region, because the shock cannot catch up with their motion. This happens when $\cos\alpha > -\beta_s$, so that the phenomenon is increasingly more important for shocks approaching the parallel configuration. This reflects in increasingly softer spectra. In the limit $\cos\alpha \to 1$, all particles escape from the upstream region and no acceleration takes place.

The slope of the spectrum as obtained from our calculations is plotted in Fig. 3.9 (solid lines and symbols) as a function of $\cos\alpha$ for three different shock speeds ($\Gamma_s\beta_s = 0.6, 1.0, 2.0$): when there is no particle escape, the slope s is actually a constant, while it increases dramatically (and in fact diverges, showing the disappearance of the acceleration process) for values of $\cos\alpha$ larger than $-\beta_s$. In the small panel in Fig. 3.9 we also plot the return probability from upstream: for very inclined shocks the return probability is still very close to unity, as in the case of upstream scattering, but it drops rapidly for increasingly less inclined shocks.

The steepening of the spectrum due to leakage of the particles towards upstream infinity can also be understood in terms of a Bell-like (Bell 1978a) calculation, when carried out for the case of a large scale coherent magnetic field. The slope of the spectrum is related to the average return probability and to the average energy gain of the particles per cycle back and forth through the shock front through the expression:

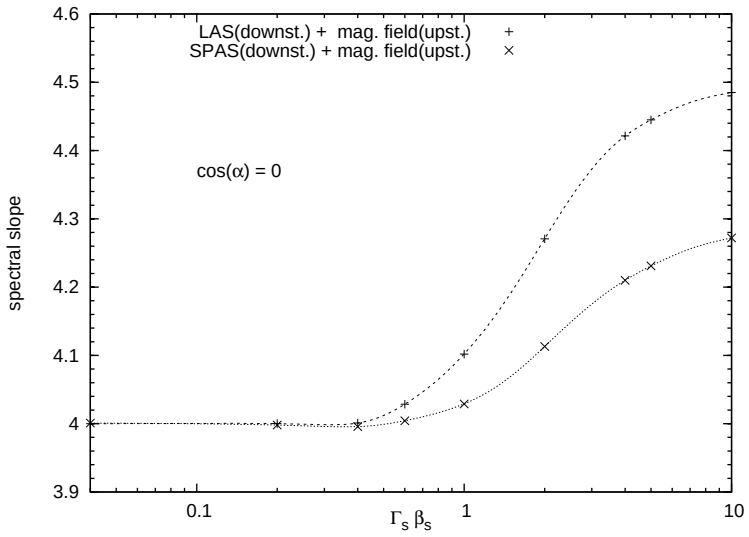

Fig. 3.7 Spectral index vs. shock speed for the same configuration as in Fig.3.6.

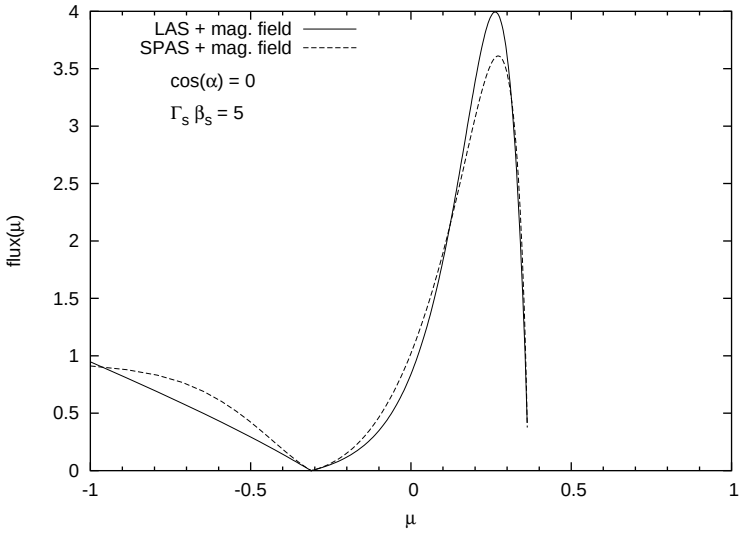

Fig. 3.8 Particle flux $J(\mu) \equiv |\mu + u_d| g(\mu)$ across the shock front, as it appears in the downstream frame, when the upstream magnetic field is parallel to the shock ($\cos\alpha = 0$) and the downstream fluid is in the LAS regime (solid line) or SPAS regime (dashed line). The shock speed is $\Gamma_s\beta_s = 5.0$. The flux entering downstream (*i.e.* for $-u_d < \mu < 1$) is normalised to 1. In this way we see that downstream return probability, *i.e.* the integrated flux for $-1 < \mu < -u_d$, is larger when the downstream region is in the SPAS regime.

$$s = 3 - \frac{\log\langle P_{\rm ret}\rangle}{\log\langle G\rangle}\,, \tag{3.18}$$

where $\langle G\rangle$ is the mean amplification in a single cycle (downstream $\rightarrow$ upstream $\rightarrow$ downstream), and $\langle P_{\rm ret}\rangle$ is the mean probability of returning to the shock. One should keep in mind that Bell's method, as expressed through the equation above is flawed in that it does not take into proper consideration the correlation between the amplification factor and the return probability. Moreover, Eq. (3.18) hides the assumption of isotropy of the distribution function of the accelerated particles, since that formula was conceived in a discussion of non relativistic shocks (Peacock (1981) introduced this formalism for particle acceleration at relativistic shock fronts). All these limitations become of particular importance for relativistic shocks. A general expression for the slope was found in Vietri (2003), and reads:

$$\langle P_{\rm ret}\rangle\langle G^{s-3}\rangle = 1. \tag{3.19}$$

In the following we use Eq. (3.18), since we only want to provide the reader with an argument of plausibility for the steepening of the spectra in those cases in which particle leakage can take place in the upstream region. In order to account for this leakage, which cannot take place in the standard scenario of diffusive particle acceleration at a shock front, we generalize Eq. (3.18) in order to include the probability of escape from the acceleration box from upstream. This is easily achieved by replacing $\langle P_{\rm ret}\rangle$ with $\langle P^{\rm (up)}_{\rm ret}\rangle \cdot \langle P^{\rm (down)}_{\rm ret}\rangle$. These mean values expressed in the downstream frame are:

$$\langle P^{\rm (down)}_{\rm ret}\rangle = \frac{\int_{-1}^{-u_d} d\mu_\circ \int_{-u_d}^{1} d\mu\, g(\mu)(u_d+\mu) P_d(\mu,\mu_\circ)}{\int_{-u_d}^{1} d\mu\, g(\mu)(u_d+\mu)} \tag{3.20}$$

and

$$\langle P^{\rm (up)}_{\rm ret}\rangle = \frac{\int_{-u_d}^{1} d\mu \int_{-1}^{-u_d} d\mu_\circ\, g(\mu_\circ)(u_d+\mu_\circ) P_u(\mu_\circ,\mu)}{\int_{-1}^{-u_d} d\mu_\circ\, g(\mu_\circ)(u_d+\mu_\circ)}\,. \tag{3.21}$$

In the last equation P_u has also to be computed in terms of quantities evaluated in the downstream frame. Energy amplification for a particle entering the upstream region with direction $\mu_\circ$ (as measured downstream) and returning with direction μ, is obtained combining two Lorentz transformations:

$$G(\mu_\circ,\mu) = \gamma^2_{\rm rel}(1-u_{\rm rel}\mu_\circ)\,\left(1+u_{\rm rel}\bar{\mu}\right)\,, \tag{3.22}$$

where $\bar{\mu} = (\mu+u_{\rm rel})/(1+u_{\rm rel}\mu)$ is the returning direction as seen in the upstream frame. Averaging the amplification we have:

$$\langle G\rangle = \frac{\int_{-1}^{-u} d\mu_\circ\, g(\mu_\circ)(u+\mu_\circ)\int_{-u}^{1} d\mu\, G(\mu_\circ,\mu) P_u(\mu_\circ,\mu)}{\int_{-1}^{-u} d\mu_\circ\, g(\mu_\circ)(u+\mu_\circ)\int_{-u}^{1} d\mu\, P_u(\mu_\circ,\mu)}\,. \tag{3.23}$$

The spectral slope as computed through Eq. (3.18) is plotted in Fig. 3.9 (large box) with dashed lines; the corresponding upstream return probability $\langle P_{\rm ret}^{(\rm up)} \rangle$ is plotted in the small box (dashed lines). The agreement with our exact results is better than 1%, proving that the reason for the softening of the spectra of accelerated particles is in the increased probability that the particles leave the acceleration region when only a large scale coherent magnetic field is present upstream.

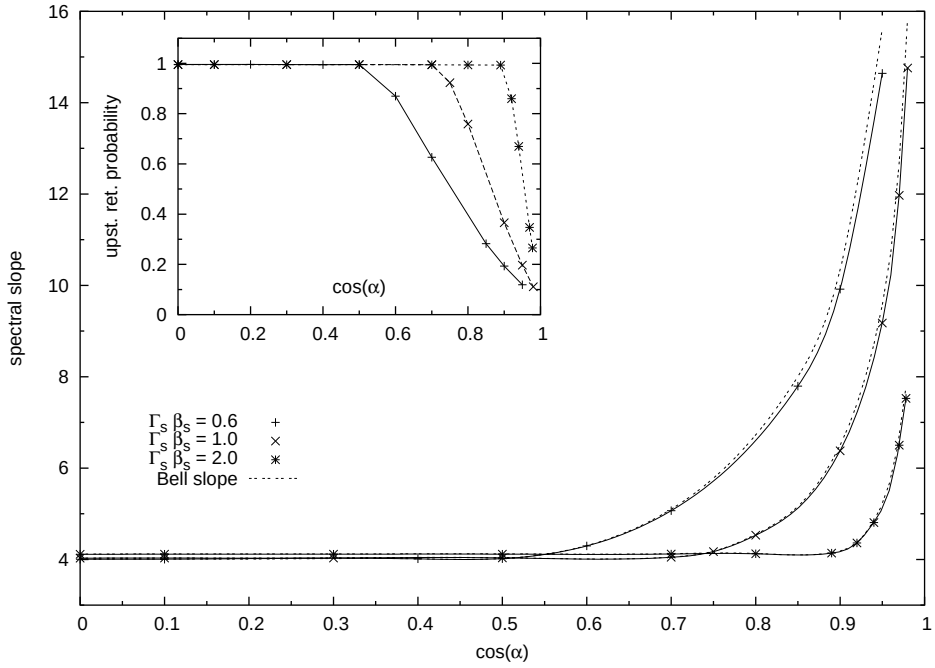

Fig. 3.9 *Large box*: spectral slope as a function of $\cos\alpha$ for three different values of the shock speed. The dashed lines show the spectral slope computed with Bell's method. *Small box*: the corresponding upstream return probabilities.

The results discussed above apply to situations in which the magnetic field in the upstream region can be considered as coherent on spatial scales exceeding the size of the acceleration box. If the coherence scale of the field is smaller than the size of the accelerator, then the direction of the particles suffer a random wandering motion and one can think of this structured field as the source of diffusion and as a physical mechanism that imposes a maximum energy to the accelerated particles (at least in the absence of radiative energy losses). Particles that escape from the shock region too fast (highest energy ones) have enough time to *feel* the effect of a coherent scale, while lower energy particles live in the accelerator for longer times and in principle may *feel* different orientations of the upstream magnetic field. This scenario is basically equivalent to having some degree of scattering upstream, and should be treated with the formalism

already discussed in Vietri (2003); Blasi & Vietri (2005). As soon as a phenomenon equivalent to scattering is present, the probability of escape to upstream infinity vanishes, for all those particles that are confined in the accelerator for sufficiently long times. Moreover, one should keep in mind that even if a large scale coherent magnetic field is present to start with, the propagation of the accelerated (charged) particles in the upstream plasma is very likely to excite fluctuations in the magnetic field structure through streaming instability Bell (1978a). These fluctuations act as scattering centers and enhance the probability of returning to the shock front.

3.3 Acceleration for shock propagating in a medium with anisotropic scattering properties

3.3.1 Anisotropic scattering: generality

In this section we consider again the standard case in which particle motion in both the upstream and downstream fluids is diffusive, due to the presence of scattering agents. However, we include the possibility that the scattering, though spatially constant, may be anisotropic. The physical motivation for this generalization is the following: in a background of Alfvèn waves with a power spectrum $P_{_W}(k)$ (such that $P_{_W}(k)dk$ is the energy density in the form of waves with wavenumber in the range dk around k) the particles suffer angular diffusion with a diffusion coefficient

$$D_{\theta\theta} = \langle \frac{\Delta\theta\Delta\theta}{\Delta t} \rangle \approx \Omega \frac{k_{_r} P_{_W}(k_{_r})}{B_0^2/8\pi}, \tag{3.24}$$

where $k_{_r} = \Omega/v\mu$ is the resonant wavenumber and Ω is the gyration frequency of particles with momentum p in the background magnetic field B_0. One can clearly see from Eq. (3.24) that the diffusion is anisotropic in general, unless the power spectrum has a specific *ad hoc* form. One should keep in mind that Eq. (3.24) is obtained in the context of quasi-linear theory. A full non-linear treatment might show how the turbulence is distributed and which is the resulting particle angular distribution.

In the calculations that follow, we quantify the effects of anisotropic scattering on the spectrum and angular distribution of the accelerated particles. The calculation of specific patterns of anisotropy in the scattering agents is beyond the scopes of this paper, therefore we adopt a few simple but physically meaningful toy models of anisotropic scattering and we carry out the calculations within those models.

3.3.2 Modeling anisotropy

We parametrize the anisotropy in such a way to reproduce the following four patterns:

- *case A*: Particles are scattered per unit length more efficiently while they move away from the shock front than they are on their way to the shock front, both upstream and downstream.

- *case B* (opposite of case *A*): Particles are scattered per unit length more efficiently on their way to the shock front than they are while they move away from the shock front, both upstream and downstream.

- *case C*: In the downstream fluid, particles are scattered per unit length more efficiently while they move away from the shock front ($\mu \to 1$) than they are on their way to the shock front ($\mu \to -1$). In the upstream fluid the situation is reversed, and scattering is more efficient for the particles that are moving toward of the shock ($\mu \to 1$).

- *case D* (opposite of *C*): Scattering is more effective around $\mu \sim -1$ both upstream and downstream.

A pictorial representation of cases *A*-*D* is shown in Fig. 3.10.

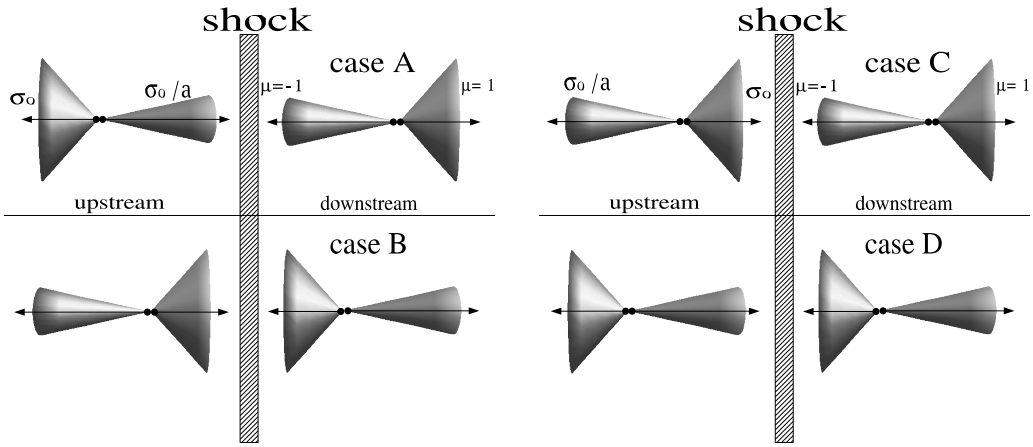

Fig. 3.10 Pictorial representation of the four patterns of anisotropic scattering considered in our calculations.

In order to simulate the cases A-D above, we adopt a scattering function similar to Eq. (2.10), but modified to introduce anisotropic scattering. In particular, to achieve this goal we allow the width σ of the scattering function to depend on both the initial and final directions $\mu^{'}$ and μ, so that:

$$w(\mu,\mu^{'}) = \frac{1}{\sigma(\mu,\mu^{'})} e^{-frac1-\mu\mu'\sigma(\mu,\mu')} I_0\left(\frac{\sqrt{1-\mu^2}\sqrt{1-\mu'^2}}{\sigma(\mu,\mu^{'})}\right) . \qquad (3.25)$$

It is worth stressing that the scattering function has to be symmetric if we exchange μ with $\mu^{'}$ as a consequence of Liouville's theorem, so we are forced to look for a symmetric function $\sigma(\mu,\mu^{'})$.

In order to apply the functional form Eq. (3.25) to the cases A-D, it is sufficient to adopt the following expression for the mean scattering angle $\sigma(\mu, \mu')$:

$$\sigma_{\mp}(\mu, \mu') = \sigma_{\circ} \cdot \left(1 - \frac{(a-1)}{4a}(\mu \mp 1)(\mu' \mp 1)\right) . \tag{3.26}$$

Both σ_{+} and σ_{-} have σ_0 as the maximum and $\sigma_{\circ}/a$ as the minimum value. For this reason we will refer to a as the *Anisotropy Factor*. For $a = 1$, isotropic scattering is recovered.

The resulting scattering function $w_{\mp}(\mu, \mu')$, obtained substituting Eq. (3.26) into (3.25), is plotted in Fig. 3.11 together with the isotropic scattering function (Eq. (2.10)), for $\sigma_{\circ} = 0.05$ and $a = 10$. These plots clarify how w_{+} and w_{-} can simulate a scattering more efficient in the $\mu = +1$ and $\mu = -1$ directions respectively.

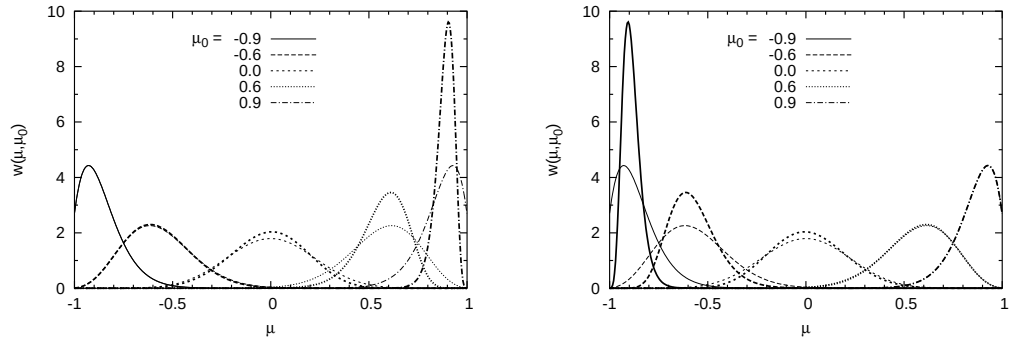

Fig. 3.11 The thick lines show the anisotropic scattering functions $w_{+}(\mu, \mu_{\circ})$ (left box) and $w_{-}(\mu, \mu_{\circ})$ (right box), as functions of μ and for different values of the incoming direction $\mu_{\circ}$. The anisotropy factor is $a = 10$ and $\sigma_{\circ} = 0.05$. For comparison the isotropic scattering function (Eq. (2.10)) is shown with thin lines and for the same values of $\mu_{\circ}$.

The condition $\int_{-1}^{1} d\mu\, w(\mu, \mu') = 1$ that states the probability conservation, is fulfilled by Eq. (3.25) provided $\sigma_0 \ll 1$. In the numerical calculations that follow we assume $\sigma_0 = 0.05$.

Using σ_{-} and σ_{+} in different combinations for the upstream and the downstream fluids, we can reproduce scenarios *A*, *B*, *C*, and *D*, as summarized in Table 3.2.

3.3.3 The particles' spectrum: results for shocks of arbitrary speed and fixed *anisotropy factor*

Following the procedure outlined in §2.2 and making use of Eqs. (3.25) and (3.26), we compute the spectral index and the angular distribution for the scenarios *A*, *B*, *C* and *D*, described above. In each case both the parameter $\sigma_{\circ}$ and the anisotropy factor a

Table 3.2 Summary of mean scattering angle used in the different scenario of Fig.3.10.

	A	B	C	D
upstream	σ_+	σ_-	σ_-	σ_+
downstream	σ_-	σ_+	σ_-	σ_+

are fixed ($\sigma_\circ = 0.05$ and $a = 10$), while the shock velocity is allowed to vary within the range $0.04 < \Gamma_s\beta_s < 5$.

The angular part of the distribution function is shown in Fig. 3.12 for all the four scenarios: A (left-upper panel), B (right-upper panel), C (left-lower panel) and D (right-lower panel). The slope of the spectrum of accelerated particles is plotted in Fig. 3.13.

For relativistic shocks, the spread in the slope of the spectrum of accelerated particles has less spread around ~ 4, although in general it remains true that harder spectra are obtained in the scenarios B and D.

A note of caution is necessary to interpret the apparent peak in the slopes at $\Gamma_s\beta_s \sim 1$ for cases A, and at $\Gamma_s\beta_s \sim 3$ for cases D. These peaks are completely unrelated to anisotropic scattering and is instead the result of the breaking of the regime of small pitch angle scattering (or SPAS), as was already pointed out in Blasi & Vietri (2005). The acceleration process does no longer take place in the SPAS regime when $\Gamma_s^2 \gtrsim 1/4\sigma$, which happens at higher Lorentz factor when σ is smaller. This is shown in Fig. 3.14, where we plot the slope for the case of isotropic SPAS for $\sigma = 0.1$ (dashed line) and $\sigma = 0.01$ (solid line), and the corresponding angular distribution for $\Gamma_s\beta_s = 5$. As already found in Blasi & Vietri (2005), the transition from SPAS to LAS is generally accompanied by a hardening of the spectra of accelerated particles. The peak seen in Fig. 3.13 is simply the consequence of an effective value of σ in the anisotropic scattering cases A and D. This is also clear comparing angular distributions of Fig. 3.14 with the angular distribution of cases A and D for $\Gamma_s\beta_s = 4$ and 5: the curves show the same behaviour with a jump at $\mu = -\beta_{\rm down}$ and a peak that moves towards $\mu = 1$ as the shock speed increase.

3.4 Discussion

In this chapter we carried out exact calculations of the angular distribution function and spectral slope of the particles accelerated at plane shock fronts moving with arbitrary velocity, generalizing a method previously described in detail in Vietri (2003); Blasi & Vietri (2005). In particular, we specialized our calculations to two situations: 1) presence of a large scale coherent magnetic field of arbitrary orientation with respect to the shock normal, in the upstream fluid; 2) possibility of anisotropic scattering in the upstream and downstream plasmas.

Our calculations allowed us to describe the importance of the inclination of the magnetic field when this has a large coherence length and there are no scattering agents upstream. For newtonian shocks, only quasi-perpendicular fields (namely perpendicular

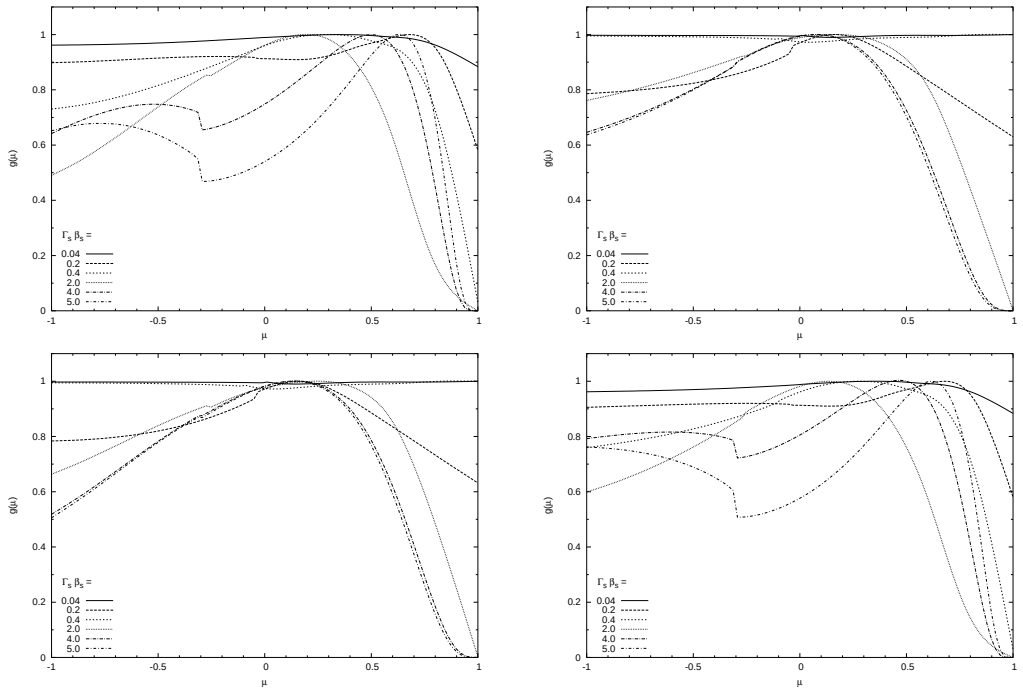

Fig. 3.12 Particle distribution function at the shock front for anisotropic scattering of type A (top-left), B (top-right), C (bottom-left) and D (bottom-right), all with $a = 10$. Each line represents a different shock speed as the labels show.

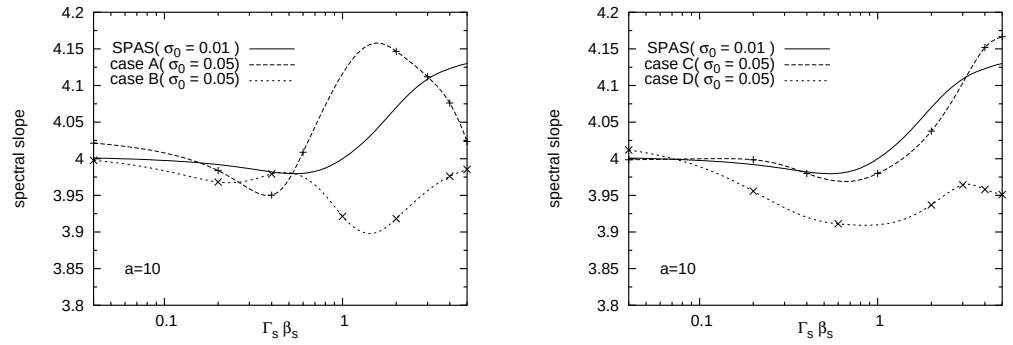

Fig. 3.13 Slope vs. shock speed in the four different anisotropic scattering scenarios: A and B in the left box, C and D in the right one. All plots are obtained with $a = 10$ and $\sigma_0 = 0.05$. Slope resulting from isotropic scattering (computed with $\sigma = 0.01$) is also shown for comparison (solid line).

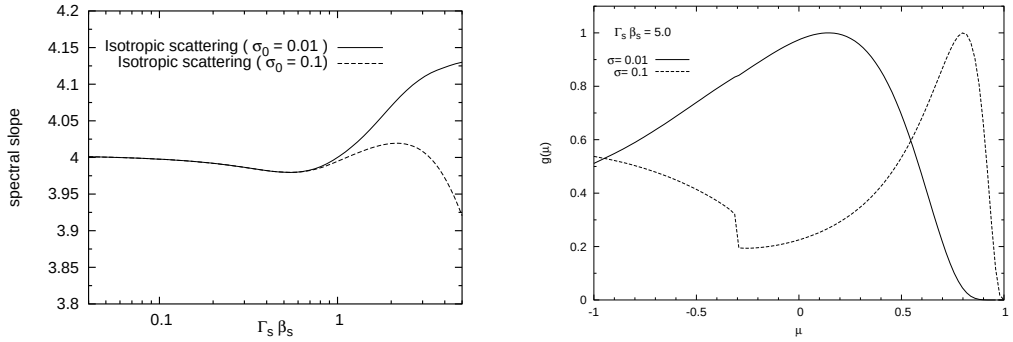

Fig. 3.14 These plots show the breaking of the SPAS approximation. *Left box:* slope of the spectrum of accelerated particles in the case of isotropic scattering with $\sigma = 0.01$ (solid line) and $\sigma = 0.1$ (dashed line). *Right box:* angular distribution for $\Gamma_s\beta_s = 5$ with $\sigma = 0.01$ (solid line) and $\sigma = 0.1$ (dashed line).

to the shock normal) are of practical importance, in that the return of particles to the shock from the upstream section is warranted. Quasi-parallel shocks imply a very low probability of return, so that the spectrum of accelerated particles is extremely soft. The process of acceleration eventually shuts off for parallel shocks. For relativistic shocks, the situation is less pessimistic because the accelerated particles and the shock front move with comparable velocities in the upstream frame. In general, the acceleration stops being efficient when the cosine of the inclination angle α of the magnetic field with respect to the shock normal is comparable with the shock speed in units of the speed of light. The slope of the spectrum of accelerated particles for $\cos\alpha = 0$ as a function of the shock velocity is plotted in Fig. 3.7 for the two cases in which SPAS or LAS is operating in the downstream plasma. The slope as a function of $\cos\alpha = 0$ for shocks moving at different speeds is shown in Fig. 3.9. In the same figure we also show the return probability from the upstream section, in order to emphasize that the presence of a large scale magnetic field upstream leads to particle leakage to upstream infinity. This latter phenomenon disappears when scattering is present, in that scattering always allows for the shock to reach the accelerated particles. In this case the probability of returning to the shock at an arbitrary direction is unity. One can ask when and how the transition from a situation in which there is no scattering to one in which scattering is at work takes place. When some scattering is present but the energy density in the scattering agents (e.g. Alfvèn waves) is very low compared with the energy density in the background magnetic field, only very low energy particles are effectively scattered. When their energy becomes large enough, they only feel the presence of the coherent field. Increasing the amount of scattering, this transition energy becomes gradually higher. Particles whose Larmor radius is larger that the coherence scale of the magnetic field can eventually escape the accelerator. In general the level of turbulence (and therefore of scattering) and the number of accelerated particles are not independent since the turbulence may be self-generated through streaming-like instabilities Bell (1978a).

In §3.3 we extended our analysis to the very interesting case of anisotropic scattering in both the upstream (unshocked) and downstream (shocked) medium. The pattern of anisotropy, which clearly depends on the details of the formation and development of the scattering centers, has been parametrized in four different scenarios, and for each one we calculated the angular part of the distribution function and the spectrum of the accelerated particles. Deviations from the predictions obtained in the context of isotropic SPAS and LAS have been quantified: the typical magnitude of these deflections is a few percent, but there are situations in which the deviation is more interesting, in particular because it goes in the direction of making spectra harder.

Chapter 4

The role of the plasma equation of state

4.1 Introduction

Chapter 3 is dedicated to the analysis of the spectrum of particles accelerated at relativistic shock with respect to the diffusive properties of the shocked and un-shocked plasmas. In the contest of test-particle theory, besides the scattering properties, the second important quantity that determines the slope of the particle spectrum is the fluid velocity jump at the shock discontinuity. This quantity strongly depends upon the fluid equation of state. In Chapter 3 we assume a relation between upstream and downstream fluid velocities as results from considering the shocked plasma as a simple monoatomic gas. No interaction between ions and electrons are assumed, besides the simple Coulomb scattering. Moreover the turbulent magnetic field play no role in the plasma equation of state, and no energy losses are considered. A more realistic plasma equation of state has to take into account these contributions. The aim of this chapter is to determine the changes to the spectral index of the accelerated particles, taking into account the possibility that different physical situations may change the equation of state of the plasma downstream of the shock. In particular collective plasma effects in the proximity of a collisionless shock may be responsible for different levels of thermalization of the electron and proton gas components behind the shock. These effects are expected to provide a channel of energy transfer from protons to electrons (see for example Begelman & Chiueh (1988); Hoshino et al. (1992); Gallant et al. (1992)) though not through particle-particle collisions. Other collective processes might result in the generation of a downstream turbolent magnetic field, which in turn may change the equation of state of the downstream fluid. We describe these effects in a phenomenological way, by introducing a parametrization of the energy exchange between electrons, protons and magnetic field energy densities in the downstream plasma, and we use such parametrization to infer the changes in the equation of state and the spectral slope of the particles accelerated at the shock front.

As a result of our calculations, we found several instances of violation of the so-called universality of the spectrum in both the newtonian and the trans-relativistic regimes.

The outline of this Chapter is the following: in §4.2 we remember the relativistic jump conditions for a strong plane shock wave propagating in a generic fluid. In §4.3 we introduce a new proton-electron plasma equation of state, adding to the classical Synge equation two contributions: *(i)* possibility of energy transfer from protons to electrons by collective plasma mechanisms and *(ii)* generation of a turbulent magnetic field (while the consequence of an upstream coherent magnetic field will be discussed in the Appendix A.2). We solve the jump conditions applying this new equation to downstream plasma

obtaining the downstream fluid velocity as a function of the upstream one. In §4.4 we show the results for the accelerated particles spectral slope computed using the new plasma equation of state. We summarize and discute the results in §4.5.

4.2 Relativistic jump conditions for strong shocks

The jump conditions describing the conservation of mass, momentum and energy across a shock front moving with velocity $V_{sh} = \beta_{sh} c$ in a medium with density n_1, pressure p_1 and energy density ϵ_1 are as follows (*e.g.* Kirk & Duffy (1999); Gallant (2002)):

$$\begin{aligned} \Gamma_1 \beta_1 n_1 &= \Gamma_2 \beta_2 n_2 && (4.1)\\ \Gamma_1^2 \beta_1 (\epsilon_1 + p_1) &= \Gamma_2^2 \beta_2 (\epsilon_2 + p_2) && (4.2)\\ \Gamma_1^2 \beta_1^2 (\epsilon_1 + p_1) + p_1 &= \Gamma_2^2 \beta_2^2 (\epsilon_2 + p_2) + p_2 \,. && (4.3) \end{aligned}$$

Number densities (n), pressures (p) and energy densities (ϵ) are all measured in the comoving frame of the plasma they refer to, while the Lorentz factor Γ_1 (Γ_2) of the upstream (downstream) plasma are measured in the shock frame (clearly $\Gamma_1 = \Gamma_{sh} = (1 - \beta_{sh}^2)^{-1/2}$). The indexes '1' and '2' refer to the upstream and downstream plasmas respectively.

The equations above can be easily generalized to the case of presence of non negligible magnetic fields upstream, but in the following we shall assume that the dynamical role of such fields is always fully negligible, and shall therefore ignore the corrections in the conservation equations.

The system of equations Eqs. (4.1)-(4.3) can be solved once an equation of state for the plasma has been fixed, in the very general form $\epsilon = \epsilon(n, p)$. For simplicity, in the following we shall limit ourselves with the case of strong shocks, namely shock waves propagating in cold pressureless media, so that $p_1 = 0$ and $\epsilon_1 \simeq n_1 m c^2 \equiv \rho_1 c^2$. In this framework Eqs. (4.2) and (4.3) become:

$$\begin{aligned} \Gamma_1^2 \beta_1 \rho_1 c^2 &= \Gamma_2^2 \beta_2 (\epsilon_2 + p_2) \qquad \text{and} && (4.4)\\ \Gamma_1^2 \beta_1^2 \rho_1 c^2 &= \Gamma_2^2 \beta_2^2 (\epsilon_2 + p_2) + p_2 \,. && (4.5) \end{aligned}$$

We assume that the equation of state has the form $\epsilon_2 = \rho_2 c^2 F(p_2/\rho_2 c^2)$, or in terms of the normalized variables $\bar{p}_2 = \frac{p_2}{\rho_2 c^2}$ and $\bar{\epsilon}_2 = \epsilon_2 / \rho_2 c^2$:

$$\bar{\epsilon}_2 = F(\bar{p}_2). \tag{4.6}$$

Most cases of astrophysical interest are well described by this functional form for the equation of state of the downstream gas, as discussed in Sec. 4.3.

Using the equation of mass conservation, Eq. (4.1), Eq. (4.4) becomes

$$\Gamma_2 = \Gamma_1 / (\bar{\epsilon}_2(\bar{p}_2) + \bar{p}_2) \equiv g_1(\bar{p}_2), \tag{4.7}$$

while from (4.5) we have

$$\Gamma_2^2 = (\bar{\epsilon}_2^2 - 1)/(\bar{\epsilon}_2(\bar{p}_2)^2 - \bar{p}_2^2 - 1) \equiv g_2^2(\bar{p}_2)\,. \tag{4.8}$$

The solution for $\bar{p}_2$ can be obtained solving numerically the equation $g_1(\bar{p}_2) = g_2(\bar{p}_2)$. Once $\bar{p}_2$ is known, the equation of state gives $\bar{\epsilon}_2$ while Eq. (4.7), or equivalently Eq. (4.8), gives Γ_2. Finally Eq. (4.1) gives the number density n_2. At this point it is also easy to determine the velocity jump and the shock $r_\beta = \beta_1/\beta_2$, which is a crucial parameter for the description of the process of particle acceleration at the shock front.

4.3 Equations of state for the downstream plasma

In this section we consider several instances of equations of state for the downstream gas, in addition to the well known and widely used Synge equation of state Synge (1957). In §4.3.1 we discuss the case of a downstream plasma made of two independent particle species that may thermalize to different temperatures. In §4.3.2 we introduce the possibility that the the proton and electron components are coupled in a collisionless way. In §4.3.3 we discuss the modification of the equation of state due to generation of a turbulent magnetic field in the downstream plasma. Finally in §4.3.4 we make an attempt to consider the most general case in which all the effects described above are taken into account.

4.3.1 The case of a plasma with independent particle species

An equation of state which is widely used in the literature was introduced by Synge (1957). The basic assumption is that the plasma consists of a single component with temperature T, and

$$\epsilon + p = \rho c^2\, G\left(mc^2/k_{\rm B}T\right) \tag{4.9}$$

where $G(x) = K_3(x)/K_2(x)$ and K_2, K_3 are the modified Bessel functions. For $x \gg 1$ (*i.e.* $k_{\rm B}T \ll mc^2$) Eq. (4.9) reduces to the classical Newtonian equation of state, $\epsilon = \rho mc^2 + 3p/2$, while in the opposite limit $x \ll 1$ (*i.e.* $k_{\rm B}T \gg mc^2$) the ultra-relativistic equation of state is recovered, $\epsilon = 3p$.

If the downstream plasma can be well described as an ideal gas ($p = nk_{\rm B}T$) made of a single component, Eq. (4.9) can be rewritten in terms of the normalized variables introduced in the previous section:

$$\bar{\epsilon} = G\,(1/\bar{p}) - \bar{p}, \tag{4.10}$$

which has the functional form assumed in §4.3 with $F(\bar{p}) = G\,(1/\bar{p}) - \bar{p}$. The Synge equation of state describes correctly the behaviour of the plasma in the ultra-relativistic and newtonian limits: applying the procedure illustrated in §4.2 we easily find the velocity jump r_β, which is plotted as a solid line in Fig. 4.1, as a function of the product $\Gamma_{sh}\beta_{sh}$. In the case of strong Newtonian shocks the well known result $r_\beta = 4$ is recovered. In the limit of an ultra-relativistic shock, when the downstream fluid obeys the ultra-relativistic equation of state for the gas, $r_\beta = 3$.

The generalization of the Synge equation of state to the case of two (or more) independent particle species with temperatures T_i is rather straightforward. Of particular interest is the case in which the temperature of the $i-$th species is simply due to the isotropization of the velocity vectors at the shock surface. In this case the energy density of the $i-$th species in the downstream plasma can be written as $\epsilon_{2(i)} = \Gamma_{\rm rel} n_i m_i c^2$, or, in terms of dimensionless variables:

$$\bar{\epsilon}_{2(i)} = \Gamma_{\rm rel}, \tag{4.11}$$

independent of the type of particles. Since the normalized energy density is the same for all species, the normalized pressures need to be the same too. It follows immediately that for the system as a whole one can write:

$$\bar{\epsilon}_{\rm T} + \bar{p}_{\rm T} = \frac{1}{\rho_{\rm T} c^2} \sum_i \rho_i c^2 \, G\left(m_i c^2 / k_{\rm B} T_i\right) = G(1/\bar{p}_{\rm T}) \,, \tag{4.12}$$

where the total quantities have the subscript $_T$.

4.3.2 Coupling between thermal protons and thermal electrons

The formation of collisionless shocks, both in the relativistic and newtonian regime still represents a subject of active investigation, in that the mechanisms that allow for an efficient transport of information among the particles in the plasma through the exchange of MHD waves are poorly known. On the other hand we know that such shocks do exist, which can be interpreted as an indirect proof of the importance of collective effects in collisionless plasmas. The same type of effects may also be responsible for total or partial thermalization of the different components of a plasma. Whether electrons and protons downstream of the shock front are in thermal equilibrium or not is a matter of debate. Most likely the answer depends on the specific conditions behind the shock of interest. In addition to the thermalization of the species, there are several other problems related to our ignorance of the complex physics that rules these effects: for instance even the spectrum of the *thermal* distribution of protons (and respectively of electrons) may not be a typical Maxwellian, in particular if a background magnetic field makes the distribution of energy in the waves anisotropic. In these conditions one should probably introduce a plasma temperature along the field and perpendicular to it. The problem of the thermalization of the plasmas around collisionless shocks is also related to the issue of the *thickness* of a collisionless shock, which is usually assumed to be of the order of the gyration radius of the thermal proton component. The same collective effects also determine the efficiency of injection of particles in the acceleration cycle: it appears intuitively clear that in a collisionless shock the processes of thermalization and particle acceleration to non-thermal energies are intimately related to each other.

Lacking a true theory of collisionless energy transport, we adopt here a phenomenological approach in that we parametrize the degree of equilibration between electron and proton temperatures in the downstream region by introducing a parameter ξ_e, such that the temperatures of electrons and protons satisfy the relation $T_e = \xi_e T_p$. On very general grounds we expect $\xi_e < 1$, at least close to the shock, before any collisional

effects may possibly equilibrate the two temperatures where the plasma has moved away from the shock front.

If we assume that the electron and proton gas separately behave as perfect fluids, the pressures of the two components are related through $p_e = nk_{\rm B}T_e = \xi_e p_p$. The equations of state of electrons and protons are easily found to be

$$\bar{\epsilon}_p = \bar{\rho}_p\, G\left(\frac{\bar{\rho}_p}{\bar{p}_p}\right) - \bar{p}_p \tag{4.13}$$

$$\bar{\epsilon}_e = \bar{\rho}_e\, G\left(\frac{\bar{\rho}_e}{\xi_e \bar{p}_p}\right) - \xi_e \bar{p}_p\,. \tag{4.14}$$

Here all the normalized quantities refer to the total matter density, namely $\bar{x} = x/n(m_e + m_p)c^2$. In order to solve the equations for the jump conditions at the shock surface we also need the total normalized energy densities and pressures:

$$\bar{\epsilon}_{\rm T}(\bar{p}_p) = \bar{\epsilon}_p(\bar{p}_p) + \bar{\epsilon}_e(\bar{p}_p) \tag{4.15}$$

$$\bar{p}_{\rm T}(\bar{p}_p) = \bar{p}_p(1+\xi_e)\,. \tag{4.16}$$

We found the appropriate solutions for the jump conditions for several values of the parameter ξ_e in the range $m_e/m_p \le \xi_e \le 1$. Fig. 4.1 shows the velocity ratio r_β as a function of the product $\Gamma_{sh}\beta_{sh}$ for $\xi_e = m_e/m_p$, 0.1, 0.3, 0.5, 1 and ∞. The case considered in section 4.3.1 corresponds to $\xi_e = m_e/m_p$, while $\xi_e = 1$ represents the limit case with protons and electrons thermalized at the same temperature.

The most peculiar feature of the curves plotted in Fig. 4.1 is the presence of a peak approximately at the place where the shock becomes trans-relativistic. The nature of this peak and the phenomenological implications of its presence are rather interesting. In order to understand the origin of the peak we consider the unphysical case $\xi_e = \infty$, which corresponds to completely cold ions in the downstream plasma. For all curves in Fig. 4.1 we can clearly identify three regimes: 1) both electrons and protons downstream are non-relativistic; 2) electrons are relativistic while protons are still non-relativistic; 3) both electrons and protons are relativistic.

The case $\xi_e = m_e/m_p$ (or equivalently $\xi_e \approx 0$) is the case that is usually studied in the literature. In the limit of non relativistic strong shocks this case leads to compression factor that asymptotically approaches 4. The derivative of the compression factor with respect to β_{sh} in this non relativistic regime is zero, as can be shown by using the Taub conditions Eqs. (4.1)-(4.3) (or equivalently, and more easily, the non relativistic version, the Rankine-Hugoniot jump conditions). On the other hand, if one expands the function $G(x)$ in the equation of state of electrons to second order in the variable $1/x$ (*i.e.* for mildly relativistic temperature), keeping the protons non relativistic, the resulting total

equation of state reads

$$\bar{\epsilon}_T = 1 + \frac{3}{2}\,\bar{p}_T + \frac{15}{8}\,\frac{\xi_e^2}{(1+\xi_e)^2}\,\frac{1}{\bar{\rho}_e}\,\bar{p}_T^{\,2}\,. \tag{4.17}$$

It is easy to show that the Rankine-Hugoniot relations give now a compression factor with a positive derivative with respect to β_{sh}, for small values of β_{sh}. Moreover the asymptotic value of r_β for ultra-relativistic shocks is always 3. This implies that at some point in between the compression factor has a peak where the derivative is zero and the compression factor is maximum. This is clearly seen in Fig. 4.1: in the trans-relativistic regime, electrons become relativistic downstream before protons do (and even if the shock is not fully relativistic) thereby making the downstream fluid more compressive. To show that this is the correct interpretation, one can estimates the value of r_β at the peak using the equation of state for non relativistic protons ($\epsilon_p = \rho_p c^2 + 3p_p/2$) and fully relativistic electrons ($\epsilon_e = 3p_e$). Under this assumption the total normalized energy reads

$$\bar{\epsilon}_T = \bar{\rho}_p + \frac{3}{2}\,\frac{1+2\xi_e}{1+\xi_e}\,\bar{p}_T\,. \tag{4.18}$$

Inserting this equation in the Rankine-Hugoniot relations one obtains the following expression for the compression ratio:

$$r_\beta = \frac{4+7\,\xi_e}{1+\,\xi_e}\,. \tag{4.19}$$

Substituting ξ_e with the values listed in Fig. (4.1), one recovers values of the compression factor close to that of the peaks within an error $\lesssim 4\%$.

4.3.3 Turbulent magnetic field production

It is interesting to investigate the possibility that part of the ram pressure of the upstream fluid may be converted into a turbulent magnetic field in the downstream region. We remember that the collisionless shock theory needs the presence of a strong magnetic turbulence within the shock layer, capable to randomize the bulk motion of the upstream particles. A possible way to produce such a turbulence is by a two-stream magnetic instability (see Medvedev & Loeb (1999) and Rossi & Rees (2003) for a discussion). This turbulence is in turn absorbed by the randomized particles themselves, but a fraction of magnetic energy can survive also far from the shock layer. Using numerical simulation Frederiksen et al. (2004) showed that for relativistic shock this is indeed the case[1].

Here we investigate this scenario and in particular we calculate the compression factor at the shock and the spectrum of the accelerated particles. In order to take into account the dynamical effect of the turbulent magnetic field it is necessary to generalize

[1]The problem of such numerical simulations is that is very difficult to follows the fluid's evolution far from the shock, hence this question remains open.

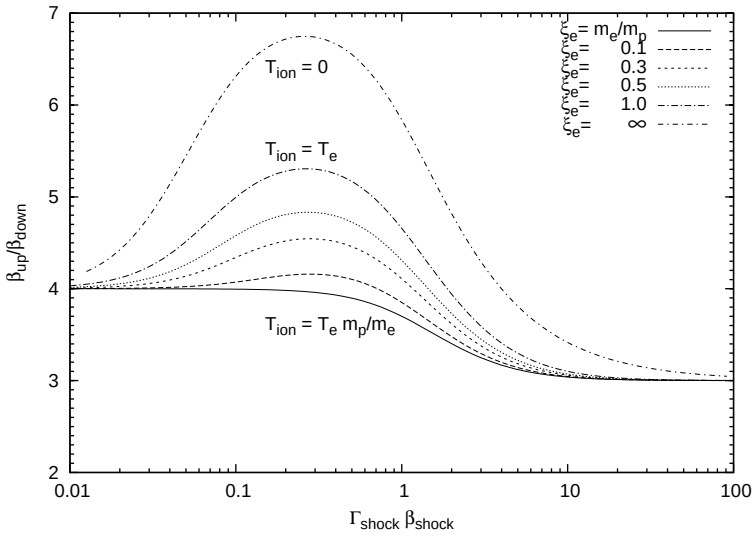

Fig. 4.1 Velocity compression factor at the shock when the downstream protons transfer a fraction ξ_e of their thermal energy to electrons.

the Taub conditions at the shock, (4.2)-(4.3), by introducing the proper components of the electromagnetic stress tensor $T^{\mu\nu}$. The specific energy density in the form of turbulent magnetic field is $\epsilon_m = T^{00}$ while the pressure in the direction identified by the index i is $p_{m,i} = T^{ii}$.

In the plasma reference frame, where no electric field is present, the electromagnetic energy tensor can be written as follows:

$$T^{\mu\nu} = \frac{1}{4\pi}\left(F^{\mu\alpha}F^{\nu}_{\alpha} - \eta^{\mu\nu}F^{\alpha\beta}F_{\alpha\beta}\right) = -\frac{1}{4\pi}\left(B^{\mu}B^{\nu} - \frac{1}{2}B^2\eta^{\mu\nu}\right) . \tag{4.20}$$

Here $B^{\mu} = (0, \mathbf{B})$ and $B^2 = B^2_x + B^2_y + B^2_z$. To be included in Eqs. (4.2)-(4.3) $T^{\mu\nu}$ has to be expressed in the shock frame, where both the scaler B and the field component along the propagation direction B_x remain unchanged. Hence the energy density and the pressure along the shock propagation direction are

$$\epsilon_m = (B^2_x + B^2_y + B^2_z)/8\pi\,, \tag{4.21}$$

$$p_{m,x} = (-B^2_x + B^2_y + B^2_z)/8\pi\,. \tag{4.22}$$

Two situations may be of interest here: 1) the turbulent field is created directly behind the shock. In this case the strength of the field is equally distributed among the three spatial dimensions. 2) the turbulent field downstream results from the compression of a turbulent field upstream. In this second case the two components of the field which are perpendicular to the shock normal are amplified at the shock while the parallel

component is left unaltered. In the former case the relation between energy density and pressure is easily obtained to be

$$p_m = \epsilon_m/3\,, \tag{4.23}$$

where the factor 1/3 suggests that the magnetic field behaves like a relativistic gas irrespective of the shock speed. On the other hand, in the latter case, if the shock is ultra-relativistic, the parallel component of the turbulent magnetic field is negligible with respect to the perpendicular components due to the shock compression. If the parallel component is neglected, the relation between energy and pressure of the magnetic field is easily obtained to be $p_m = \epsilon_m$.

In the following we limit ourselves with the case $p_m = \epsilon_m/3$, but we discuss the case $p_m = \epsilon_m$ in Sec. 4.4.

If ξ_m is the fraction of magnetic energy density with respect to the proton kinetic energy density, we can write

$$\bar{\epsilon}_m = \xi_m\,(\bar{\epsilon}_p - \bar{\rho}_p)\,. \tag{4.24}$$

When the magnetic energy equals the kinetic energy of protons, the magnetic pressure is smaller than that of protons in the Newtonian limit. On the other hand the two pressures become equal in the ultra-relativistic limit. It follows that we expect the compression ratio to increase in the Newtonian limit as the magnetic contribution increases, while the compression factor levels off when the relativistic regime is approached. The total downstream equation of state when only protons and a turbulent magnetic field are taken into account is:

$$\bar{\epsilon}_{\rm T} = \bar{\epsilon}_p + \bar{\epsilon}_m = \bar{\epsilon}_p(1+\xi_m) - \xi_m\bar{\rho}_p\,. \tag{4.25}$$

Fig. 4.2 shows the compression factor r_β for this situation, for several values of ξ_m, in the range $0 < \xi_m < 1$. The velocity compression factor ranges from 5.0 in the Newtonian limit to 3.0 in the ultra-relativistic limit, when protons and the magnetic field are considered in equipartition (*i.e.* $\xi_m = 1$).

4.3.4 The general case

As a natural conclusion of our exercise, we consider now the case of an electron-proton plasma with all the effects introduced above. The total energy of the system is given by the sum of the Eqs. (4.13), (4.14) and (4.24). The total pressure is the sum of

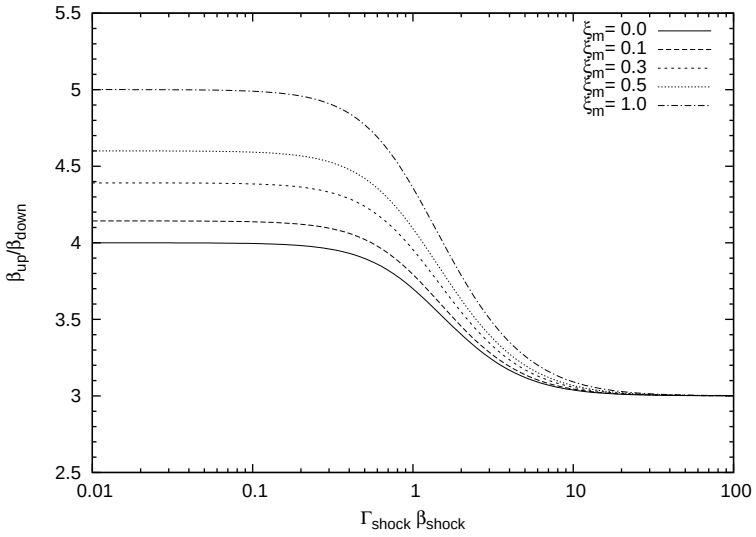

Fig. 4.2 Velocity compression factor at the shock when a turbulent magnetic field is present inside the electron-proton plasma, and ξ_m is the fraction of magnetic field energy density with respect to the protons kinetic energy.

the three contributions due to protons, electrons and magnetic pressure. We can write:

$$\begin{aligned}
\bar{\epsilon}_{\rm T}(\bar{p}_p) &= \bar{\epsilon}_p + \bar{\epsilon}_e + \bar{\epsilon}_m \\
&= \bar{\epsilon}_p(1+\xi_m) + \bar{\epsilon}_e - \bar{\rho}_p\xi_m \\
&= (1+\xi_m)\bar{\rho}_p\, G\left(\frac{\bar{\rho}_p}{\bar{p}_p}\right) + \bar{\rho}_e\, G\left(\frac{\bar{\rho}_e}{\xi_e\bar{p}_p}\right) \\
&\quad -\bar{p}_p(1+\xi_m+\xi_e) - \bar{\rho}_p\xi_m\,, \qquad (4.26) \\
\bar{p}_{\rm T}(\bar{p}_p) &= \bar{p}_p + \bar{p}_e + \bar{p}_m \\
&= \bar{p}_p\left(1+\xi_e-\frac{\xi_m}{3}\right) + \frac{\xi_m}{3}\bar{\rho}_p\left[G\left(\frac{\bar{\rho}_p}{\bar{p}_p}\right)-1\right], \qquad (4.27)
\end{aligned}$$

where we also introduced the proton and electron normalized densities $\bar{\rho}_p = m_p/(m_p + m_e)$ and $\bar{\rho}_e = m_e/(m_p + m_e)$.

In order to avoid the effects of proliferation of free parameters, in the following we limit ourselves with a sort of equipartition situation, in which $\xi_e = \xi_m \equiv \xi$. Fig. 4.3 shows the resulting compression factor r_β for $m_e/m_p \le \xi \le 1$.

It is important to stress that for shocks in the newtonian and trans-relativistic regime, the magnetic field and the thermal electrons both result in making the plasma more compressible (the compression factor is as high as 5.6 at the peak $\Gamma_{sh}\beta_{sh} \simeq 0.3$, when equipartition $\xi = 1$ is assumed). On the other hand for highly relativistic shocks all the three components behave in the same way resulting in a compression factor equal

to 3. The electron contribution turns out to be especially important in the intermediate velocity range ($0.1 \lesssim \Gamma_s \beta_s \lesssim 1$).

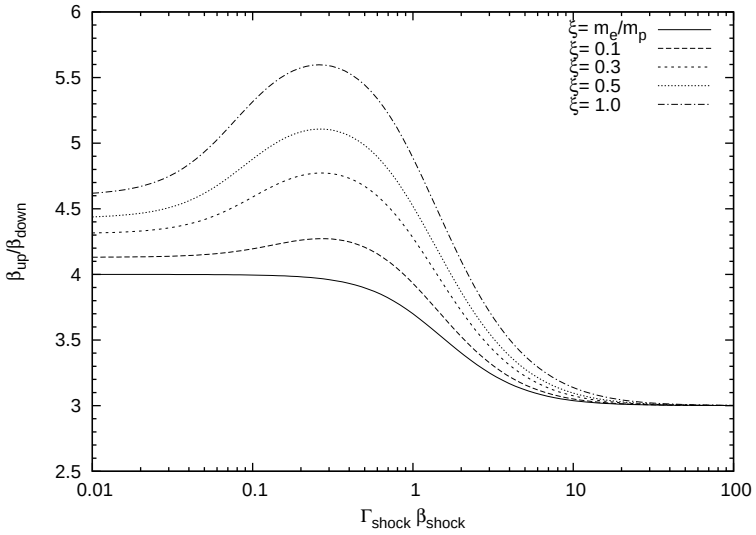

Fig. 4.3 Velocity compression factor when the equation of state of the downstream plasma takes into account the exchange of energy between electrons and protons, and the generation of a turbulent magnetic field. Here we assumed $\xi_e = \xi_m \equiv \xi$.

4.4 The particles' spectrum

The spectrum and angular distribution of the particles accelerated at shocks with arbitrary speed and arbitrary scattering properties of the fluid can be calculated following the theory of particle acceleration reviewed in chapter 2. This approach requires the calculation of the conditional probabilities of a particle returning from upstream or downstream at some direction given the entrance direction. These conditional probabilities were described by Blasi & Vietri (2005) in terms of two non-linear integral equations, that were solved iteratively.

The theoretical approach of Vietri (2003) and Blasi & Vietri (2005) applies equally well to cases of Small Pitch Angle Scattering (SPAS) and Large Angle Scattering (LAS) and to the case of a large scale coherent field upstream, as shown in chapter 3. Here we limit ourselves with considering only two situations, namely that of SPAS, both upstream and downstream, and that of a large scale field upstream, with orientation perpendicular to the shock normal (perpendicular shock). In 3.2.3 it was shown that the spectral shape does not change dramatically with the inclination, with the exception of the cases where the shock is quasi-parallel, but these cases lead to insignificant acceleration and are therefore physically irrelevant.

Before showing our results for the different equations of state discussed above, it is useful to show the spectral slope and the distribution function of the accelerated particles for different values of the velocity compression factor. In Fig. 4.4 we show the spectral slope as a function of the compression factor for several values of $\Gamma_{sh}\beta_{sh}$, ranging from 0.05 to 5.0. The solid line corresponds to the case of a strong newtonian shock, $s(r_\beta) = (r_\beta + 2)/(r_\beta - 1)$. In Fig. 4.5 we also show the distribution function of the accelerated particles as a function of the direction μ measured in the downstream frame.

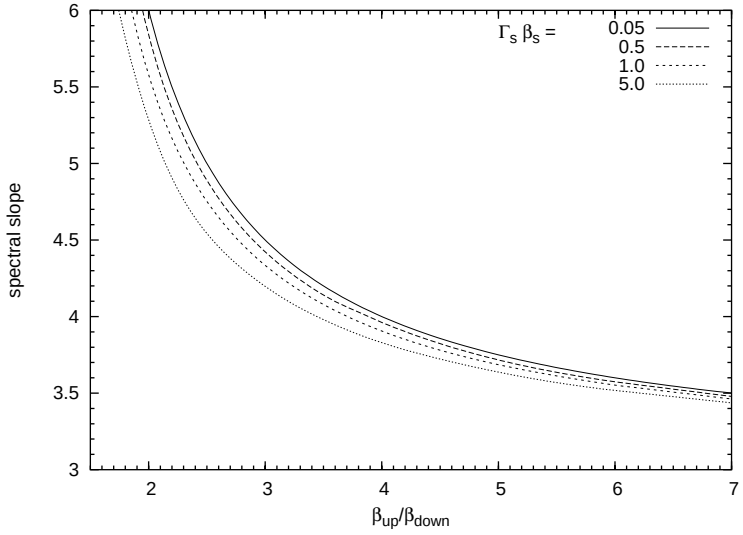

Fig. 4.4 Slope of the spectrum of accelerated particles as a function of the velocity compression factor for different values of the shock speed. The scattering in the SPAS regime both upstream and downstream.

4.4.1 The case of electron-proton coupling

As discussed in §§4.3.1-4.3.4, the basic effect of changing the equation of state is to change the compression factor at the shock and thereby the shape of the spectrum of the accelerated particles. In the following we discuss separately the effect of the interaction between electrons and protons in the downstream plasma, and the effect of the generation of magnetic field. Finally we shall use Eqs. (4.26) and (4.27) in order to quantify the combined effect of the two phenomena.

Fig. 4.6 shows the spectral slope as a function of the shock speed for different values of the parameter ξ_e which characterizes the degree of coupling between thermal electrons and thermal protons, as introduced in §§4.3.1. The left panel refers to the case of SPAS both upstream and downstream, while the right panel refers to the case of a regular perpendicular field upstream (and SPAS downstream).

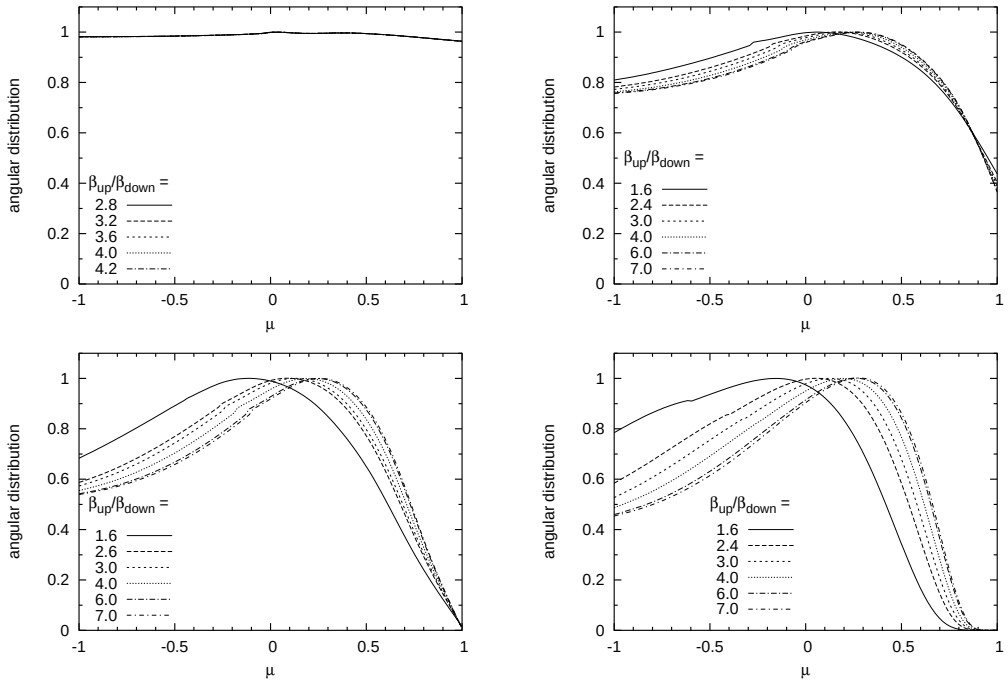

Fig. 4.5 Angular distribution of accelerated particles at the shock front as measured in the downstream fluid frame. μ is the cosine of the angle between the particle direction and the shock normal. The different lines correspond to different values of the velocity compression factor, as indicated in the labels, while the shock velocity has a fixed value for each plot: $\Gamma_{sh}\beta_{sh} = 0.1$ (top-left), 0.5 (top-right), 1.0 (bottom-left) and 5.0 (bottom-right).

Some comments are in order: for very non-relativistic shocks (not shown in the plot) the spectrum has the standard slope $s = 4$. In the ultra-relativistic limit universality is also reached, being the results independent on the value of ξ_e. Most differences in the slope of the spectrum of accelerated particles is present for trans-relativistic shocks: a minimum in the slope appears for these shocks, deeper for larger values of ξ_e. This flattening of the spectrum is due to the increasing compression ratio at trans-relativistic shock speed, as explained in the last paragraph of §4.3.2. A very similar behaviour was found also in Kirk & Duffy (1999) (compare their Fig 3 with left panel of our Fig. 4.6) where they use a different technique, the eigenvalue expansion firstly introduced by Kirk & Schneider (1987), and an equation of state for a gas consisting of both hydrogen and helium.

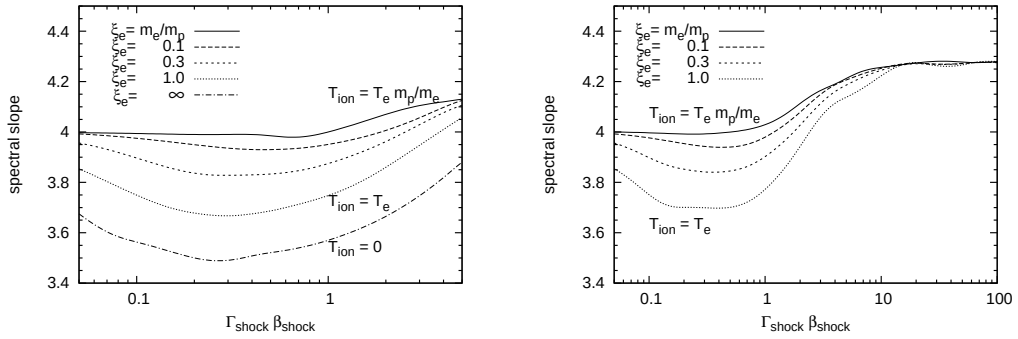

Fig. 4.6 Slope of the spectrum of accelerated particles as a function of $\beta_{sh}\Gamma_{sh}$ when the electrons have a temperature $T_e = \xi_e T_p$. The left panel refers to the case of SPAS in both the upstream and downstream plasmas. The right panel refers to the case in which a regular perpendicular field is present upstream.

4.4.2 The case of turbulent magnetic field production

Based on the discussion in §4.3.3, the effect of a turbulent magnetic field is expected to depend upon the shock speed. As illustrated in Fig. 4.7 (left and right panel as in Fig. 4.6) the spectrum of accelerated particles is harder than in the absence of magnetic fields for newtonian and trans-relativistic shocks (the minimum slope is $s = 3.75$ in the equipartition regime, $\xi_m \sim 1$). In the ultra-relativistic regime all the curves approach the same value: the configuration of magnetic field adopted here does not produce any change in the particle spectra with respect to the case where no magnetic field is present. On the other hand this is easy to guess simply looking at Eq. (4.23).

The spectrum of the accelerated particles is however rather sensitive to the structure of the magnetic field. As we discussed in §4.3.3 and A.2, the equation of state of the field depends on whether the field is generated downstream and is therefore isotropic in the local frame, or it is rather compressed in its perpendicular components. In this

latter case the equation of state of the field is not the same as that of a relativistic fluid and this affects the compression factor at the shock. As an instance we consider here the case $\Gamma_{sh}\beta_{sh} = 5$ and we introduce a magnetization parameter $\alpha = (\delta B^2/8\pi)/\rho c^2$ in the upstream region, where δB is the amplitude of the average magnetic turbulence. $\alpha = 0$ corresponds to the unmagnetized case, which leads to a compression factor 3.12 and a spectral slope $s = 4.12$, as already found earlier. On the other hand, for $\alpha = 10^{-2}$ ($\alpha = 3 \times 10^{-2}$) the compression factor becomes 2.71 (2.16) and the spectral slope is $s = 4.4$ ($s = 4.95$). The corresponding value of the parameter ξ_m downstream, as resulting from the compression of the perpendicular components of the magnetic field is $\xi_m = 0.11$ ($\xi_m = 0.28$). This softening of the spectrum may have very important phenomenological consequences for those classes of sources where particle acceleration occurs at ultra-relativistic shocks.

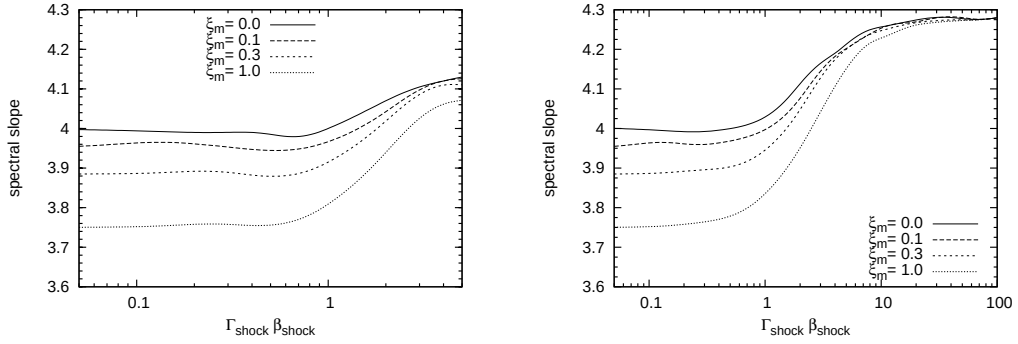

Fig. 4.7 Slope of the spectrum of accelerated particles as a function of $\beta_{sh}\Gamma_{sh}$ when a turbulent magnetic field is present with $\epsilon_m = \xi_m(\epsilon_p - \rho_p c^2)$. The left panel refers to the case of SPAS in both the upstream and downstream plasmas. The right panel refers to the case in which a regular perpendicular field is present upstream.

4.4.3 The general case

Finally we consider the case in which both the effects of turbulent magnetic field downstream and energy exchange between the thermal components of electrons and protons are taken into account. More specifically we concentrate on the so called *equipartition case*, in which $\xi_e = \xi_m = \xi$ and we illustrate our results for different values of ξ. Here we restrict our attention to the case in which the turbulent field is generated downstream and does not result from the compression of an upstream field. As usual, the left panel in Fig. 4.8 refers to SPAS both upstream and downstream and the right panel to a large scale field upstream (and SPAS downstream).

For $\xi = m_e/m_p$ the standard result is recovered in the SPAS case (left panel). The case $\xi = 0$ when a large scale magnetic field is present upstream was discussed in

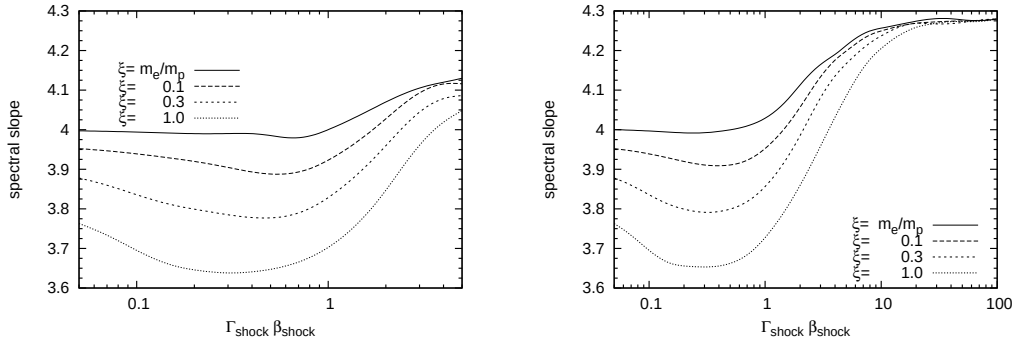

Fig. 4.8 Slope of the spectrum of accelerated particles as a function of $\beta_{sh}\Gamma_{sh}$ with the full equation of state for the downstream plasma. The left panel refers to the case of SPAS in both the upstream and downstream plasmas. The right panel refers to the case in which a regular perpendicular field is present upstream.

Section 3.2 and the results are very close to the case $\xi = m_e/m_p$ used as the lower limit in Fig. 4.8.

In the other extreme case $\xi = 1$ the spectrum of accelerated particles is harder than 4 in the non-relativistic limit and approaches the *universal* spectrum in the ultra-relativistic case. In both cases of SPAS and regular field upstream, a minimum in the slope of the spectrum is reached at $\beta_{sh}\Gamma_{sh} \approx 0.4$ corresponding to $s \approx 3.65$. This is a result of the interaction between electrons and protons in the trans-relativistic regime.

In Figs. 4.6, 4.7 and 4.8 the range of shock velocities adopted for the cases of upstream ordered magnetic field and of SPAS are quite different. This is not due to any deep reason, but simply to the fact that the computation method introduced in Blasi & Vietri (2005) becomes very challenging when the Lorentz factor becomes too large. This is related to the fact that in order to describe the regime of small pitch angle scattering we need to adopt a finite aperture σ of the scattering function which however must stay smaller than $1/4\Gamma_{sh}^2$ in order to operate in the SPAS regime. As discussed in §3.2 this problem is absent in the case of ordered magnetic field.

4.5 Discussion

We used the theoretical framework introduced in Chapter 2 to determine the spectrum of particles accelerated at shocks with arbitrary speed and scattering properties, with different equations of state of the gas downstream. In particular we investigated two situations: 1) the downstream gas is made of thermal electrons and protons that may exchange energy with each other, thereby changing the equation of state; 2) the downstream gas includes a turbulent magnetic field. We also considered the case in which both effects are at work at the same time.

In the downstream frame the scattering has always been assumed to be in the SPAS regime, while in the upstream fluid we considered two scenarios, namely SPAS

and regular field with no turbulent scattering. We limited our attention to the case of strong shocks, namely the case in which the inflowing plasma has zero pressure.

When the downstream plasma is made of electrons and protons and their temperatures are different, for newtonian and ultra-relativistic shocks the shape of the spectrum is not appreciably changed. However, for trans-relativistic shocks the compression factor increases appreciably when the electron temperature is $\gg \frac{m_e}{m_p} T_p$, causing a flattening in the spectrum of the accelerated particles. In particular this is true for $T_e = T_p$, a situation which might be achieved due to some efficient collisionless plasma process, able to equilibrate the electron and proton components more efficiently than the simple isotropization of the velocity vectors.

The effect of a turbulent magnetic field on the compression factor and on the spectral slope is more complex. We identified two situations of interest that arise when the magnetic field is introduced in the conservation equations at the shock surface: 1) the turbulent field is created downstream and is isotropic; 2) the magnetic field downstream is the result of the compression of the turbulent field upstream (only the perpendicular components are compressed). In the former case it can be demonstrated that the equation of state of the magnetic field is identical to that of an ideal relativistic gas, Eq. (4.23), irrespective of the shock speed. When the shock is non-relativistic the compression factor at the shock is increased and the spectra become harder than in the absence of field. For relativistic shocks the usual asymptotic spectrum is reached both in the case of upstream regular deflection or small pitch angle scattering.

The second case is more interesting: when the perpendicular components of the turbulent upstream field are amplified by crossing the shock surface, the resulting magnetic field downstream is strongly anisotropic and the equation of state of the magnetic field is $p_m = \epsilon_m$, not resembling that of a relativistic gas. In this case, for relativistic shocks the spectra of accelerated particles are softer than in the first scenario. For instance for $\Gamma_{sh}\beta_{sh} = 5$ and $\alpha = 10^{-2}$ ($\alpha = 3 \times 10^{-2}$) the compression factor becomes 2.71 (2.16) and the spectral slope is $s = 4.4$ ($s = 4.95$). The corresponding value of the parameter ξ_m downstream, as resulting from the compression of the perpendicular components of the magnetic field is $\xi_m = 0.11$ ($\xi_m = 0.28$). The important effect consisting of a spectral steepening was found by Lemoine & Revenu (2006) and was attributed to the fact that the compression in the downstream gas makes the magnetic field quasi-perpendicular, thereby reducing significantly the probability of return from the downstream frame. This effect is limited, in the analysis of Lemoine & Revenu (2006) to the particles with gyration radius smaller than the coherence scale of the turbulent field. The steepening of the spectrum as found in our calculations, is due to a change in the equation of state of the downstream plasma (electrons, protons and magnetic field) and concerns all of the spectrum of the accelerated particles. The relevance of this finding for the phenomenology of several astrophysical sources of accelerated particles, in particular those where a relativistic shock is expected or observed, is evident.

Chapter 5

Nonlinear CRs acceleration for newtonian shock

5.1 Introduction

Past chapters were dedicated to analyse the shock acceleration process assuming that the energy transferred from the shock motion to the non-thermal particles were negligible. This assumption, commonly called *test-particle* approximation, allows us to separate the study of the acceleration process into two different steps: firstly the determination of the shock structure, witch depends only on the thermal component of the gas, than the study of the non-thermal particles production as a function of the fixed shock structure. For obvious reasons this approach is also called *linear theory*.

In spite of the important results achieved, test-particle theory presents serious deficiencies when used to explain the existence of CRs. First of all we note that, in the contest of SNR paradigm, the linear theory can account only for CRs up to an energy around $Z \times 10^{14} - 10^{15}$ eV (Lagage & Cesarsky 1983). The maximum energy is limited by the combination of some quantities: the size L of the shock, the time τ during which the shock propagates at hight velocity, v_s, and the spatial diffusion coefficient of the particles, $D(p)$. Tipical values for a SNRs shock are $v_s = 10^4 \mathrm{Km\,s^{-1}}$, $L = 10\,\mathrm{pc}$ and $\tau = 10^3\,\mathrm{yr}$. The simplest assumption for the diffusion is the Bohm like diffusion, which assumes the mean free path of a particle to be of the order of its Larmor radius, namely $D_{\mathrm{B}}(p) = r_L c/3 = pc/(3ZeB)$. Energies up to $Z \times 10^{15}$ eV can be obtained using $B = 3\,\mu\mathrm{G}$, the tipical value for the interstellar magnetic field. Acceleration to higher energies is improbable unless the magnetic field would be larger.

If one belives the SNRs to be the factories of galactic CRs, the maximum energy predicted by the linear theory has serious problems in explaining the spectrum as observed at the Earth. Following the recent results of KASCADE experiment, protons are observed up to energies of $2 - 4 \times 10^{16}$eV (Hoerandel 2005). This problem become worst if one supposes that the galactic CRs extend up to the energy of the *ankle*[1], i.e. $\sim 5 \times 10^{18}\,\mathrm{eV}$. Similar difficulties arises if one try to apply the shock acceleration model in some extra-galactic environments to explain the most energetic part of the CRs spectrum.

[1] Up to now the value of the cross energy, where the extragalactic CRs start to dominate on the galactic component, is still a matter of debate. Two different scenario has been proposed: the *ankle* scenario identifies the cross energy at $5 \times 10^{18}\,\mathrm{eV}$, where a change of slope occurs. Most recently the *deep* scenario has been proposed, where the ankle is interpreted as a feature of the extragalactic CRs alone, due to the interaction with the CMBR photons. In this case the cross energy is located at 10^{18} where a feature called *second knee* has been identified. See Aloisio et al. (2007) and references therein for a detailed discussion.

CRs are believed to be scattered by the magnetic field irregularities exited by the CRs themselves through the *streaming instability* (Bell 1978a). In the contest of linear theory these irregularities have an amplitude $\delta B \leq B_\circ$, where $B_\circ$ is the background magnetic field into the unshocked region. But this condition holds only if the energy channelled into the CRs is small compared with the bulk energy of the gas, $P_{CR} \ll \rho u^2$. McKenzie & Volk (1982) firstly point out the possibility that CRs themselves can amplify the turbulent magnetic field above the background field value. Using the equation that describes the linear amplification of the turbulence (e.g. Bell & Lucek 2001), a back to the envelope calculation gives the following estimate for the total energy of the amplified field:

$$\frac{\delta B^2}{B_\circ^2} = 2M_A \frac{P_{CR}}{\rho u^2}\,, \tag{5.1}$$

where $M_A = u/v_A$ is the Alfvén Mach number. If we suppose $P_{CR} \sim \rho u^2$, the amplification can be as hight as $M_A^{1/2}$. For a SNRs shock propagating into the interstellar medium, with tipical density of 1 proton$\cdot$cm^{-3} and a tipical temperature of 10^5 K, Mach number as hight as 1500 can be obtained. Numerical simulation reported in Lucek & Bell (2000) confirms this effect, predicting an amplification factor around 100. As a consequence the maximum energy predicted could be as hight as $Z \times 10^{16} - 10^{17}$ eV. However such estimate can be strongly reduced by non linear effects which occurs when $\delta B \sim B_\circ$, and can saturate the amplification effect.

Some recent analysis of the hight resolution X-rays images of several SNRs provided the first clue about a probable magnetic field amplification in the post shock region (Berezhko et al. 2003; Berezhko & Völk 2004; Völk et al. 2005; Parizot et al. 2006). Relativistic electrons lose energy by bremmstralung and emit X-rays. Both the brightness and the size of the emitting region depend on the magnetic field intensity: strongest is the field, brightest and smaller is the emitting region. Combined measure of these two quantities allow one to estimate the field intensity. In all cases considered by the cited authors values around few thousand μG are deduced. Hence, if we suppose to start with the tipical interstellar field, $3\,\mu G$, amplification around a factor 100 are required. Recently a second mechanism of amplification has been proposed by Bell (2004), who identified a non-resonant, nearly purely growing modes driven by the CRs current. Such modes grow more rapidly than the resonant Alfvén waves usually considered, and can account for a strong field amplification.

Previous considerations justify the importance of developing a non linear approach for the shock acceleration problem. The non linearity reflects into two distinct aspects. The first point concerns the mutual interaction between the CRs and the Alfvén waves: from one hand the CRs produce and amplify the Alfvén waves; from the other hand the Alfvén waves scatter the CRs themselves. From the mathematical point of view this interaction translates into a dependence of the diffusion coefficient by the CRs distribution function, $D[f(x,p)]$.

The second aspect regards the backreaction of CRs onto the shock dynamics: CRs exert a pressure against the incoming gas flux, reducing progressively its speed. In turn the modification of the shock structure produces modification of the CRs spectrum

because the particles feel a different velocity jump between the upstream and downstream fluids, depending on their momentum. Three different approaches exist to include the backreaction of CRs onto the shock dynamics. Numerical simulations play an important role because the ability of a self-consistent treatment of several effects (Jones & Ellison 1991; Bell 1987; Ellison et al. 1990, 1995, 1996; Kang & Jones 1997; Kang et al. 2002). The second approach are the fluid models, that treats the CRs component as a relativistic fluid with a specific energy density and pressure (Drury & Voelk 1981; Drury et al. 1982; Axford et al. 1982; Duffy et al. 1994). These models can handle with the CRs total energy and pressure but they are unable to provide information about the non-thermal particle spectrum that has to be provided *a priori*. The third approach is kinetic, and attempts to study the CRs transport in a plasma, by the use of a transport equation for the non-thermal particles.

Blandford (1980) tackles the problem considering the pressure of CRs a small perturbation. This perturbative approach can only handle weakly modified shock. A different approach was used in (Eichler 1984; Ellison & Eichler 1984; Eichler 1985; Ellison & Eichler 1985) where some simplified assumpions are used to express the diffusion coefficient.

Always in the contest of non linear theory, Berezhko et al. (1994) showed that even when a small fraction of particles is involved in the acceleration process ($\sim 10^{-4}$ of the gas density), CRs can absorb about 20% of the SN explosion energy, while in (Berezhko 1996) both the effect of CRs back reaction and geometrical factors on the maximum energy were investigated.

More recently Malkov (1997); Malkov et al. (2000); Blasi (2002) developed an approximate solution for the transport equation able to provide self-consistently both the particle spectrum and the structure of the hydrodynamic flow.

All the previous approaches has been applied under the assumption that the particle injection occurs at the shock position from the thermal pool. But important effects could arise from a pre-existing population of non-thermal particles, also called *seed* particles. Indeed shocks usually propagates into media where pre-accelerated particle already exist. This is true not only for isolated supernovae, which explode in the ISM, where the *regular* Galactic CRs are present, but it is even more important for those SN that explode in the so called OB associations. These associations are group of massive stars where most of SN progenitor are observed. The wind activity of such stars generates large structures calls *superbubbles*, inside which the SN explosion rate is sufficiently high, and the diffusion coefficient is sufficiently low, that particles can be accelerated repeatedly before they can escape the superbubble region (Parizot et al. 2004). In such structures, when a SN explode, the pre-existing CRs component can be even more important than the fresh injected particles at the shock.

The linear theory of acceleration including seed particles was presented by Bell (1978b), while the first analytical attempt to calculate the non-linear effect of pre-existing non-thermal particle was developed by Blasi (2004) using an approximate solution for the transport equation.

Here we present the full solution of the stationary-transport equation for a plane geometry, including the back reaction of the CRs and the presence of a seed particles. Although we assume e simple Bohm diffusion instead of including the correct treatment

of the self-generated diffusion coefficient, the solution founded can be easily generalized for every form of D also if it depends upon the spatial coordinate. We specialize our solution to the case of a tipical SNRs shock in two different situations: we firstly consider only the presence of seed particles, than we add the contribution of thermal injection according to the *thermal leakage* model. As previously founded by Blasi (2004) we confirm that the shock modification produced by the seed particles can dominate on the same effect produced by the injection. Moreover the presence of seed particles also changes the shape of the spectrum in the low energy region.

A problem arises when the shock acceleration mechanism is formulated with a non-linear approach under the assumption of the stationarity of the solution: multiple solutions appear. It is needless to say this is a very common aspect of non-linear phenomena. Both the two fluid and the kinetic approaches have find that three solutions arises for a large region of the parameters space. At the present it is still not clear how to resolve such a problem. A possibility is that one or more solution could be unstable. Using the two fluid approach Mond & O'C. Drury (1998) demonstrate that the intermediate solution is indeed unstable to corrugations in the shock structure and emission of acoustic waves. A second possibility put forward in Malkov et al. (2000) is that the shock can sit at the critical point, self-regulating the value of the maximum achievable momentum and the injection from the thermal pool. The latter hypothesis turns out to be less clear when applied in a situation where also the seed particles are added, because, as we will discuss, the shock has no way to reduce the effect of modification induced by the pre-existing particles, as can done for the injected particles. One can also suspect that the stationarity is an incorrect assumption and that the actual solution continously evolves with time.

This chapter is organized as follows: in the next section we summarize the gas dynamics under the effect of the CRs, obtaining the expression of the fluid velocity as a function of the CRs distribution. In §5.3 we solve the diffusive-transport equation using the pre-existing CRs distribution as the upstream infinity boundary condition and a mono-energetic injection at the shock discontinuity. §5.4 summarizes the procedure to obtain the complete solution in a self-consistent manner. The results for a tipical scenario of a SNRs shock are shown and commented in §5.5. We conclude in §5.6.

5.2 The gas dynamics

In the contest of non-linear shock theory the dynamic and thermodynamic properties of the gas result from the interaction with the CRs component. As sketched in Figure 5.1 we expect that the CRs pressure slows down the upstream gas flux, producing a curved velocity profile (the region were this occurs is called *precursor*). The remaining sub-shock step is only a discontinuity for the gas, because it is too thin compared with the mean free path of accelerated particles.

The first step consist to include CRs into the mass and momentum conservation. We write these equations between the upstream infinity, where the gas has velocity $u_\circ$ and density $\rho_\circ = m\, n_{g,\circ}$, and a generic point x. The mass conservation for the gas is simply

$$\rho_\circ u_\circ = \rho(x) u(x)\,. \tag{5.2}$$

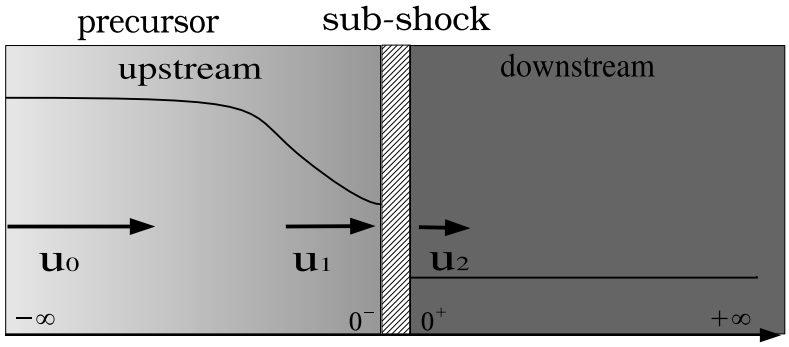

Fig. 5.1 Generic modified shock structure as seen in the shock reference frame. The solid line shows the the plasma velocity profile. The discontinuity at $x = 0$ is usually called *sub-shock*

Obviously the mass contribution of CRs can be neglected. The momentum conservation reads:

$$\rho_\circ {u_\circ}^2 + P_{g,0} + P_{CR,0} = \rho(x) u(x)^2 + P_g(x) + P_{CR}(x)\,, \tag{5.3}$$

where P_g and P_{CR} are the gas and the CRs pressure respectively. The CRs pressure at a fixed point x can be expressed using the distribution function of the particles:

$$P_{CR}(x) = \frac{4\pi}{3} \int_{p_{\min}(x)}^{p_{\max}(x)} dp\, p^3\, v(p) f(p,x)\,, \tag{5.4}$$

The second step requires the gas equation of state. The simplest assumption is to suppose that the gas is adiabatically compressed, hence the pressure reads:

$$P_g(x) = P_{g,\circ} \left(\frac{\rho(x)}{\rho_\circ} \right)^{\gamma_g}\,, \tag{5.5}$$

where γ_g is the adiabatic index of the gas. At the end of this section we will make some comments on the validity of the adiabatic assumption. Now we want to rewrite the momentum equation in a usefull adimensional form. Taking into account the conservation of mass flux and the definition of the Mach number, $M_0 = c_s^2/u_\circ^2 = (\gamma P_{g,0})/(\rho_\circ u_\circ^2)$, we can divide equation (5.3) for $\rho_\circ {u_\circ}^2$. The result is

$$\xi_c(x) - \xi_{c,\circ} = 1 - U(x) + \frac{1}{\gamma_g {M_0}^2} \left(1 - U(x)^{-\gamma_g} \right)\,. \tag{5.6}$$

Here ξ_c is the CRs pressure normalized with respect to the total momentum flux, i.e. $\xi_c(x) = P_{CR}(x)/(\rho_\circ u_\circ^2)$, and $U(x) \equiv u(x)/u_\circ$. $\xi_{c,\circ}$ is the normalized pressure at upstream infinity. Equation (5.6) is the first stone of the non-linear shock model; once inverted it allows us to get the gas speed $u(x)$ as a function of the CRs distribution $f(x,p)$.

The boundary values of gas speed are usually expressed using the total and the sub-shock compression factors, $R_{\rm tot} = u_\circ/u_2$ and $R_{\rm sub} = u_1/u_2$. Equation (5.6) provide us an usefull relation between the CRs pressure at the sub-shock position and $R_{\rm sub}$:

$$\xi_c(0) - \xi_{c,\circ} = 1 + \frac{1}{\gamma_g {M_0}^2} - \frac{R_{\rm sub}}{R_{\rm tot}} - \frac{1}{\gamma_g {M_0}^2}\left(\frac{R_{\rm sub}}{R_{\rm tot}}\right)^{-\gamma_g} . \tag{5.7}$$

This relation will be used in §5.4 to obtain $\xi_{c,\circ}$ only as a function of once $R_{\rm sub}$. But to get this aim we also need to express $R_{\rm tot}$ as a function of $R_{\rm sub}$. If the upstream gas is adiabatic compressed, as we assumed previously, the Mach number at upstream infinity and the one at the subshock are related by:

$$M_1^2 = M_0^2 \left(\frac{R_{\rm sub}}{R_{\rm tot}}\right)^{\gamma_g+1} \tag{5.8}$$

On the other hand the Rankine-Hugoniot jump conditions applied at the sub-shock provide use the well-know relation between $R_{\rm sub}$ and M_1:

$$R_{\rm sub} = \frac{(\gamma_g+1)M_1^2}{(\gamma_g-1)M_1^2+2} \tag{5.9}$$

Substituting M_1 as results from (5.9) into equation (5.8), we get the final expression for $R_{\rm tot}$:

$$R_{\rm tot} = {M_0}^{2/(\gamma_g+1)} \left[\frac{(\gamma_g+1)R_{\rm sub}^{\gamma_g} - (\gamma_g-1)R_{\rm sub}^{\gamma_g+1}}{2}\right]^{\frac{1}{\gamma_g+1}} . \tag{5.10}$$

Some comments are in order about the adiabatic hypothesis. It is worth noting that the equations (5.3) and (5.5) implies a non trivial assumption about the interaction process that occurs between thermal and non-thermal particles. As many times stressed, the interaction between particles in a tenuous plasma, as those present in almost all astrophysical situations, is mediated only by non local field effects; the contribution of Coulomb scattering is completely negligible. For an approach like this, where the particles are divided in two different component, thermal (plasma) and non thermal (CRs), the interactions can be sketched as:

$$\text{Plasma} \leftrightharpoons \text{Wave} \leftrightharpoons \text{CRs}.$$

Both thermal and non-thermal particles produce and react to the waves. The question is which kind of wave can transmit the pressure from CRs to the thermal plasma and *vice-versa*. As generally known CRs can excite two kind of waves: magnetosonic and Alfvén waves. The former are dumped very quickly through the Landau-damping mechanism, hence they contribute to heat the plasma in a non adiabatic way. On the other hand

Alfvén waves are only slightly dumped [2] and can persist long time after their generation: they are the true responsables of the adiabatic compression [3].

We mention also a second process that produce a non-adiabatic gas heating, originally discovered by Drury & Falle (1986): the so called *acoustic instability*. When a pressure gradient is present in the plasma, the CRs presence can amplify the sound waves up to the development of a train of shock waves that heat the gas.

The plasma wave-component should be taken into account also in the jump conditions at the sub-shock. The pressure and energy flux exerted by the waves can reduce considerably the gas compression factor $R_{\rm sub}$, especially in the case of strong modified shock where CRs produce a strong Alfvén wave turbulence[4]. Hence also our equation (5.9) turn out to be an approximation.

As it is clear from the previous discussion, a complete solution of the problem should include the contribution of the waves in the momentum equation and their effect onto the gas equation of state. The net effect of the non-adiabatic heating is the reduction of the acceleration efficiency because a larger fraction of the initial energy flux is channeled into the internal energy of the gas[5]. But we note that a correct treatment requires a non liner theory of the wave-particle interaction that, in our knowledge, has not still developed. In any case all this discussion does non invalidate our main conclusion.

5.3 The diffusive-transport equation for CRs

In this section we find the most general expression for the cosmic rays distribution function, solving the convection-diffusion equation under the assumption of stationarity. As in the chapter 2 we assume a plane geometry, so the problem is one-dimensional, and we chose the frame where the shock is stationary and is located at $x = 0$, while both the upstream and downstream fluids move with positive velocity $u(x)$ along the x direction (see Figure 5.1). The cosmic rays are injected according to a function $Q(x, p)$, where p is the injection momentum. With $f_{\infty}(p)$ we indicate the pre-existing CRs distribution, *i.e.*, the boundary condition at upstream infinity ($x = -\infty$). Under this assumptions, the diffusive-transport equation reads[6]:

$$\frac{\partial}{\partial x}\left[D(x,p)\frac{\partial}{\partial x}f(x,p)\right] - u(x)\frac{\partial f(x,p)}{\partial x} + \frac{1}{3}u'(x)p\frac{\partial f(x,p)}{\partial p} + Q(x,p) = \frac{\partial f}{\partial t} = 0\,. \quad (5.11)$$

[2]Despite the fact that Alfvén waves do not undergo the Landau damping, when the Alfvén velocity is greater than the sound speed, they produce magnetosonic waves in a similar fashion then Alfvén waves produced by particles with velocity greater than the Alfvén speed (see Skilling (1975)). Because magnetosonic waves are in turn dumped, the whole process produce a non adiabatic heating precisely called *Alfvén-heating*.

[3]For an extensive discussion see e.g. McKenzie & Volk (1982).

[4]See Vainio & Schlickeiser (1999) for a self-consistent treatment of the jump conditions in the presence of Alfvén waves.

[5]See Amato & Blasi (2006) for a quantitative estimation of this effect in the case of weak turbulence.

[6]For the derivation of the diffusive-transport equation starting from the Vlasov equation see (e.g. Vietri 2006, chap. 4).

In this equation the first and the second terms represent the particle diffusion and convection respectively, and $D(x,p)$ is the diffusion coefficient. The third term takes into account the effect of the adiabatic compression of the fluid. Note that $u' \equiv du/dx$.

The non-linearity of equation (5.11) is twofold: first of all the fluid velocity $u(x)$ depends on the CRs pressure, as we saw in §5.2. Secondly, as is now generally accepted, the diffusion process is caused by the CRs self-generated turbulence. Hence a full self-consistent treatment requires the inclusion of the self-generated turbulence and the description of the diffusion coefficient in terms of turbulence density. In this work we neglect the self-generated turbulence, and we will assume a Bohm diffusion with an uniform magnetic field. This simplification will not invalidate our main conclusions; however the inclusion of self-generated diffusion is not difficult, at least in the quasi-linear approach, as done by Amato & Blasi (2006).

Injection problem. We assume that the particle injection occurs immediately upstream of the shock, hence $Q(x,p) = Q_\circ(p)\delta(x)$. The generally accepted picture describes the injection process as due to the sub-shock discontinuity itself: the same collective processes responsable of the fluid thermalization from the upstream to the downstream state should be provide a fraction of supratermal particle able to cross the shock discontinuity and start the Fermi acceleration mechanism. The detailed description of the injection mechanism is still a matter of investigation, but numerical simulations show that this is the correct picture. As usually done in the literature, we will use a mono-energetic injection at a single momentum value $p_{\rm inj}$:

$$Q_\circ(p) = \frac{\eta\, n_{g,1} u_1}{4\pi p_{\rm inj}^2}\, \delta(p - p_{\rm inj})\,. \tag{5.12}$$

Here u_1 and $n_{g,1}$ are the fluid velocity and the gas density immediately upstream while η rapresents the fraction of the upstream gas injected as suprathermal particles. In passing we note that from the numerical simulations η is usually of the order of $\sim 10^{-4}$; this means that both the energy and momentum lost by the gas are negligible, hence could be neglected in the computation of gas jump conditions. Although η is an unknown parameter, because it hides all the bad know physics of collisionless shock, it can be related to the subshock compression factor through a simple argument. We suppose that only particles from the downstream thermal bath with larmor radii grater than the shock thickness can start the acceleration process. Because the shock thickness is of the order of the larmor radii of the thermal particles, and the downstream temperature is related to $R_{\rm sub}$, the result is a relation $\eta(R_{\rm sub})$. This picture is called *thermal leakage* model. We adopt here the recipe proposed by Blasi et al. (2005) that gives the following result for η:

$$\eta = \frac{4}{3\sqrt{\pi}}\,(R_{\rm sub} - 1)\,\xi^3 \mathrm{e}^{-\xi^2}\,. \tag{5.13}$$

The paramete ξ identifies the effective injection momentum as a multiple of the thermal momentum, i.e.

$$p_{\rm inj} \equiv \xi\, p_{\rm th}\,, \tag{5.14}$$

whit the thermal momentum defined as $p_{\rm th} \equiv \sqrt{2\, m_{_p} K_{_B} T}$. The fraction of particle injected is $\eta \sim 10^{-4}$ for $\xi = 3.5$. As is clear from equation (5.13) more the shock is modified ($R_{\rm sub}$ approaching 1) less are the injected particles. This feedback mechanism allows the shock to self-regolate and, as shown by Blasi et al. (2005), strongly reduces the problem of multiple solutions.

Following Malkov (1997) and Blasi (2004) the solution of equation (5.11) can be expressed in an implicit form using the boundary conditions at upstream infinity, $f_{\infty}(x) \equiv f(-\infty, p)$, and at the shock position, $f_{\circ}(p) \equiv f(0, p)$. While the cited authors use an approximated solution, we will compute the exact expression. Before doing this, in §5.3.3, in the next section we will remember how to express $f_{\circ}(p)$.

5.3.1 Boundary conditions at the shock position

As showed by Blasi (2002), the expression for the distribution at the shock position can be obtained integrating equation (5.11) along the shock discontinuity, between the points 0^{-} and 0^{+} (see Figure 5.1). An important point ha to be stressed: the CRs distribution is assumed to be continuous at the sub-shock discontinuity. The physical motivation is that CRs has a mean free path longer than the sub-shock thickness hence they don't feel the discontinuity. Moreover the downstream section is considered uniform in space, therefore we can assume $(\partial f/\partial x)_{0^{+}} = 0$, the result of the integration become

$$[D \partial_{_x} f]_{0^{-}} = \frac{1}{3}\, p\, \partial_{_p} f\, (u_2 - u_1) + Q_{\circ}(p)\,. \tag{5.15}$$

Now equation (5.11) can be integrated again, but this time between $-\infty$ and 0^{-}; substituting the expression (5.15) in the result we finally get a first-order differential equation for $f_{\circ}$, i.e.

$$p\, \partial_{_p} f_{\circ}(p) = -\frac{3}{u_{_p}(p) - u_2} \left\{ f_{\circ}(p) \left[u_{_p}(p) + \frac{1}{3}\, p\, \partial_{_p} u_{_p}(p) \right] - u_{\circ} f_{\infty}(p) - Q_{\circ}(p) \right\}, \tag{5.16}$$

where $u_{_p}(p)$ is defined as follows

$$u_{_p}(p) = u_1 + \frac{1}{f_{\circ}(p)} \int_0^{\infty} \frac{du(x')}{dx'} f(x', p) dx'\,. \tag{5.17}$$

As underline by Blasi (2002) $u_{_p}$ has a simple physical meaning: it represents the mean fluid velocity experienced by a particle with momentum p in the upstream section. Integration of equation (5.16) allow us to express $f_{\circ}(p)$ as an implicit function of $f(x, p)$ by the use of the expression (5.17); moreover it is usefull to distinguish between the contribution of the injection and that resulting from the seed particles. The injection is

written out according to the expression (5.12). The final solution is

$$\begin{aligned} f_\circ(p) &= f_\circ^{\rm inj}(p) + f_\circ^{\rm seed}(p) \\ &= \frac{\eta\, n_{\rm gas,1}}{4\pi p_{\rm inj}^3}\,\frac{3R_{\rm sub}}{R_{\rm tot}U_p(p)-1}\exp\left\{-\int_{p_{\rm inj}}^{p}\frac{3R_{\rm tot}U_p(p')}{R_{\rm tot}U_p(p')-1}\frac{dp''}{p''}\right\} \\ &+ \frac{3R_{\rm tot}}{R_{\rm tot}U_p(p)-1}\int_{p_{\rm min}}^{p}\exp\left\{-\int_{p'}^{p}\frac{3R_{\rm tot}U_p(p'')}{R_{\rm tot}U_p(p'')-1}\frac{dp''}{p''}\right\} f_\infty(p')\frac{dp'}{p'}\,. \end{aligned} \quad (5.18)$$

As usual $R_{\rm tot}$ and $R_{\rm sub}$ are the total and the sub-shock compression factor and $U_p \equiv u_p/u_\circ$. Some attention has be paid with the value of $p_{\rm min}$: it means the minimum momentum allowed for the $f_\circ^{\rm seed}$ at the shock position. Because we suppose that only particles with $p > p_{\rm inj}$ can take part to the acceleration, $p_{\rm min}$ is the maximum between $p_{\rm inj}$ and the minimum momentum that seed particles have when they encounter the sub-shock at the first time. In fact, because of the effect of the gas compression, seed particles arrive at the sub-shock with momentum greather than what they have at upstream infinity. We will derive $p_{\rm min}$ in the §5.3.4.

5.3.2 The test-particle limit

Before to compute the complete solution for the distribution function, let us re-analyse the test-particle limit case to show why such a solution cannot be a physical one. When we assume that the dynamical role of accelerated particles is negligible, the upstream plasma speed reduces to a constant, $u(x) = u_0$, and $U_p \to 1$, hence the distribution function at the shock, Eq. (5.18), turn out to be a simple power law in the momentum, i.e.:

$$\begin{aligned} f_\circ(p) &= f_\circ^{\rm inj}(p) + f_\circ^{\rm seed}(p) \\ &= \frac{\eta\, n_{\rm gas}}{4\pi p_{\rm inj}^3}\, s\left(\frac{p}{p_{\rm inj}}\right)^{-s} + s\,p^{-s}\int_{p_{\rm min}}^{p} p'^{s-1} f_\infty(p')\,dp'\,. \end{aligned} \quad (5.19)$$

Now, let us compare the pressure generated by CRs with respect to the plasma thermal pressure. For simplicity we assume that only the injection at the shock occurs. Moreover we set $s = 4$. Substituting Eq. (5.19) into Eq. (5.4) we get the following estimate for the CRs pressure:

$$P_{CR} = \frac{4\pi}{3}\int_{p_{\rm inj}}^{p_{\rm max}} p^4 v(p) f_\circ(p)\, d\ln(p) \lesssim \frac{4}{3}\,\eta\, n_{\rm gas}\, p_{\rm inj} c\, \ln\left[\frac{p_{\rm max}}{m_p c}\right]\,, \quad (5.20)$$

where the last passage is obtained considering only the pressure due to particle with $p > m_p c$ for which the approximation $v(p) = c$ holds. The ratio between CR and gas

pressure can be estimate as follows:

$$\frac{P_{CR}}{P_{\rm gas}} = \frac{P_{CR}}{n_{\rm gas} K_B T} \lesssim \eta \frac{8\, p_{\rm inj} c}{3\, p_{\rm th} v_{\rm th}} \ln\left[\frac{p_{\rm max}}{m_p c}\right] \approx 2.3 \cdot 10^5 \eta\, \xi\, \ln\left[\frac{p_{\rm max}}{10^5 m_p c}\right] \left(\frac{T}{10^5 K}\right)^{-1/2}, \tag{5.21}$$

where we use the definition of $p_{\rm inj}$, Eq. (5.14). It is clear that even for a fraction of injected particles as small as 10^{-5}, the CR pressure can be greather than the gas pressure, hence it cannot be neglected into the Eq. (5.3).

Always using the test-particle solution we can show that the contribution of seed particles can be relevant if one considers as seed the CR spectrum as observed at the Earth. Let us assume that f_∞ is a power law with index s_0, starting from the minimum momentum $p_{\rm min}$:

$$f_\infty(p) = \frac{n_{CR,0}}{4\pi p_{\rm min}^3} (s_0 - 3) \left(p/p_{\rm min}\right)^{-s_0} . \tag{5.22}$$

It is convenient to express the number density $n_{CR,0}$ as a function of CRs energy density, $\mathcal{E}_{CR,0}$, and $p_{\rm min}$:

$$n_{CR,0} = \frac{\mathcal{E}_{CR,0}}{c p_{\rm min}} \frac{s_0 - 4}{s_0 - 3} = 3.6 \cdot 10^{-10} {\rm cm}^{-3} \left(\frac{\mathcal{E}_{CR,0}/{\rm eV\,cm^{-3}}}{p_{\rm min} c/{\rm GeV}}\right) . \tag{5.23}$$

where the value $s_0 = 4.7$ is assumed. Substituting Eq. (5.22) into Eq. (5.19) we can easily get the ratio between the re-accelerated seed particles and the freshly injected ones:

$$\frac{f_\circ^{\rm seed}(p)}{f_\circ^{\rm inj}(p)} \quad \underset{p \gg p_{\rm min}}{\longrightarrow} \quad \frac{n_{CR,0}}{\eta\, n_{\rm gas}} \left(\frac{s_0 - 4}{s_0 - s}\right) \left(\frac{p_{\rm min}}{p_{\rm inj}}\right)^{s-3} \tag{5.24}$$

$$\approx \quad 3.6 \cdot 10^{-2} \left(\frac{10^{-5}}{\eta}\right) \left(\frac{{\rm cm}^{-3}}{n_{\rm gas}}\right) \left(\frac{\mathcal{E}_{CR,0}}{{\rm eV\,cm^{-3}}}\right) \left(\frac{10^{-3} m_p c}{p_{\rm inj} c}\right) . \tag{5.25}$$

The previous estimate has to be taken carefully. It is worth stressing that the result in Eq. (5.24) is sensitive to the value of the spectral index s in the range $p_{\rm inj} < p < p_{\rm min}$. As we will show, in the low momentum range, the nonlinear theory predict a greather value for s, in such a way that Eq. (5.24) can easily reach the a value of order unity and even greather, especially in case of low ambient medium density.

5.3.3 General solution for the distribution function

Now we can write out the solution for $f(x,p)$. Using the shortening $\nu \equiv \ln(p)$, the equation (5.11) can be rewritten as follows:

$$\partial_x [D(x,\nu) \partial_x f] - u(x) \partial_x f + \frac{1}{3} u'(x) \partial_\nu f + Q(x,\nu) = 0 . \tag{5.26}$$

We make the following substitutions:

$$g(x,\nu) \equiv D(x,\nu)\partial_x f(x,\nu)\,, \tag{5.27}$$

$$b(x,\nu) \equiv \frac{1}{3}u'(x)\partial_\nu f(x,\nu)\,. \tag{5.28}$$

Eq. (5.26) become:

$$\partial_x g(x,\nu) = \frac{u(x)}{D(x,\nu)}g(x,\nu) - b(x,\nu)\,. \tag{5.29}$$

The solution of this equation is the sum of the solution of the homogeneous associated equation, $g_1(x,\nu)$, plus a particular solution $g_2(x,\nu)$:

$$g_1(x,\nu) = g_\circ(\nu)e^{-A(x,\nu)}\,, \tag{5.30}$$

$$g_2(x,\nu) = e^{-A(x,\nu)}\int_x^0 e^{A(x',\nu)}b(x',\nu)dx'\,, \tag{5.31}$$

$$\tag{5.32}$$

where

$$A(x,\nu) = \int_x^0 \frac{u(x')}{D(x',\nu)}\,dx'\,. \tag{5.33}$$

The boundary condition $g_\circ(\nu) \equiv g(x=0,\nu)$ can be derived from the boundary conditions of $f(x,\nu)$, as we will show in a while. Integrating the equation (5.27) from upstream infinity up to x, we get the implicit solution for f:

$$f(x,\nu) = f_\infty(\nu) + \int_{-\infty}^{x} \frac{g_1(x',\nu)+g_2(x',\nu)}{D(x',\nu)}dx'\,. \tag{5.34}$$

In the limit $x \to -\infty$, equation (5.34) give us no new information, while for $x \to 0$ it provides the following expression for $g_\circ$:

$$g_\circ(\nu) = \frac{f_\circ(\nu) - f_\infty(\nu) - \int_{-\infty}^0 g_2(x',\nu)/D(x',\nu)dx'}{\int_{-\infty}^0 e^{A(x',\nu)}/D(x',\nu)dx'}\,. \tag{5.35}$$

The final step is the substitution of equation (5.35) into (5.34). The full solution can be expressed as follows:

$$f(x,\nu) = f_\infty(\nu)\left[1 - G_1(x,\nu)\right] + f_\circ(\nu)\,G_1(x,\nu) + h(\nu)\left[G_2(x,\nu) - G_1(x,\nu)\right]\,, \tag{5.36}$$

where:

$$G_1(x,\nu) = \int_{-\infty}^{x} \frac{e^{A(x',\nu)}}{D(x',\nu)}dx' \Bigg/ \int_{-\infty}^{0} \frac{e^{A(x',\nu)}}{D(x',\nu)}dx' \; ; \tag{5.37}$$

$$G_2(x,\nu) = \int_{-\infty}^{x} \frac{g_2(x',\nu)}{D(x',\nu)}dx' \Bigg/ \int_{-\infty}^{0} \frac{g_2(x',\nu)}{D(x',\nu)}dx' \; ; \tag{5.38}$$

$$h(\nu) = \int_{-\infty}^{0} \frac{g_2(x',\nu)}{D(x',\nu)}dx' \, . \tag{5.39}$$

From their definitions, the functions G_1 and G_2 have the same value 1 for $x \to 0$, and 0 for $x \to -\infty$, hence equation (5.36) provides the correct boundary condition in these limits: $f(x \to 0, \nu) = f_\circ(\nu)$, and $f(x \to -\infty, \nu) = f_\infty(\nu)$. Equations (5.36)-(5.39) rapresent the formal solution of the problem in an iterative form: once both $D(x,p)$ and $u(x)$ are known, we can chose an arbitrary well defined $f^{(0)}(x,p)$ to compute u_p and $f_\circ$ using equations (5.18) and (5.17) respectively. This functions are in turn used to compute the new distribution function $f^{(1)}(x,p)$ by equation (5.36). The procedure can be iterated until the convergence is getted.

But a piece still misses: the value of $p_{\min}$ as appears in the equation (5.18) is not specified until now. At a first stage, one can argues that the value of $p_{\min}$ at the shock position should be an output of the solution, because the only relevant boundary conditions are $f_\infty(p)$, defined in the interval $[p_{\min,\infty}, p_{\max,\infty}]$, and the spatial derivative at infinity, i.e. $\partial_x f(x,p)|_{x=-\infty} = 0$. This turn out to be incorrect because in the equation (5.36) the distribution function is defined by iteration and we will show in the next section that when the solution of a PDE is expressed by an iterative form, the resulting domain could be different with respect to the exact solution.

5.3.4 Effect of compression on the momentum

The solution for the distribution function founded in the previous section is not complete because it does not include the correct domain in the phase-space (x,p). Such a problem arises because we use an iterative definition for $f(x,p)$ in therms of the boundary conditions $f_\infty(p)$ and the velocity function $u(x)$. If we use $f^{(0)}(x,p) \equiv f_\infty(p)$ as the first step of the iteration procedure, the domain of the solution turn out to be the simple Cartesian product $\mathcal{D}_p(f_\infty) \times \mathcal{D}_x(u)$. But this is not correct as we clarify with the following example.

Let us consider the problem of particle transport when the diffusion is not present. As for the full diffusion-convection problem, the solution can be expressed with an iterative formula. The convection equation without the diffusion term reads:

$$-u(x)\partial_x f + \frac{1}{3}u'(x)\, p\, \partial_p f(x,p) = 0 \, . \tag{5.40}$$

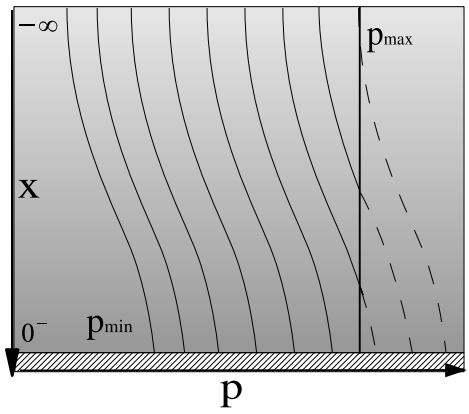

Fig. 5.2 Caracteristic lines for the convection equation.

If we divide equation (5.40) by $u(x)$ and integrate it from $-\infty$ up to x, we get the solution through the following iterative formula:

$$f(x,p) = f_{\infty}(p) + \int_{-\infty}^{x} p\,\partial_p f(x',p)\frac{1}{3\,u}\frac{du}{dx'}\,dx'\,. \tag{5.41}$$

Now if we chose f_{∞} as the first step of the iteration, we easily get the solution in form of a series:

$$f(x,p) = \sum_{n=0}^{\infty}\frac{1}{n!}\left(\frac{\log(u/u_{\circ})}{3}\right)^{n}\frac{d^n}{d\log^n p}f_{\infty}(p)\,. \tag{5.42}$$

If the upstream boundary condition is expressed as the usual power-law, $f_{\infty} \propto p^{-s}$, in the interval $[p_{\mathrm{min},\infty}, p_{\mathrm{max},\infty}]$, the series can be easily summed and gives us:

$$f(x,p) = f_{\infty}(p)\left[u(x)/u_{\circ}\right]^{-s/3}\,. \tag{5.43}$$

The solution (5.43) is correct, as one can easily check substituting it into equation (5.40), and it is defined in the rectangular domain $\mathcal{D}_p(f_{\infty})\times\mathcal{D}_x(u)$. But this is incorrect: if $u(x)$ is not constant, the fluid compression (or expansion) increases (or decreases) both the maximum and the minimum momenta. This conclusion can be recovered in a natural way if the compression equation is analyzed with the method of characteristics for first-order PDE. One as to find the first integral witch determines the characteristic lines $\phi(x,p)$. The solution does not depend on x and p as independent variables, but only by the function $\phi(x,p)$, i.e. $f(x,p) = f(\phi(x,p))$. The first integral is the solution of the following equation

$$\frac{dx}{3u/u'} = -\frac{dp}{p}\,. \tag{5.44}$$

which integrated from upstream infinity up to a point x gives the following results:

$$\phi(x,p) = p\,u(x)^{-1/3}\,. \tag{5.45}$$

Calling s the parameter along the characteristic lines, the convection equation can be rewritten in the new variables ϕ and s as:

$$u(\phi,s)^{2/3}\partial_s f(\phi,s) = 0\,. \tag{5.46}$$

This equation has the trivial solution $f = \text{const}$ along the caracteristic lines, i.e. $\phi = \text{const}$ (showed in the figure 5.2). This represents the correct consequence of the compression effect: if a particle has momentum $p_\circ$ at upstream infinity, at a point x its momentum become:

$$p(x) = p_\circ\left(\frac{u_\circ}{u(x)}\right)^{1/3}, \tag{5.47}$$

As a consequence the correct domain is $\phi_{\min} < \phi < \phi_{\max}$ i.e.

$$p_{\min,\infty}\left(u_\circ/u(x)\right)^{1/3} < p(x) < p_{\max,\infty}\left(u_\circ/u(x)\right)^{1/3}\,. \tag{5.48}$$

Now we can return to consider the full diffusion-convection problem. Firstly we note that the diffusion does not change the particle momentum modulus, but only its direction. This means that the fluid compression produces the same effect as in the simple convection problem, hence the particles momentum obey the compression equation (5.47). (Now the difference is that f is no more a constant along the $\phi = \text{const}$ lines). Following also the discussion about the injection process, the correct expression for the minimum momentum in the equation (5.18) is

$$p_{\min} = \max\left[p_{\rm inj}, p_{\min,\circ}\right] = \max\left[p_{\rm inj}, p_{\min,\infty}\left(R_{\rm tot}/R_{\rm sub}\right)^{1/3}\right]\,. \tag{5.49}$$

The tipical value of $p_{\min,\infty}$ is taken to be $10^{-3}mc$. When the shock is only slightly modified $p_{\rm inj} \gg p_{\min,\circ}$, but this relation can be reversed if the shock is strongly modified. Assuming that the injection obey the thermal leakage model, we can compute the value of $R_{\rm sub}$ at which $p_{\rm inj} = p_{\min,\circ}$:

$$\bar{R}_{\rm sub} = \left[\frac{\gamma_g - 1}{\gamma_g + 1} + \frac{2}{\gamma_g + 1}A^{3(\gamma_g+1)/4}M_0^{(3\gamma_g-5)/4}\right]^{-1}, \tag{5.50}$$

where

$$A = 2\,\xi\,\left(\frac{2(\gamma_g+1)}{\gamma_g - 1}\right)^{1/2}\left(\frac{p_{\min,\infty}}{mc}\right)^{-1}\left(\frac{K_B T_0}{mc^2}\right)^{1/2}\,. \tag{5.51}$$

It is worth to note that in the case of monoatomic non relativistic gas, i.e. $\gamma_g = 5/3$, $\bar{R}_{\rm sub}$ does not depend on M_0:

$$\bar{R}_{\rm sub} = \left[\frac{1}{4} + \frac{15}{16}\xi^2 \left(\frac{p_{\rm min,\infty}}{mc}\right)^{-2} \left(\frac{K_B T_0}{mc^2}\right)\right]^{-1} . \tag{5.52}$$

For the tipical values of the parameter assumed in this work ($T_0 = 10^5$K, $p_{\rm min,\infty} = 10^{-3}mc$ and $\xi = 3.5$) the value of $\bar{R}_{\rm sub}$ is ~ 2.813.

5.4 Algorithm to get the solution

In this section we will summarize the procedure to get the full solution. We start from the boundary values of the gas state at upstream infinity: $u_\circ$, M_0 and $P_{CR,0}$; than we chose a value for R_{sub} which in turn fixes the value of CRs pressure at the sub-shock front $\xi_c(0)$ through equation (5.7). At this point we start the iterative process using for the first step the functions $u^{(0)}(x) \equiv u_\circ$ and $f^{(0)}(x,p) \equiv f_\infty(p)$. For the pre-existing CRs distribution we adopt the spectrum as observed at the Earth, i.e a power-law with index $s = 4.7$ and normalized in such a way that the CRs pressure and the gas pressure are equal at upstream infinity. The next steps are made using in sequence the equations (5.18), (5.36), (5.4), (5.6), (5.49) and again (5.18) to get the following chain:

$$\left\{ \begin{matrix} u_\circ \\ f_\infty(p) \end{matrix} \right\} \overset{(4.16)}{\Longrightarrow} f^{(0)}_\circ(p) \overset{(4.27)}{\Longrightarrow} f^{(1)}(x,p) \overset{(4.4)}{\Longrightarrow} \xi^{(1)}_c(x) \overset{(4.6)}{\Longrightarrow} u^{(1)}(x) \overset{(4.40)}{\Longrightarrow} p^{(1)}_{\rm min}(x) \overset{(4.16)}{\Longrightarrow} f^{(1)}_\circ(p) \, .$$

Now we note that the resulting $f^{(1)}_\circ(p)$ cannot be used as the starting function for a new iteration, because when integrated it give rise to a CRs pressure at the sub-shock different from $\xi_c(0)$. To go beyond this difficulty we define the re-normalized function $\bar{f}^{(1)}_\circ = \lambda_1 f^{(1)}_\circ$, where

$$\lambda_1 = \frac{4\pi}{3\xi_c(0)} \int dp\, p^3 v(p) f^{(1)}_\circ(p) \, , \tag{5.53}$$

and we use it as the new input for the algorithm. The procedure is repeated until the convergence is getted. The resulting value of λ tell us if the solution is a good one or not: $\lambda = 1$ correspond to a physically acceptable solution. Varying $R_{\rm sub}$ in the whole allowed range, i.e. between 1 (completely modified shock with no sub-shock) and $M_0^2(\gamma_g + 1)/(2 + M_0^2(\gamma_g - 1))$ (unmodified shock) we look for such solutions.

We note that the procedure just described is equivalent to solve a non linear eigenvalue problem for $f_\circ$, i.e.

$$G[f_\circ] = \lambda\, f_\circ(p) \, , \tag{5.54}$$

and looking for an eigenfunction with eigenvalue equal to 1. The operator G hides all the previous described operations.

Two comments are in order. The first question that one can ask is whether the solution actually exists or not. Unfortunately from the theoretical point of view there are no theorem that guarantee neither the existence of a solution and not even its unicity.

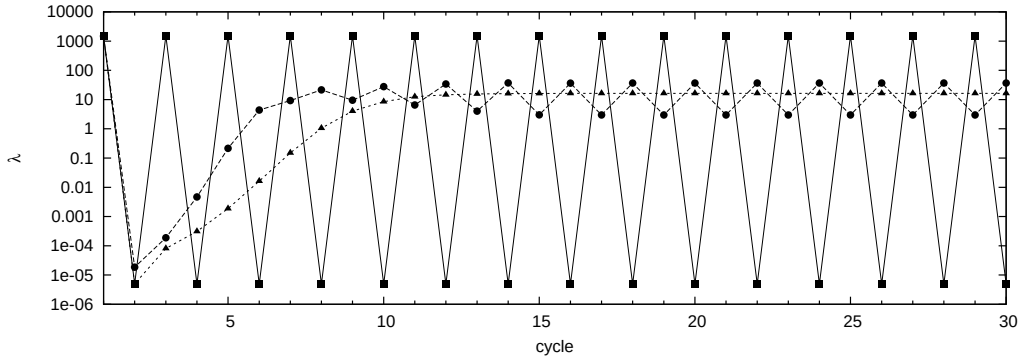

Fig. 5.3 Behaviour of the iterative algorithm described in §5.4: comparison between convergent and oscillating cases iterative algorithm resulting from the use of different recipes for the normalized function $\bar{f}_\circ(p)$. $M_0 = 100$, $T_0 = 10^5$K, $p_{\max,\infty} = 10^6$ and $R_{\rm sub} = 2.4$. See the text for the detailed description of each case.

The second non trivial question is: assumed that the solution exist, does the algorithm actually converge? The algorithm as described above converge only some values of $R_{\rm sub}$ and M_0 (basically when the shock is only slightly modified). As an example we report in Figure 5.3 (with filled square points and solid line) the behaviour of the algorithm for $M_0 = 100$, $T_0 = 10^5$K, $p_{\max,\infty} = 10^6$ and $R_{\rm sub} = 2.4$. The plot shows how λ oscillates between two values, to which correspond two different functions for $f_\circ(p)$.

A possible way to get the convergence in the whole region of space parameters we are interested in, is by changing the definition of $\bar{f}_\circ$ (obviously without changing the normalization at $x = 0$). The most general expression for $\bar{f}^{(n)}_\circ$ can be build as a linear combination of the $f^{(k)}_\circ$ with $k \leq n$:

$$\bar{f}^{(n)}_\circ = \alpha_1 \lambda_n f^{(n)} + \alpha_2 \lambda_{n-1} f^{(n-1)} + ... + \alpha_k \lambda_{n-k+1} f^{(n-k+1)}, \qquad (5.55)$$

with the constraint $\alpha_1 + \alpha_2 + ... + \alpha_k = 1$. In Figure 5.3 we have plotted what happen choosing only the first two functions with $\alpha_1 = \alpha_2 = 1/2$ (filled-triangle) and $\alpha_{k>2} \equiv 0$: the convergence is getted after few iterations. Choosing three function, with $\alpha_1 = \alpha_2 = \alpha_3 = 1/3$ (filled-circle), the solution oscillate again. We fix our attention to the former case with two functions. Different behaviour can be observed changing the relative values of α_1 and α_2. Figure 5.4 shows what happen for $\alpha_1 > \alpha_2$ (upper panel) and for $\alpha_1 < \alpha_2$ (lower panel). While in the former case the behaviour is chaotic, in the latter case the convergence is always getted and the combination $\alpha_2 = 3\,\alpha_1$ allows to get the convergence in the shortest number of cycles.

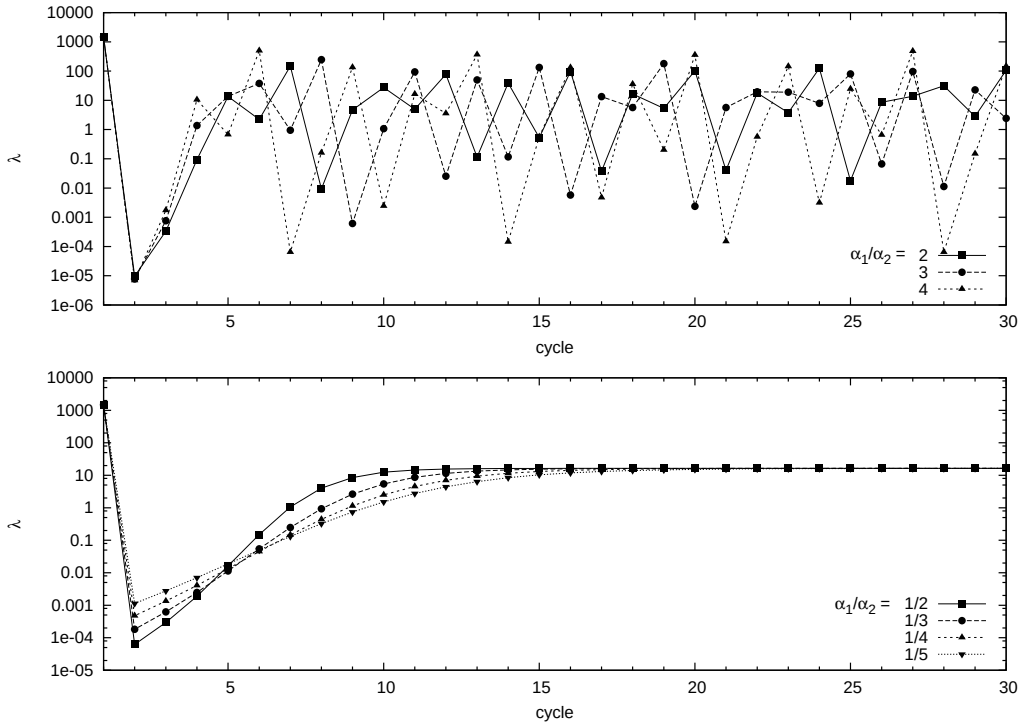

Fig. 5.4 Behaviour of the algorithm when $\bar{f}_{\circ}^{(n)} = \alpha_1 \lambda_n f^{(n)} + \alpha_2 \lambda_{n-1} f^{(n-1)}$. For $\alpha_1 > \alpha_2$ (*upper panel*) the convergence is never getted, the behaviour is somehow chaotic (the plot shows only three cases with $\alpha_1/\alpha_2 = 2, 3, 4$). On the other hand, when $\alpha_1 < \alpha_2$ (*lower panel*) the algorithm converges always. All the other parameters are the same as in Figure 5.3.

5.5 Results

Now that all the mathematical machinery has been described in the previous sections, the rest of the chapter will be devoted to present some results about the modification of the shock structure under the influence of non-thermal particles. We first analyse the results when only a pre-existing population of non-thermal particles is presents (§5.5.1). Secondly, in §5.5.2, we investigate the situation where both seed particles and injection at the sub-shock discontinuity are take into account.

5.5.1 Re-acceleration of seed particles

In this section we explore the consequence of a shock propagating into a region with a pre-existing non-thermal particle population. In the introduction we just emphasize the importance of this study: while the possibility of particles injection at the shock, although widely accepted, suffers from big uncertainties, the presence of cosmic rays into the Galaxy is well established. A shock propagating into the interstellar medium cannot avoid the dynamical effect of galactic CRs, hence the knowledge of such effect turn out to be of primary importance to understand the evolution of a shock. We expect that such effect is expecially important during the early stage of a shock, when the contribution of the injection is negligible. Moreover, as we will show in the next section, the knowledge of the effect of seed particles onto the shock could help us to understand better the injection process itself.

As found by Blasi (2004) the presence of a CRs component is able to modify a shock also if the injection is neglected. The cited author use an approximate solution for the equation (5.11). Here, using the correct solution as developed in the previous sections, we will show that such conclusions are correct.

In the following we assume that a plane shock propagates with velocity $u_\circ$ into a plasma with temperature $T_0 = 10^5$K. Because we have in mind a SNRs shock propagating into the interstellar medium, we adopt a power-law spectrum to describe the non-thermal particle distribution:

$$f_\infty(p) = N_\infty p^{-s}. \tag{5.56}$$

For the spectral index we use the value $s = 4.7$ as results from the CRs spectrum observed at the Earth below the knee. The normalization is determined assuming the pressure equilibrium between the gas and the CRs component, i.e $P_{g,0} = P_{CR,0}$, a relation roughly respected into the interstelar medium. We note that the assumption of pressure equilibrium can be easily relaxed if one wants to study a shock propagating into a different environment, as could be the high density stellar formation regions, or shock produced into the AGNs jets or lobes.

The seed particle distribution is defined in the range $[p_{\min,\infty}, p_{\max,\infty}]$. The maximum momentum is fixed by the shock acceleration process and its detailed calculation is a very difficult task. $p_{\max,\infty}$ is determined not only by the dimension of the acceleration region and by the energy losses; a crucial role is played by the magnetic field amplification as firstly pointed out by Bell & Lucek (2001). As shown by Blasi et al. (2007)

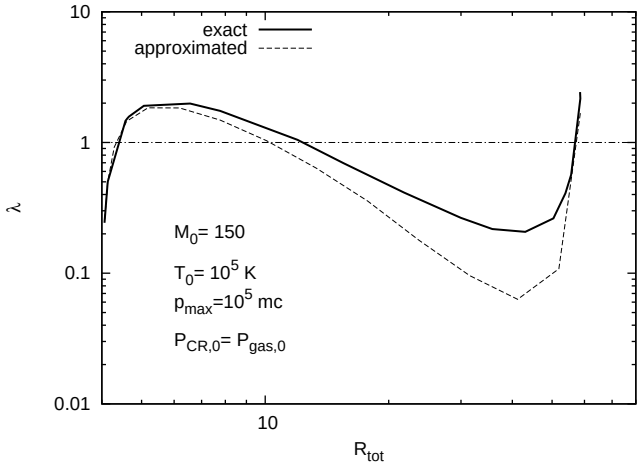

Fig. 5.5 Comparison between the approximated method used in Blasi (2004) (*dotted-line*) and the exact method developed here (*solid-line*). The plot shows the eigenvalue λ as a function of $R_{\rm tot}$ for a single case with the parameters value as show in the caption. The physical acceptable solution are those for which $\lambda = 1$.

the $p_{\rm max,\infty}$ can be as hight as $10^6 mc$ when the effect of magnetic field amplification are take into account. Here we adopt $p_{\rm max,\infty} = 10^6 mc$ unless differently specified. We note that if the seed particle spectrum extends above $p_{\rm max,\infty}$, particles with $p > p_{\rm max,\infty}$ can be neglected because they escape from the acceleration region without take part to the acceleration process. The minimum momentum of the seed particle is taken to be $p_{\rm min,\infty} = 10^{-3} mc$.

Following the procedure described in §5.4 we find the solution varying the value of $R_{\rm sub}$ (and hence also $R_{\rm tot}$ by equation (5.10)) and looking for the solution with $\lambda = 1$. Because we are considering only the seed particles, equation (5.18) can be simplified dropping out the first addend $f_{\circ}^{\rm inj}$. For what concern the diffusion coefficient $D(p)$, we adopt a Bohm diffusion with a spatially-constant magnetic-field density. We are aware that such a choice is unrealistic, but it does not affect our main conclusions.

The first comment concerns the comparison between our results and that of Blasi (2004). As pointed out by the cited author, the major problem concerns the appearance of multiple solutions. This problem is not resolved using our correct solution for the particle distribution. Figure 5.5 compares the results for the function $\lambda(R_{\rm tot})$ using the approach of Blasi (2004) (dotted line) and the one presented here (solid line) for the following value of the parameters: $M_0 = 100$, $T_0 = 10^5$K and $p_{\rm max} = 10^5 mc$. First of all we note that both the curves presents 3 solutions. The main difference concerns the middle solution, while the unmodified ($R_{\rm tot} \sim 4$) and the strong-modified ($R_{\rm tot} \sim 58$ solutions are essentially the same. A detailed study performing the variation of the parameters value shows that our approach reduces somehow the region of the space parameter where the multiple solutions are present, but it is far from resolve the problem.

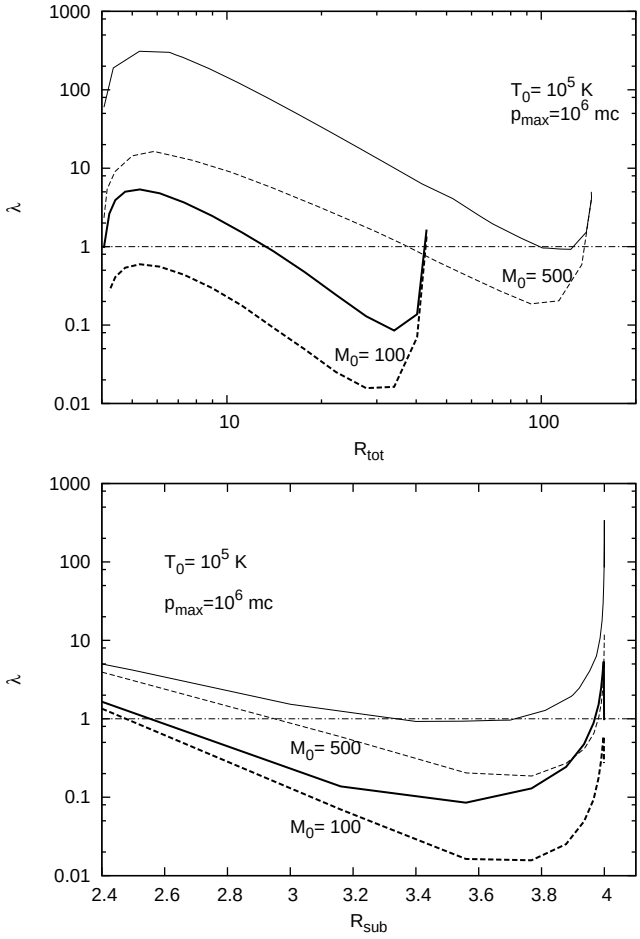

Fig. 5.6 *Upper panel*: this plot shows the difference between the results with and without the constraint on $p_{\rm inj}$. Each curve represents the value of the eigenvalue λ as a function of $R_{\rm tot}$. The solutions of the problem correspond to $\lambda = 1$. Two values of Mach number are shown, $M_0 = 100$ (thick lines) and $M_0 = 500$ (thin lines) with the same temperature and maximum momentum (as indicated in the figure). The dashed lines result from the calculation under the assumption that all the seed particles undergo the acceleration process, while for the solid lines only particle with $p > p_{\rm inj}$ are consideres. It is clear that the problem of multiple solution is still present, but the region of the parameter space where multiple solutions appear is somehow translated.
Lower panel: the same as the upper panel but for λ as a function of $R_{\rm sub}$.

As occurs for the injection at the sub-shock, one can suppose that only particles with the momentum above a defined threshold, namely $p > p_{\rm inj}$, can cross the shock and start the acceleration process. If we adopt this recipe also for the seed particles, with $p_{\rm inj}$ determined by the thermal leakage model itself (but excluding the injection of thermal particles) multiple solutions persist. Figure 5.6 compares the results when all the incoming particles take part to the acceleration (dashed lines) with the situation where the restriction $p > p_{\rm inj}$ is applied (solid lines). Two value of Mach number are considered, $M_0 = 100$ and 500, with $T_0 = 10^5$K and $p_{\rm max} = 10^6 mc$. One time more the multiple solutions appear but the space parameter region where this happens is somehow translated towards lower value of the Mach number. We also note that the strong modified solution (the one with the greatest $R_{\rm sub}$) remain almost unaltered.

We are aware that the appearance of multiple solutions is connected to the non-linear nature of the modified-shock problem and does not depend on the approximations made, for example, either on the form of the diffusion coefficient or on the value of $p_{\rm max}$. From one hand we can suspect that one or more solutions could be unstable, hence unimportant from the physical point of view. Such a conclusion is achieved by Mond & O'C. Drury (1998) who use the two-fluid model approach to demonstrate that the intermediate solution is unstable to corrugations in the shock structure and emission of acoustic waves. On the other hand the stationarity assumption itself could be unphysical, hence the problem should be solved in a time dependent way.

5.5.2 Acceleration in presence of seed particles and injection

In the previous section we showed how the Galactic component of CRs can modify the shock structure in a significative way. In the present section we address the more complicated scenario where, besides the pre-existing population of CRs, also the injection of particles at the sub-shock front occurs.

It is worth remembering that in the situation where only injection is take into account, the problem of multiple solutions is strongly reduced if a feedback mechanism, like the thermal leakage recipe (equation (5.13)) is implemented into the shock dynamics. This happens because the thermal leakage acts in such a way to allow the shock to self regulate (see Blasi et al. (2005)): more is the modification less are the particles injected. When the seed particles are added the situation become generally worse, because the feedback mechanism does not apply to them. In spite of this, for what may concern the SNRs shock scenario, the parameters region of physical interest presents only a single solution.

As an example, in Figure 5.7 we compare the three different cases that take into account *(i)* only the seed particles (dashed line), *(ii)* only the injection (dotted line) and finally *(iii)* both the contributions (solid line). The parameters are fixed as shown in the caption. The situations *(ii)* and *(iii)* both present a single solution. The figure shows only the case with $M_0 = 100$, but the same conclusion apply for a wide range of the Mach number value: Figure 5.8 shows the results for M_0 ranging from 50 to 500 when both the pre-existing CRs and the injection are take into account.

Restricting our discussion to that cases that present only a single solution, it is interesting to analise the particle spectrum depending on whether the seed particles

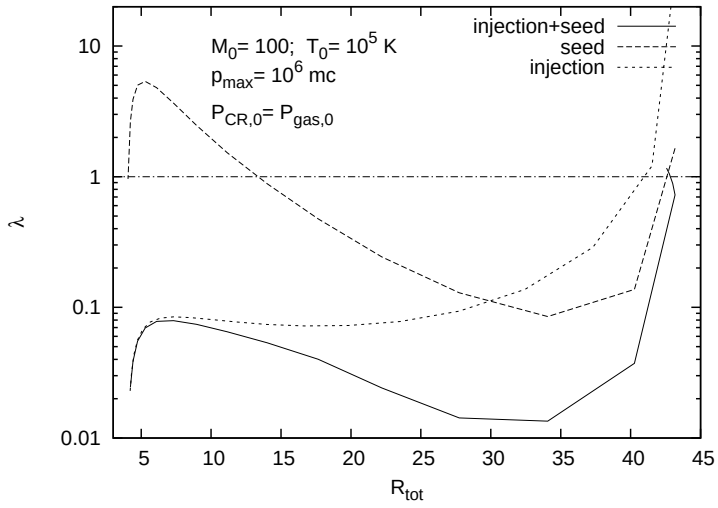

Fig. 5.7 Comparison between the solutions of the modified shock problem obtained in the three different situations: only seed particles (*dashed-line*), only injection from the thermal bath (*dotted-line*) and both the previous (*solid-line*). For all the three cases the parameters are fixed as shown in the caption.

are included or not. Such a comparison is shown in Figure 5.9, as usual, for several values of the Mach number. The upper panel shows the particle spectrum $f_\circ(p)$ at the sub-shock position. In the case where the galactic CRs are take into account (solid line), the spectrum turns out to be steeper at low energy, while at high energy remains unchanged with respect to the case where only injection is considered. The steepness of the spectrum is enhanced going from hight Mach numbers towards lower ones. This result can be confirmed looking at the corresponding values of the sub-shock and the total compression factors. Lower panels of the same figure show $R_{\rm sub}$ (left side) and $R_{\rm tot}$ (right side) as a function of M_0. While the value of $R_{\rm tot}$ changes very little in passing from the solution without seeds to that with both seeds and injection, $R_{\rm sub}$ results in a strong reduction, in accordance with the modification of the spectrum only at low energy.

The reason of such behaviour at low energies lies in the different shape of the spectrum derived by the seed particles and the one resulting only from the injection, namely the functions $f_\circ^{(\rm seed)}(p)$ and $f_\circ^{(\rm inj)}(p)$ as defined in the equation (5.18). In the limit $p \to p_{\rm inj}$ the former goes to zero while the latter increases towards higher values. In principle this difference can be used to measure the relative weight of the two contributions, as we will show in a while. It is worth to remember that $f_\circ^{(\rm inj)}(p)$ strongly depends on the parameter ξ that regulates the efficiency of the injection process (see Eq. (5.13)). Until now we have assumed the arbitrary value 3.5, but it is needless to say that we are not able to compute the exact value of ξ because the very poorly-know physics that stays behind the injection mechanism. It could be very interesting if such

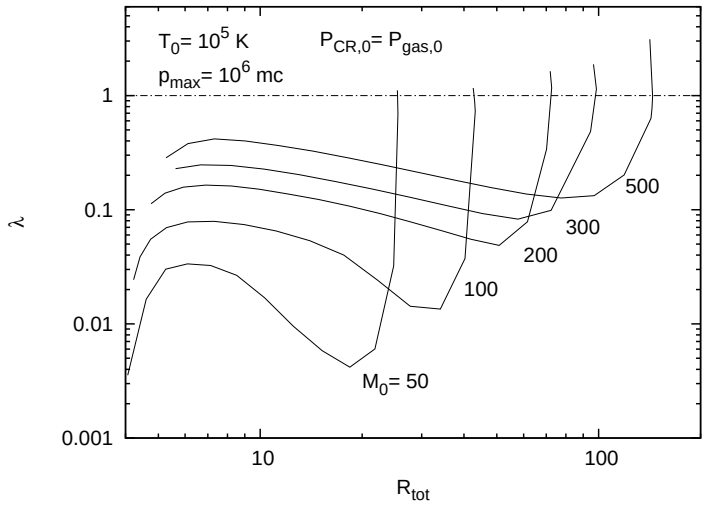

Fig. 5.8 Result of the modified shock problem when both injection and seed particles are considered for several values of Mach number as shown in the caption.

parameter could be estimated from the observations. For this aim we have shown in Figure 5.10 what happens to the particle spectrum when the value of ξ changes. Both the component $f_\circ^{(\mathrm{seed})}(p)$ and $f_\circ^{(\mathrm{inj})}(p)$ are shown, together with their sum $f_\circ(p)$. We have performed the computation at a fixed Mach number (100) for three different values of ξ, namely 3.25, 3.5 and 3.75, which correspond to an injection efficiency η of about $6.6\cdot10^{-4}$, $1.9\cdot10^{-4}$ and $4.8\cdot10^{-5}$ respectively. The corresponding change in spectrum at low energy is significative: going from $\xi = 3.25$ up to $\xi = 3.75$ the spectrum varies over an order of magnitude in the region where $p \sim p_{\mathrm{inj}}$. Also the local slope $q(p) \equiv -\frac{d\log f_\circ}{d\log p}$ changes, decreasing from ~ 5.2 down to 4.3, as shown in the lowest panel of the same figure. For lower Mach numbers the difference become more pronounced.

Unfortunately we have no way to measure such difference in the low energy region of the spectrum.

5.6 Conclusions

In this chapter we presented the full solution for the stationary problem of a shock propagating into a plasma including the back reaction of the non-thermal particles. Our main goal is the study of shock modification under the action of a pre-existing non-thermal particle population. This study is motivated by a trivial remark: astrophysical shocks like SNRs shocks, propagates into the interstellar medium where a Galactic Cosmic Rays population already exists. This is true for every SNR, expecially those that expand in the so called *superbubbles*, i.e. regions with a high concentration of massive stars, where the rate of supernovae explosions can be so frequent that energetic particles can be accelerated by several shocks, before leaving the region.

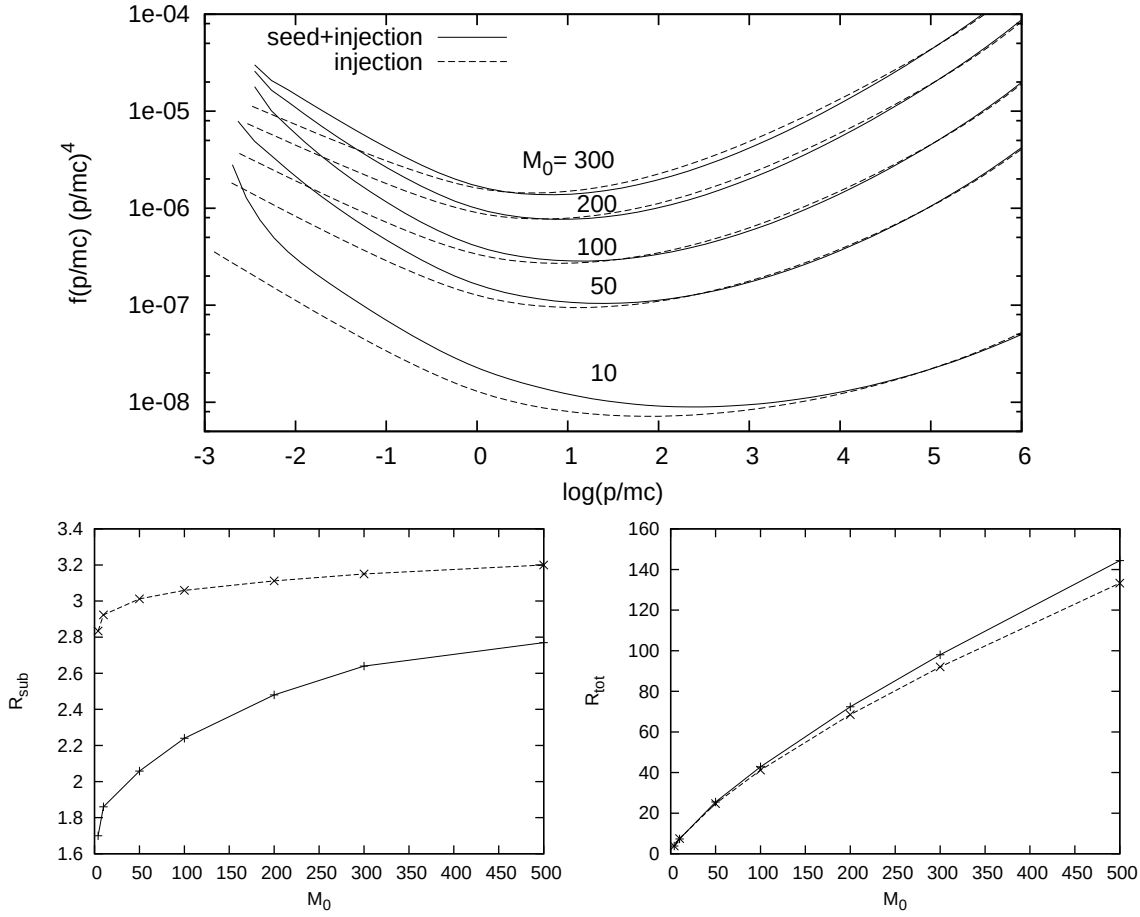

Fig. 5.9 Comparison between the solutions obtained when only the injection at the shock front in considered (*dashed lines*) and when also the seed particles are added (*solid lines*). Temperature and $p_{\max}$ are fixed at $10^5 K$ and $10^6 mc$ respectively, while the injection efficiency is fixed at $\xi = 3.5$. The *upper panel* shows the non-thermal spectrum as observed at the sub-shock front for several values of the Mach number, as reported in the caption. In the *lower panels* the relatives values of $R_{\rm sub}$ and $R_{\rm tot}$ are shown as a function of the Mach number (left and right side respectively).

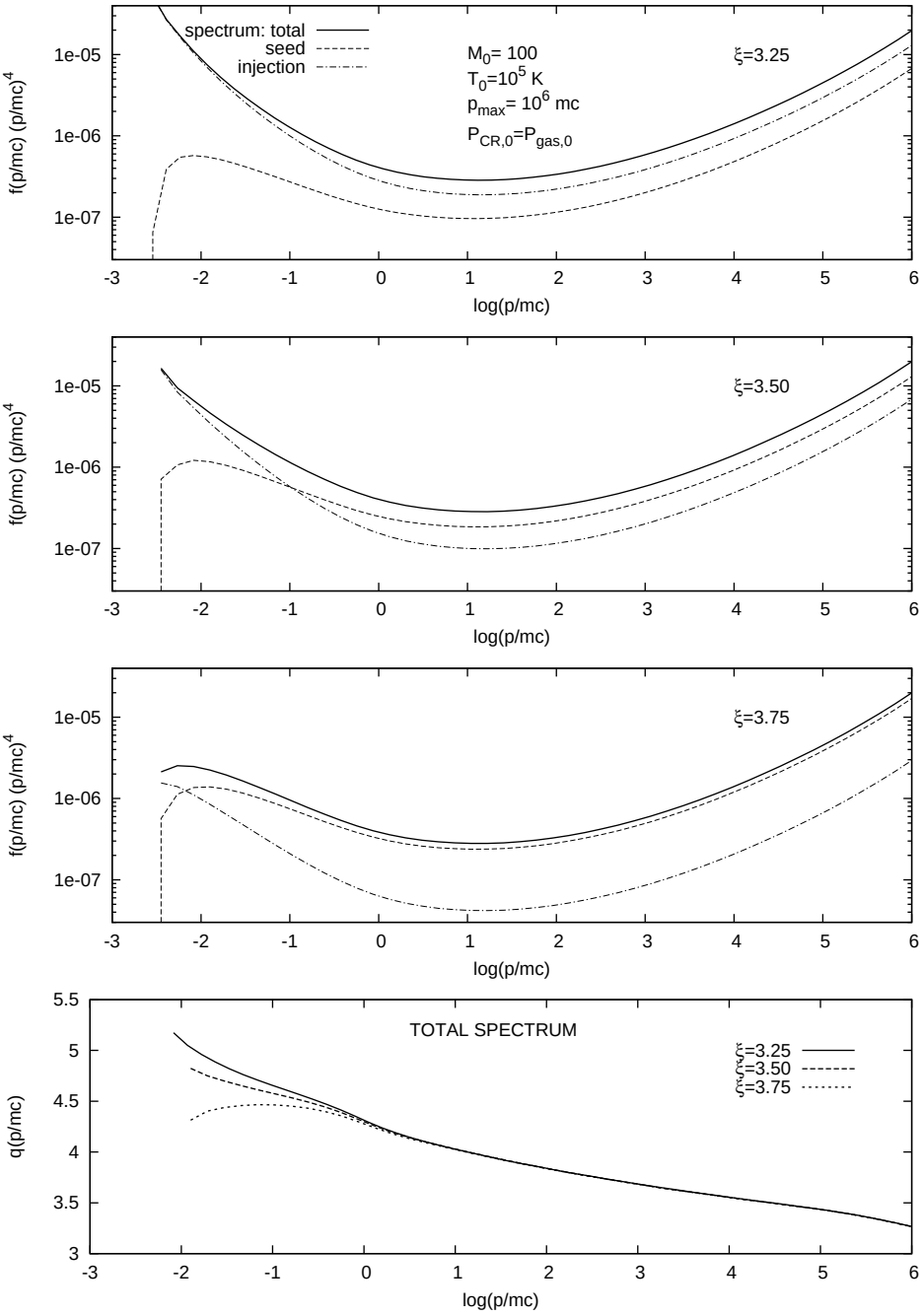

Fig. 5.10 The total non-thermal particle spectrum $f_\circ(p)$ as a function of the momentum is shown in the three upper panels (solid lines) as results for three different values of the parameter ξ, namely 3.25, 3.50 and 3.75. The other parameters are fixed as shown in the caption. The two components of the spectrum, $f_\circ^{(\mathrm{seed})}$ and $f_\circ^{(\mathrm{inj})}$, are also shown separately with dashed and dot-dashed lines respectively. The lower panel compares the local slope of the total spectrum for the three cases.

The test-particle theory of re-acceleration of non-thermal particle was firstly presented by Bell (1978b), who estimated that each shock passage can enhance the particle energy by an order of magnitude. He further pointed out that, in the limit of infinite number of shocks passing in the same region, the particle spectrum tends to a power low in energy $E^{-3/2}$. This means that a lot of energy is channelled into non-thermal particles. Hence a non linear treatment is clearly required.

The first attempt to develop the non-linear generalization of such theory was presented by Blasi (2004), which used an approximate solution for the diffusion-convection equation. The author recognized the role of the seed particles in producing modified shocks, also in the absence of the injection from the thermal pool.

With respect to the previous studies, here we solve exactly the diffusion-convection equation. Hence we use the correct solution for the spectrum to perform detailed calculation of the particle spectrum in the tipical scenario of a SNR expanding into the interstellar medium. We confirm the result of Blasi (2004), finding that the pre-existing CRs can modify a shock in a stronghest way with respect to what injected particles can do alone. This means that test-particle approach can never been used, also if the injection would be negligible.

We also perform the computation of the spectrum fixing the contribution of the pre-existing cosmic rays, assumed in pressure equilibrium with the interstellar gas, and varying the injection efficiency. We find that the low energy region of the spectrum is remarkable affected by the variation of the injection efficiency, while the high energy region remains unchanged.

The main problem concerning the modified shocks is the presence of multiple solutions, that persist also when the diffusion-convection equation is solved without approximations. In spite of the fact that the problem presents only a single solution in a wide range of the parameter space of physical interest, the multiple-solution problem may hide a subtle issue. First of all it is possible that one or more solutions are not stable. While in the contest of the two fluid model this turn out to be the case, stability study of the kinetic approach had not been performed yet. A second possibility is that the assumption of stationarity could be incorrect. It is possible that the shock continuously evolves and never settle in a stationary solution, like many non linear systems. If this were the case, the problem should be solved in a time dependent way.

Conclusions and final remarks

In this work we investigate several aspects of the particle acceleration mechanism at shock waves. The work is structured into two macroscopic parts. In the first part (Chapters 2, 3 and 4) we study acceleration mechanism in the test-particle approximation for shocks with arbitrary velocity , while Chapter 5 is dedicated to the non-linear shock theory restricted to Newtonian shocks.

In Chapter 3 we carried out exact calculations of the angular distribution function and spectral slope of the particles accelerated at plane shock fronts moving with arbitrary velocity, generalizing a method previously described in detail in Vietri (2003) and Blasi & Vietri (2005) (which is summarized in Chapter 2). In particular, we specialized our calculations to two situations:

1. presence of a large scale coherent magnetic field of arbitrary orientation with respect to the shock normal, in the upstream fluid;

2. anisotropic scattering of the particles both in the upstream and in the downstream plasmas.

Our calculations allowed us to describe the importance of the inclination of the magnetic field when this has a large coherence length and there are no scattering agents upstream. For newtonian shocks, only quasi-perpendicular fields (namely perpendicular to the shock normal) are of practical importance, in that the return of particles to the shock from the upstream section is warranted. Quasi-parallel shocks imply a very low probability of return, so that the spectrum of accelerated particles is extremely soft. The process of acceleration eventually shuts off for parallel shocks. For relativistic shocks, the situation is less pessimistic because the accelerated particles and the shock front move with comparable velocities in the upstream frame. In general, the acceleration stops being efficient when the cosine of the inclination angle α of the magnetic field with respect to the shock normal is comparable with the shock speed in units of the speed of light. As a matter of fact, in this case the presence of only a large scale magnetic field upstream leads to particle leakage to upstream infinity. This latter phenomenon disappears when scattering is present, in that scattering always allows for the shock to reach the accelerated particles. In this case the probability of returning to the shock at an arbitrary direction is unity. One can ask when and how the transition from a situation in which there is no scattering to one in which scattering is at work takes place. When some scattering is present but the energy density in the scattering agents (e.g. Alfvén waves) is very low compared with the energy density in the background magnetic field, only very low energy particles are effectively scattered. When their energy becomes large enough, they only feel the presence of the coherent field. Increasing the amount of scattering, this transition energy becomes gradually higher. Particles whose Larmor radius is larger that the coherence scale of the magnetic field can eventually escape the accelerator. In general the level of turbulence (and therefore of scattering) and the number of accelerated particles are not independent since the turbulence may be self-generated through streaming-like instabilities (Bell 1978a).

Always in Chapter 3 we extended our analysis to the very interesting case of anisotropic scattering in both the upstream (unshocked) and downstream (shocked) medium. The pattern of anisotropy, which clearly depends on the details of the formation and development of the scattering centers, has been parameterized in four different scenarios, and for each one we calculated the angular part of the distribution function and the spectrum of the accelerated particles. Deviations from the predictions obtained in the context of isotropic small angle scattering (SPAS) and large angle scattering (LAS) have been quantified: the typical magnitude of these deflections is a few percent, but there are situations in which the deviation is more interesting, in particular because it goes in the direction of making spectra harder.

In Chapter 4 we develop a general parametric plasma equation of state to handle in a more realistic way the problem of acceleration at shock waves propagating through a plasma. This equation of state is applied to the shocked downstream plasma to get the velocity ratio needed to compute the spectrum of accelerated particles. We consider a simplified model of proton-electron plasma to take into account:

1. collective plasma effects that allow energy transfer from protons to electrons;

2. generation of turbulent magnetic field.

We analyse how these processes alter the compression factor of downstream plasma. We find values for the downstream fluid velocity very different from what predicted assuming that the plasma behaves like an ideal gas, a simplification that is generally adopted in the literature.

These results for the downstream fluid velocity are combined with the theory of shock acceleration of Chapter 2, to get the spectral slope s of accelerated particles. Two different regimes for particles diffusion are considered in the upstream fluid: small angle scattering and deflection by a static magnetic field. For the downstream fluids only the SPAS regime is considered. The spectral slope is shown as a function of shock speed from Newtonian to fully relativistic values, and for several values of equation of state parameters. We show how the presence of a turbulent magnetic field lead to softer spectra as a consequence of strong magnetic pressure contribution. On the other hand, energy transfer from protons to electrons have the opposite effect: it reduces the total pressure leading to harder spectra.

Fermi I order mechanism is usually believed to give the same results independently from the microphysics. This is true only at a superficial glance. The results presented in Chapter 4 show that a correct shock acceleration theory cannot neglect the microphysics of a plasma even if this could not directly affect the diffusion process of high energetic particles. Hence we belive that a deep study of the complex microphysics that regulate plasma interactions is needed.

In the last part of this thesis, Chapter 5, we presented the general solution for the stationary diffusion-convection equation describing the acceleration at shock that propagates with constant (Newtonian) speed, including the dynamical reaction of the accelerated particles, and for arbitrary diffusion coefficient. Our solution allows one to include the effect of a pre-existing nonthermal particle population. We try to answer two principal questions: *i)* whether a correct mathematical treatment can help to solve

the problem of multiple solutions, and *ii)* under which conditions the presence of a pre-existing nonthermal particle population can affect the shock dynamic.

The answer to the first question is negative. Multiple solutions are still present even when the diffusion-convection equation is solved without approximations. Even if some authors have demonstrated that this problem is alleviated when a reasonable recipe for the injection is assumed (Blasi et al. 2005), the multiple solutions is not a mere mathematical question, but can hide a subtle issue: it is either possible that one or more solutions are not stable (like happens in the context of the two fluid model) or the assumption of stationarity could be incorrect. It is indeed possible that the shock continuously evolves and never settle into a stationary solution, like it happens in many non linear systems. If this were the case, the problem should be solved in a time dependent way.

For what concerns the point *ii)*, we showed that the contribution of a pre-existing energetic particle's flux, like the Galactic CRs, whose pressure is comparable to that of the ISM, can in general affect the shock dynamics. As a consequence shocks like those generated in a SN explosion, that propagates into the Galactic environment can evolve in a nonlinear way even if the injection of fresh particles were not an efficient process. This consideration could be even more important in situations where CRs pressure is supposed to be stronger, like stellar regions with high rate of SN explosions (OB association).

Appendix

Jump Conditions for perpendicular shocks

In this Appendix we want to discuss to some extent the dynamical role of a coherent magnetic field in the shock process. In Chapter 3 we have just discussed how the coherent field can diffuse particles and drive the acceleration process also in the absence of a random diffusion. In that case we completely neglect the contributions of magnetic pressure and energy in computing the jump conditions. This is correct when we deal with a magnetic field whose energy density is negligible with respect to the shock's kinetic energy, as is the case for the interstellar field. Nevertheless in some astrophysical environments the field contribution to the energy density could be strongest and the shock dynamic can significantly be altered. It is also worth to remember that when we deal with strictly parallel shocks, as we done in Chapter 5, the field has no influence onto the shock, no matter its energy density is. In that case the field's only role is to support the Alfvén waves that tie together the plasma and the CRs.

On the other hand, when the field is not parallel to the shock normal (*oblique shock*) it can alter significantly the shock jump conditions. In the Figure A.1 we sketch an oblique shock in the normal incident frame. A straight magnetic field exerts an isotropic pressure equal to $B^2/(8\pi)$, that has to be included in the momentum and energy conservation. Moreover, because the orthogonal component of the field is compressed at the shock, the field direction changes and, as a consequence, at the discontinuity the field exerts a tension force onto the plasma in the $x - y$ plane. This means that the plasma can convert momentum from the x to the y direction.

In this case the jump condition become more complicated than the Rankine-Hugoniot or Taub jump conditions, because we need to add the components of the energy-momentum tensor along the y direction. For simplicity we consider here only the case of perpendicular shocks. In this case the tension force disappear and the problem return to be one-dimensional. We only need to take into account the magnetic pressure and energy. We firstly resolve the problem for Newtonian shocks, obtaining an analytic expression for the compression factor, than we solve numerically the relativistic case.

A.1 The Newtonian limit

For the sake of completness we report in the following the full MHD jump conditions for the oblique non-relativistic shocks. Besides the fluid's mass, momentum and energy conservation along the x direction, we need to add the source-free Maxwell equations for the magnetic field, $\nabla \cdot \mathbf{B} = 0$ and $\nabla \times (\mathbf{u} \times \mathbf{B}) = 0$. Expressed in a vectorial

form, the jump conditions reads:

$$[\rho\,\mathbf{u}\cdot\hat{\mathbf{n}}] = 0\,, \tag{A.1}$$

$$\left[\rho\,\mathbf{u}\,(\mathbf{u}\cdot\hat{\mathbf{n}}) + p + B^2/8\pi - (\mathbf{B}\cdot\hat{\mathbf{n}})\,B/4\pi\right] = 0\,, \tag{A.2}$$

$$\left[\mathbf{u}\cdot\hat{\mathbf{n}}\left(\frac{1}{2}\rho u^2 + \frac{\gamma_g}{\gamma_g - 1}\,p + \frac{B^2}{4\pi}\right) - \frac{(\mathbf{B}\cdot\hat{\mathbf{n}})(\mathbf{B}\cdot\mathbf{u})}{4\pi}\right] = 0\,, \tag{A.3}$$

$$[\mathbf{B}\cdot\hat{\mathbf{n}}] = 0\,, \tag{A.4}$$

$$[\hat{\mathbf{n}}\times(\mathbf{u}\times\mathbf{B})] = 0\,. \tag{A.5}$$

Here $[x]$ means the difference between the downstream and the upstream values, i.e $[x] = x_2 - x_1$. $\hat{\mathbf{n}}$ is the normal to the shock surface and the fluid is considered ideal with the adiabatic index γ_g. In the case of orthogonal shocks the jump conditions strongly simplified: Eqs. (A.4) and (A.5) simply give $B_{2,x} = B_{1,x}$ and $B_{2,y} = r\,B_{1,y}$, where r is the usual compression factor, $r = u_1/u_2$. Eqs. (A.2) and (A.3) become respectively:

$$1 + \frac{1}{\gamma_g M_1^2} + \frac{1 - r^2}{2\,M_A^2} = \frac{1}{r}\left(1 + \frac{1}{\gamma_g M_2^2}\right)\,, \tag{A.6}$$

$$\frac{1}{2} + \frac{1}{M_1^2(\gamma_g - 1)} + \frac{1 - r}{M_A^2} = \frac{1}{r^2}\left(\frac{1}{2} + \frac{1}{M_2^2(\gamma_g - 1)}\right)\,. \tag{A.7}$$

Here the magnetic contribution is parametrized using the Alfvénic Mach number of the shock, namely $M_A \equiv u_1/v_A = \rho_1 u_1^2/(B^2/4\pi)$. We recover the standard R-H relations for $M_A \to \infty$. Solving together (A.6) and (A.7) the only physical acceptable solution,

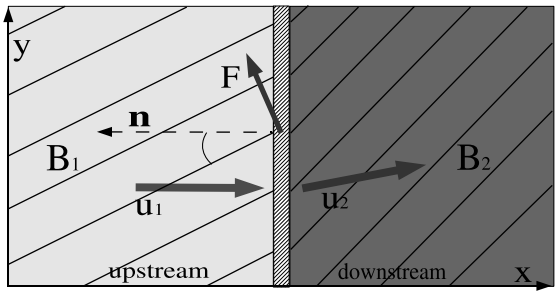

Fig. A.1 Sketch of an oblique shock in the *normal incident* frame. F is the tension force caused by the change of the field direction, and exerted by the field onto the plasma.

besides the trivial one, $r = 1$, is the following:

$$r = \frac{2 + M_1^2\left(\gamma_g - 1 + \frac{\gamma_g}{M_A^2}\right) - \left\{\left[2 + M_1^2\left(\gamma_g - 1 + \frac{\gamma_g}{M_A^2}\right)\right]^2 - 4(\gamma_g + 1)(\gamma_g - 2)\,\frac{M_1^4}{M_A^2}\right\}^{1/2}}{2(\gamma_g - 2)\,\frac{M_1^2}{M_A^2}}\,. \tag{A.8}$$

The Figure A.2 show the compression factor as a function of M_1 for several value of M_A. In the limit of negligible magnetic energy density we recover the usual hydrodynamic result $r = [(\gamma_g + 1)M_1^2)]/[(\gamma_g - 1)M_1^2 + 2]$.

We note that the shock to exist requires $r > 1$. This condition imposes an upper limit for the magnetic energy density, that translates into a lower limit for the Alfvénic Mach number:

$$M_A^2 > M_1^2/(M_1^2 - 1)\,. \tag{A.9}$$

An interesting result is that the minimum value of M_A does not depend on the adiabatic index of the plasma. In the following we also report the expression for the downstream Mach number:

$$M_2^2 = \left[\gamma_g(r-1) + \frac{r}{M_1^2} - \frac{\gamma_g r(r^2-1)}{2M_A^2}\right]^{-1}\,. \tag{A.10}$$

For what concern the downstream pressure and temperature, for an ideal gas the following relations hold:

$$T_2/T_1 = M_1^2/(r^2 M_2^2)\,, \tag{A.11}$$

$$p_2/p_1 = M_1^2/(r\,M_2^2)\,. \tag{A.12}$$

Using the solution for r it is easy to see that the condition $M_1 > 1$ implies $r > 1$ and $M_2 < 1$ and, in turn, also $T_2 > T_1$ and $p_2 > p_1$, as required by the second principle of the thermodynamics.

A.2 The relativistic treatment

As described in §4.3.3, to get the MHD generalization of the relativistic jump conditions, we simply need to add the Maxwell-energy tensor, Eq. (4.20), to the fluid momentum-energy tensor. The results are the same Equations (4.1)-(4.3) plus the magnetic energy and pressure contributions both for upstream and downstream sections. As for the Newtonian case, the upstream values are $\epsilon_{m,1} = p_{m,1} = B^2/(8\pi)$. The downstream values can be computed using the source-free Maxwell equations in the shock frame around the shock discontinuity

$$\nabla_\mu(B'^\mu u^\nu - u^\mu B'^\nu) = 0\,, \tag{A.13}$$

where B'^μ is the field in the shock frame and u^μ is the plasma 4-velocity. Equation (A.13) joint with the Lorentz transformation for B'^μ between the plasma and the shock frame, gives us the parallel and the orthogonal field components: $B_{x,2} = B_{x,1}$ and

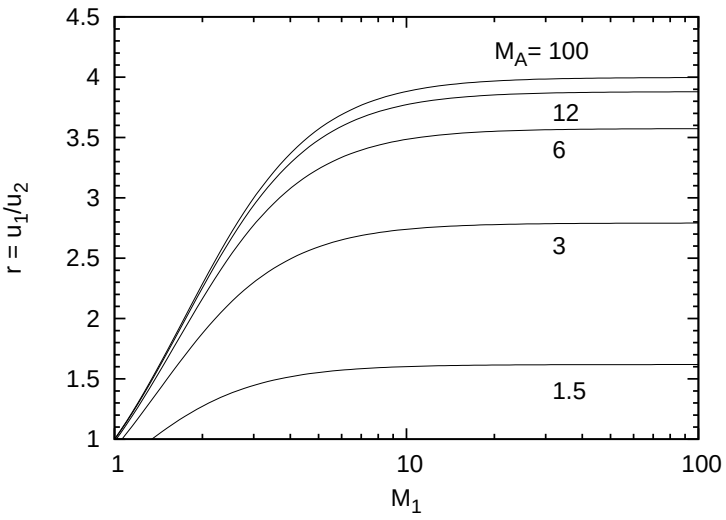

Fig. A.2 Compression factor for Newtonian perpendicular shock as a function of the Mach number in the presence of a coherent magnetic field, for different values of the Alfvénic Mach number, M_A.

$B_{\perp,2}\beta_1\Gamma_1 = B_{\perp,2}\beta_2\Gamma_2$. Because we have only the orthogonal component, the result reads:

$$\epsilon_{m,2} = p_{m,2} = \epsilon_{m,1}\left(\frac{\Gamma_1\beta_1}{\Gamma_2\beta_2}\right)^2 , \tag{A.14}$$

As usual we limit our analysis to the strong shocks ($p_1 = 0$). Obviously the mass conservation, Eq. (4.1), does not change, while Eqs. (4.2) and (4.3) with the magnetic contribution can be expressed as follows:

$$\Gamma_2^2\beta_2^2\left(1+\Gamma_1^2\beta_1^2\right)\left(1+2\alpha_m\right)^2 = \left(1+\Gamma_2^2\beta_2^2\right)\left(\bar{w}_2(\bar{p})\Gamma_2\beta_2 + 2\alpha_m\Gamma_1\beta_1\right)^2 , \tag{A.15}$$

$$\Gamma_1\beta_1\Gamma_2^3\beta_2^3\bar{w}(\bar{p}) - \Gamma_1^2\beta_1^2\Gamma_2^2\beta_2^2 + \Gamma_1\beta_1\Gamma_2\beta_2\bar{p} + 2\alpha_m\left(\Gamma_1^2\beta_1^2 - \Gamma_2^2\beta_2^2\right) = 0 . \tag{A.16}$$

In the present case we use the magnetization parameter $\alpha_m = \frac{B^2/8\pi}{\rho_1 c^2}$ instead of the Alfvénic Mach number. The Equations (A.15) and (A.16) can be solved numerically once the equation of state for the downstram gas is provided in term of the normalized enthalpy $\bar{w} = \bar{\epsilon}(\bar{p}) + \bar{p}$.

The simplest example of solution is shown in Figure A.3 where the velocity ratio r_β vs. the shock velocity is plotted for a non-interacting electron-proton plasma (i.e. we do not take into account any of the collective plasma processes described in the Chapter 4). Different values of magnetic energy density are considered, ranging from $\alpha_m = 5\times10^{-4}$ up to 0.1. The presence of magnetic pressure makes the plasma less compressible, hence the compression factor can be strongly reduced.

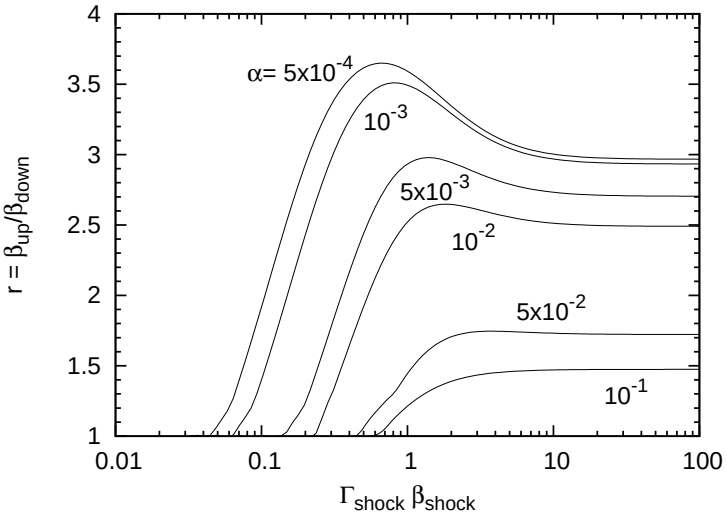

Fig. A.3 Velocity ratio for perpendicular shocks as a function of $\Gamma_{\rm sh}\beta_{\rm sh}$, for several values of the magnetized parameter α_m.

It is worth noting that while in the Newtonian limit there exist a maximum value for α_m (i.e. a minimum value for M_A), above which the shock cannot exist, in the ultra-relativistic limit the magnetic energy density is not limited by any value, and $r_\beta \to 1$ when $\alpha_m \to \infty$.

Bibliography

Achterberg, A., Gallant, Y. A., Kirk, J. G. & Guthmann, A. W. (2001) Particle acceleration by ultrarelativistic shocks: theory and simulations. Mon. Not. R. Astron. Soc. 328:393–408.

Aloisio, R., Berezinsky, V., Blasi, P., Gazizov, A., Grigorieva, S. & Hnatyk, B. (2007) A dip in the UHECR spectrum and the transition from galactic to extragalactic cosmic rays. Astroph. Phys. 27:76–91.

Amato, E. & Blasi, P. (2006) Non-linear particle acceleration at non-relativistic shock waves in the presence of self-generated turbulence. Mon. Not. R. Astron. Soc. 371:1251–1258.

Axford, W. I., Leer, E. & Skadron, G. (1977) The Acceleration of Cosmic Rays by Shock Waves. In: International Cosmic Ray Conference. vol. 11 of *International Cosmic Ray Conference*, pp. 132–+.

Axford, W. I., Leer, E. & McKenzie, J. F. (1982) The structure of cosmic ray shocks. Astron. Astroph. 111:317–325.

Baade, W. & Zwicky, F. (1934) Cosmic Rays from Super-novae. Proceedings of the National Academy of Science 20:259–263.

Bednarz, J. & Ostrowski, M. (1998) Energy Spectra of Cosmic Rays Accelerated at Ultrarelativistic Shock Waves. Physical Review Letters 80:3911–3914.

Begelman, M. C. & Chiueh, T. (1988) Thermal coupling of ions and electrons by collective effects in two-temperature accretion flows. Astrophis. J. 332:872–890.

Bell, A. R. (1978a) The acceleration of cosmic rays in shock fronts. I. Mon. Not. R. Astron. Soc. 182:147–156.

Bell, A. R. (1978b) The acceleration of cosmic rays in shock fronts. II. Mon. Not. R. Astron. Soc. 182:443–455.

Bell, A. R. (1987) The non-linear self-regulation of cosmic ray acceleration at shocks. Mon. Not. R. Astron. Soc. 225:615–626.

Bell, A. R. (2004) Turbulent amplification of magnetic field and diffusive shock acceleration of cosmic rays. Mon. Not. R. Astron. Soc. 353:550–558.

Bell, A. R. & Lucek, S. G. (2001) Cosmic ray acceleration to very high energy through the non-linear amplification by cosmic rays of the seed magnetic field. Mon. Not. R. Astron. Soc. 321:433–438.

Berezhko, E. G. (1996) Maximum energy of cosmic rays accelerated by supernova shocks. Astroparticle Physics 5:367–378.

Berezhko, E. G. & Völk, H. J. (2004) Direct evidence of efficient cosmic ray acceleration and magnetic field amplification in Cassiopeia A. Astron. Astroph. 419:L27–L30.

Berezhko, E. G., Yelshin, V. K. & Ksenofontov, L. T. (1994) Numerical investigation of cosmic ray acceleration in supernova remnants. Astroparticle Physics 2:215–227.

Berezhko, E. G., Ksenofontov, L. T. & Völk, H. J. (2003) Confirmation of strong magnetic field amplification and nuclear cosmic ray acceleration in SN 1006. Astron. Astroph. 412:L11–L14.

Blandford, R. D. (1980) On the mediation of a shock front by Fermi-accelerated cosmic rays. Astrophis. J. 238:410–416.

Blandford, R. D. & McKee, C. F. (1976) Fluid dynamics of relativistic blast waves. Physics of Fluids 19:1130–1138.

Blandford, R. D. & Ostriker, J. P. (1978) Particle acceleration by astrophysical shocks. Astrophis. J. Lett. 221:L29–L32.

Blasi, P. (2002) A semi-analytical approach to non-linear shock acceleration. Astroph. Phys. 16:429–439.

Blasi, P. (2004) Nonlinear shock acceleration in the presence of seed particles. Astroparticle Physics 21:45–57.

Blasi, P. & Vietri, M. (2005) On Particle Acceleration around Shocks. II. A Fully General Method for Arbitrary Shock Velocities and Scattering Media. Astrophis. J. 626:877–886.

Blasi, P., Gabici, S. & Vannoni, G. (2005) On the role of injection in kinetic approaches to non-linear particle acceleration at non-relativistic shock waves. Mon. Not. R. Astron. Soc. 361:907–918.

Blasi, P., Amato, E. & Caprioli, D. (2007) The maximum momentum of particles accelerated at cosmic ray modified shocks. Mon. Not. R. Astron. Soc. 375:1471–1478.

De Hoffman, F. & Teller, E. (1950) Magneto-Hydrodynamic Shocks. Physical Review 80:692–703.

Drury, L. O. & Falle, S. (1986) On the stability of shock modified by particle acceleration. Mon. Not. R. Astron. Soc. 223:353–376.

Drury, L. O. & Voelk, J. H. (1981) Hydromagnetic shock structure in the presence of cosmic rays. Astrophis. J. 248:344–351.

Drury, L. O., Axford, W. I. & Summers, D. (1982) Particle acceleration in modified shocks. Mon. Not. R. Astron. Soc. 198:833–841.

Duffy, P., Drury, L. O. & Voelk, H. (1994) Cosmic ray hydrodynamics at shock fronts. Astron. Astroph. 291:613–621.

Eichler, D. (1984) On the theory of cosmic-ray-mediated shocks with variable compression ratio. Astrophis. J. 277:429–434.

Eichler, D. (1985) Nonlinear shock acceleration. III - Finite wave velocity, wave pressure, and entropy generation via wave damping. Astrophis. J. 294:40–46.

Ellison, D. C. & Eichler, D. (1984) Monte Carlo shock-like solutions to the Boltzmann equation with collective scattering. Astrophis. J. 286:691–701.

Ellison, D. C. & Eichler, D. (1985) Relativistic cosmic-ray spectra in the fully nonlinear theory of shock acceleration. Physical Review Letters 55:2735–2738.

Ellison, D. C., Möbius, E. & Paschmann, G. (1990) Particle injection and acceleration at earth's bow shock - Comparison of upstream and downstream events. Astrophis. J. 352:376–394.

Ellison, D. C., Baring, M. G. & Jones, F. C. (1995) Acceleration Rates and Injection Efficiencies in Oblique Shocks. Astrophis. J. 453:873–+.

Ellison, D. C., Baring, M. G. & Jones, F. C. (1996) Nonlinear Particle Acceleration in Oblique Shocks. Astrophis. J. 473:1029–+.

Fermi, E. (1949) On the Origin of the Cosmic Radiation. Physical Review 75:1169–1949.

Fermi, E. (1954) Galactic magnetic field and the origin of cosmic radiation. Astrophis. J. 119:1–6.

Frederiksen, J. T., Hededal, C. B., Haugbølle, T. & Nordlund, Å. (2004) Magnetic Field Generation in Collisionless Shocks: Pattern Growth and Transport. Astrophis. J. Lett. 608:L13–L16.

Gallant, Y. A. (2002) Particle Acceleration at Relativistic Shocks. In: Guthmann, A. W., Georganopoulos, M., Marcowith, A. & Manolakou, K. (eds.), Relativistic Flows in Astrophysics. vol. 589 of *Lecture Notes in Physics, Berlin Springer Verlag*, pp. 24–+.

Gallant, Y. A. & Achterberg, A. (1999) Ultra-high-energy cosmic ray acceleration by relativistic blast waves. Mon. Not. R. Astron. Soc. 305:L6–L10.

Gallant, Y. A., Hoshino, M., Langdon, A. B., Arons, J. & Max, C. E. (1992) Relativistic, perpendicular shocks in electron-positron plasmas. Astrophis. J. 391:73–101.

Hoerandel, J. R. (2005) A review of experimental results at the knee.

Hoshino, M., Arons, J., Gallant, Y. A. & Langdon, A. B. (1992) Relativistic magnetosonic shock waves in synchrotron sources - Shock structure and nonthermal acceleration of positrons. Astrophis. J. 390:454–479.

Jones, F. C. & Ellison, D. C. (1991) The plasma physics of shock acceleration. Space Science Reviews 58:259–346.

Kang, H. & Jones, T. W. (1997) Diffusive Shock Acceleration in Oblique Magnetohydrodynamic Shocks: Comparison with Monte Carlo Methods and Observations. Astrophis. J. 476:875–+.

Kang, H., Jones, T. W. & Gieseler, U. D. J. (2002) Numerical Studies of Cosmic-Ray Injection and Acceleration. Astrophis. J. 579:337–358.

Kirk, J. G. & Duffy, P. (1999) TOPICAL REVIEW: Particle acceleration and relativistic shocks. Journal of Physics G Nuclear Physics 25:163–+.

Kirk, J. G. & Schneider, P. (1987) On the acceleration of charged particles at relativistic shock fronts. Astrophis. J. 315:425–433.

Kirk, J. G., Guthmann, A. W., Gallant, Y. A. & Achterberg, A. (2000) Particle Acceleration at Ultrarelativistic Shocks: An Eigenfunction Method. Astrophis. J. 542:235–242.

Krymskii, G. F. (1977) A regular mechanism for the acceleration of charged particles on the front of a shock wave. Akademiia Nauk SSSR Doklady 234:1306–1308.

Lagage, P. O. & Cesarsky, C. J. (1983) The maximum energy of cosmic rays accelerated by supernova shocks. Astron. Astroph. 125:249–257.

Lemoine, M. & Pelletier, G. (2003) Particle Transport in Tangled Magnetic Fields and Fermi Acceleration at Relativistic Shocks. Astrophis. J. Lett. 589:L73–L76.

Lemoine, M. & Revenu, B. (2006) Relativistic Fermi acceleration with shock compressed turbulence. Mon. Not. R. Astron. Soc. 366:635–644.

Lucek, S. G. & Bell, A. R. (2000) Non-linear amplification of a magnetic field driven by cosmic ray streaming. Mon. Not. R. Astron. Soc. 314:65–74.

Malkov, M. A. (1997) Analytic Solution for Nonlinear Shock Acceleration in the Bohm Limit. Astrophis. J. 485:638–+.

Malkov, M. A., Diamond, P. H. & Völk, H. J. (2000) Critical Self-Organization of Astrophysical Shocks. Astrophis. J. Lett. 533:L171–L174.

McKenzie, J. F. & Volk, H. J. (1982) Non-linear theory of cosmic rays shock including self-generated Alfvén waves. Astron. Astroph. 116:192–200.

Medvedev, M. V. & Loeb, A. (1999) Generation of Magnetic Fields in the Relativistic Shock of Gamma-Ray Burst Sources. Astrophis. J. 526:697–706.

Mond, M. & O'C. Drury, L. (1998) Acoustic emission and corrugational instability of shocks modified by strong particle acceleration. Astron. Astroph. 332:385–390.

Niemiec, J. & Ostrowski, M. (2004) Cosmic-Ray Acceleration at Relativistic Shock Waves with a "Realistic" Magnetic Field Structure. Astrophis. J. 610:851–867.

Parizot, E., Marcowith, A., van der Swaluw, E., Bykov, A. M. & Tatischeff, V. (2004) Superbubbles and energetic particles in the Galaxy. I. Collective effects of particle acceleration. Astron. Astroph. 424:747–760.

Parizot, E., Marcowith, A., Ballet, J. & Gallant, Y. A. (2006) Observational constraints on energetic particle diffusion in young supernovae remnants: amplified magnetic field and maximum energy. Astron. Astroph. 453:387–395.

Peacock, J. A. (1981) Fermi acceleration by relativistic shock waves. Mon. Not. R. Astron. Soc. 196:135–152.

Pierre AUGER Collaboration (2008) Upper limit on the cosmic-ray photon flux above 10^{19} eV using the surface detector of the Pierre Auger Observatory. Astroparticle Physics 29:243–256.

Rossi, E. & Rees, M. J. (2003) Gamma-ray burst afterglow emission with a decaying magnetic field. Mon. Not. R. Astron. Soc. 339:881–886.

Skilling, J. (1975) Cosmic ray streaming. II - Effect of particles on Alfven waves. Mon. Not. R. Astron. Soc. 173:245–254.

Synge, J. (1957) The relativistic gas. North-Holland, Amsterdam.

Vainio, R. & Schlickeiser, R. (1999) Self-consistent Alfvén-wave transmission and test particle acceleration at parallel shock. Astron. Astroph. 343:303–311.

Vietri, M. (2003) On Particle Acceleration around Shocks. I. Astrophis. J. 591:954–961.

Vietri, M. (2006) Astrofisica Delle Alte Energie. Bollati Boringhieri, 1st edn.

Völk, H. J., Berezhko, E. G. & Ksenofontov, L. T. (2005) Magnetic field amplification in Tycho and other shell-type supernova remnants. Astron. Astroph. 433:229–240.